

Structure-Function Studies of Nicotinic Acetylcholine Receptors Using Selective Agonists and Positive Allosteric Modulators

Thesis by

Christopher Bruno Marotta

In Partial Fulfillment of the Requirements for the Degree of

Doctor of Philosophy



CALIFORNIA INSTITUTE OF TECHNOLOGY

Pasadena, California

2015

(Defended May 22, 2015)

© 2015

Christopher Bruno Marotta

All Rights Reserve

*Dedicated To My Friends, Family, And
All Of Those Who Have Helped Me Along The Way*

Perfection is not attainable, but if we chase perfection we can catch excellence.

-Vince Lombardi

Acknowledgements

During my tenure at Caltech I have met numerous wonderful people who have shaped me into the scientist – and person – I am today. Everyone here has in some way aided me in accomplishing my dissertation; a feat I never thought I would be capable of achieving. I would like to take this time to thank all the positive influences that pushed me to be better in all aspects of my life.

First, I must thank my advisor, Dennis Dougherty. He has provided an enriching environment filled with freedom to experiment and explore new ideas for projects. This has allowed me to venture out to solve unique problems that arise. Although frustrating at times, it has taught me how to look critically at problems and develop new solutions. The constant encouragement to have discussions between lab peers generated numerous useful perspectives on data interpretation. All of these factors have taught me invaluable critical thinking skills and allowed me to embark on numerous endeavors and collaborations. It is satisfying to say my thesis is comprised of projects that I had a significant hand in developing and succeeding in finishing. I am truly grateful for all his guidance and support throughout my time at Caltech.

I am also extremely thankful to my thesis committee: Professors Jackie Barton, Tom Miller, and Doug Rees. They have provided me with wonderful discussions and encouragement throughout all of our meetings over the years. I'd also like to thank Professor Rees for taking on the role as my committee chair and guiding the meetings in a timely and professional manner.

The Dougherty lab is fortunate to work in close collaboration with Professor Henry Lester and his staff and students. His knowledge and insight toward ion channel function and electrophysiology are incredible. His persistence in the pursuit of perfection has driven me to be thorough, critical, and to have plenty of control experiments. In addition, his lab has provided me with plenty of scientific discussions, which have even sparked several collaborations. Dr. Bruce Cohen has provided invaluable information and suggestions during many phases of nearly all my projects. His passion for research and attention to detail kept me sharp during all of our meetings. I would like to thank Dr. Crystal Dilworth with whom I had the pleasure of collaborating on a project that was eventually published. She was an encouraging friend and guided me during my most impressionable beginning years. I would also like to thank Dr. Weston Nichols for seeking me out for the collaboration discussed in Appendix 1. I would also like to thank Dr. Brandon Henderson for all our scientific and non-scientific talks. He is a tremendously smart and hard working role model, and I wish him the best for his future endeavors. Finally, I would also like to thank all of the other Lester Lab members (former and present) who took the time to talk with me and be part of my daily life over the years.

All the members of the Dougherty lab have been important in my growth and have been great influences and friends to me. First, a thank you to all the members who have already graduated. I will be joining you all on the other side shortly. Dr. Nyssa Puskar, Dr. Angela Blum, and Maggie Thompson initiated me into the Dougherty lab techniques and electrophysiology of oocytes. Thank you all for your patience as I fumbled about and killed so many oocytes. Also, thank you Angela for being so hard and demanding on me in the beginning. You were influential in so many ways and really

whipped me into shape – both scientifically and physically at our boot camp classes. Dr. Jai Shanata was a fun presence during the late hours in lab and always encouraging and supportive. Thank you Dr. Sean Kedrowski for all the sports conversations. You were one of the few at the time that enjoyed talking about anything and everything that came on ESPN. To Erin Lamb, Ramrod! Thanks for always making me laugh. Thank you Dr. Walrati (Kay) Limapichat for teaching me how to salsa and for being a beacon of hard work and dedication in the lab. Thank you Dr. Ximena Da Silva for your insights on lab techniques. To my Connecticut brethren, Dr. Ethan Van Arnham and Dr. Kristina Daeffler, go Huskies! Ethan, your impersonations and passionate outbursts were always a source of wonder and laughter. Kristina, thank you for always being there to listen and give advice. Your friendship has meant a lot over the years. I enjoyed our collaboration and actually getting some positive results from a project that looked like it was doomed. I promise this year is the Buffalo's year. The Bills *will* make the playoffs, or at least they will next year. To Dr. Noah Duffy, thank you for being a great friend and knowledgeable lab mate. I miss our late night lab sessions that devolved into YouTube viewing as the hours got later and later. Also, your MacGyver skills always left me in awe. No one fixes things like you do. Dr. Tim Miles, I am impressed with your success in lab and being able to graduate in four years. It was definitely due to your passion and knowledge. Congratulations on having a successful teaching post-doc and best of luck in your new research post-doc. I know you will continue being great. To Kayla Busby, I miss the bubblyness you always brought to lab. I'm sure you still bring that same air of optimism everywhere you go. And finally, thank you Iva Rreza. It was a pleasure being your TA for the first year and a half. It was even more rewarding being you lab mentor and to work on a project that was a

success in the end. I know you will be great at Columbia and will be even more successful at your PhD.

To all the current lab members, thank you all for the support over the years and help during this exit process. It has been an awesome experience getting to know everyone and I am proud to have you all as lab mates and as friends. Clinton Regan was my TA in Chem 242a, so it was pleasure to be able to teach him something when he joined the lab. Your excitement and curiosity is always invigorating. Oliver Shafaat is a dedicated and determined individual who always amazes me with his knowledge of instrumentation and science in so many diverse fields. It has been a pleasure getting to know you and work alongside your side (especially when you do your annual rotation of oocyte experiments). Thank you Matt Rienzo and Mike Post for being supportive friends through these years. I appreciate all the insight into experiments as well as helping me dress for success. Also, thank you for helping me complete a Tough Mudder, Matt. And thank you Mike for being a dedicated “Copus” captain and helping to tackle all the problems that arose with the Opus. Matt Davis, I have enjoyed all our sports watching and lunch bets for our fantasy football face-offs. Tryptoman is in good hands and will continue to be a model of fun and sportsmanship with your leadership. You are a great person and friend. Also, don’t change; the puns never get old. Paul (DPPD) Walton, your work ethic and enthusiasm are an inspiration to all. What’s even better is that you can kick back and have a good time as well. I will miss your quick quips and the humor that you bring to lab. It’s good to be a little absurd and it has always brightened my day. I am glad to call you my friend, and I know you will be tremendously successful. To Betty Wong, Catie Blunt, Annet Blom, and Bryce Jarmon, watching you all grow over the last

few years has been a pleasure. I am glad I got to know you all, and I know you all will be great scientists in this lab. And to Richard Mosesso, even though we only overlapped briefly, I believe you will have an excellent career here, from the work ethic you have already shown.

I have also made many friends in other labs and other departments at Caltech that have been instrumental in my thesis completion. They have provided me with new perspectives and relief when I needed to take a break from my lab work. So many people have been there for me and I am truly grateful for all those that I have met over the years. I lived in a house full of (mostly) GPS students and lived vicariously through their research travel adventures. David Case, my first and continued roommate at Caltech, has been one of my best friends. Thank you for always being there to listen and being supportive through all the ups and downs. I will miss our pick up football and softball as well as our Sunday ritual of watching the NFL in the fall. Brian Kohan, we were the non-GPS people in a house full of them. You're an extremely talented and loyal friend. I have always got your back and I know you have mine. Also, we will always have Vegas. Elizabeth Trembath-Reichert, you have been an amazing friend and extremely supportive person. I enjoyed all the cooking advice, and I learned a great deal in the kitchen from you. Thank you for always listening and giving great advice. Jeff Prancevic and Sophie Hines, you both are caring and compassionate people and I am glad to have you as friends. Also, thank you for teaching me proper bicycle maintenance and how to change a flat. It has come in handy more than once.

Others I would like to thank include Lindsay Repka. It was fun being co-captains of our joint Dougherty-Reisman softball team, Tryptoman. Also, it was fun working on

our joint collaboration and actually getting a hit on a compound made from your synthesis. Thank you Agnes Tong for all your help and support over the years. You are a vital resource to all the chemistry graduate students. Thank you, Amanda Shing, for being a good and inclusive friend. Thank you Sunita Darbe, Kevin Fiedler, and Sam Johnson. It has been a pleasure getting to know you all over the last two years, and I value your friendship immensely. Also, thank you Sam for all the meals you prepared during my proposal exam writing period. You are a wonderful, caring person and a life-long friend I am glad to have. Finally, thank you Gabriela Venturini for being a great friend and an awesome roommate. It has been fun watching all the TV shows and having our vanilla cone moments. Thank you for sharing the “chickens” – Jacob and Nessie – with me over the last two years. I’m sorry the big one loves me so much but he loves you the same. Also, thank you for letting me tag along on your trip back home to Argentina. It was an amazing experience, and I can’t wait to visit again.

One very important person in my life that I have a tremendous amount of gratitude and respect for is Lisa Mauger. I am so grateful to have met you. You are a strong, companionate, and dedicated person who I try and emulate everyday. Your sense of community and giving back are inspirational. Also, your child-like enthusiasm for world travel is infectious. We have had several exciting traveling adventures (Germany was out of this world), and I can’t wait to continue exploring with you. Your constant support and love has gotten me through injuries (sorry about that) and stressful times. I will be there to support you, as I know you will be there to help me. Together, we can accomplish anything. I am excited to be graduating with you and starting the next phases of our lives together. Thank you for everything. I love you.

Finally, I must thank my family. Their love and support throughout the years have guided me and empowered me to excel in all aspects of my life. I grew up with my extended family and they deserve a lot of credit. It is a wonderful feeling to know I always have support from them and they would do anything for me – just as I would do anything for any one of them. As for my immediate family, my little brother, Derek Marotta, has always pushed me to be a good role model – to study hard and work harder. Despite the natural sibling rivalry, we grew up close and have mutual respect for one another. I know he has the same strength and determination to accomplish his dreams and passions. My stepdad, Bill Fleischer, has always been supportive in all my activities and always provides fun conversations. I am grateful to have him in my life.

My father, Chris Marotta, has always been proud of my achievements but also keeps them from going to my head. He is a hard working individual and always puts family above all else. Of all the things my dad taught me over the years from cooking to car maintenance, the one thing that I am most proud to say I got from him was my dedication to my family. He instilled that passion and love early on and continues to live by it to this day. I know I will always be able to find support, and with that I am not afraid to try anything. No matter when or how many times I fall down, there are always people there to help pick me back up.

My mother, Tammy Fleischer, is an extremely selfless person and has always been there to support both my brother and me. She has made many sacrifices for us, and I am always grateful for that. My mom has also taught me many life skills and lessons as well, but the one that sticks out the most, and I am truly thankful for, is her altruism. She always looks out for other people's welfare and gets great joy from putting a smile on

someone else's face. I saw that from an early age and still see it today. I try to live by the same rules of conduct, treating everyone with respect and compassion. Being able to cheer someone up provides the best feeling in the world. I have made several close, life-long friends from this, which is a true blessing. Thank you all so very much for everything that you have given me. You all mean the world to me. I love you all

My parents, family, friends, and loved ones all shaped me into the person I am today. I am glad I can make them all proud by achieving a PhD. from such a prestigious institution. This thesis and work is as much theirs as it is mine.

Abstract

This dissertation primarily describes chemical-scale studies of nicotinic acetylcholine receptors (nAChRs) in order to better understand ligand-receptor selectivity and allosteric modulation influences during receptor activation. Electrophysiology coupled with canonical and non-canonical amino acids mutagenesis is used to probe subtle changes in receptor function.

The first half of this dissertation focuses on differential agonist selectivity of $\alpha 4\beta 2$ -containing nAChRs. The $\alpha 4\beta 2$ nAChR can assemble in alternative stoichiometries as well as assemble with other accessory subunits. Chapter 2 identifies key structural residues that dictate binding and activation of three stoichiometry-dependent $\alpha 4\beta 2$ receptor ligands: sazetidine-A, cytisine, and NS9283. These do not follow previously suggested hydrogen-bonding patterns of selectivity. Instead, three residues on the complementary subunit strongly influence binding ability of a ligand and receptor activation. Chapter 3 involves isolation of a $\alpha 5\alpha 4\beta 2$ receptor-enriched population to test for a potential alternative agonist binding location at the $\alpha 5$ - $\alpha 4$ interface. Results strongly suggest that agonist occupation of this site is not necessary for receptor activation and that the $\alpha 5$ subunit only incorporates at the accessory subunit location.

The second half of this dissertation seeks to identify residue interactions with positive allosteric modulators (PAMs) of the $\alpha 7$ nAChR. Chapter 4 focuses on methods development to study loss of potentiation of Type I PAMs, which indicate residues vital

to propagation of PAM effects and/or binding. Chapter 5 investigates $\alpha 7$ receptor modulation by a Type II PAM (PNU-120596). These results show that PNU-120596 does not alter the agonist binding site, thus is relegated to influencing only the gating component of activation. From this, we were able to map a potential network of residues from the agonist binding site to the proposed PNU-120596 binding site that are essential for receptor potentiation.

Table of Contents

Acknowledgements.....	iv
Abstract.....	xii
Table of Contents.....	xiv
 Chapter 1: Introduction	1
1.1 Neuronal Communication.....	1
1.2 Ligand Gated Ion Channels: Nicotinic Acetylcholine Receptors	2
1.3 Non-Canonical Amino Acid Mutagenesis	5
1.4 Electrophysiology Assays: The EC ₅₀ and Voltage Jump Experiments	10
1.5 Mutant Cycle Analyses	11
1.6 Orthosteric vs. Allosteric	13
1.7 Summary of Dissertation Work	14
1.8 References.....	17
 Chapter 2: Selective Ligand Behaviors Provide New Insights into Agonist Activation of Nicotinic Acetylcholine Receptors.....	21
2.1 Abstract.....	21
2.2 Introduction.....	22
2.3 Results and Discussion	24
2.3.1 Hydrogen Bonding: Non-Canonical Amino Acid Analysis	24
2.3.2 Sazetidine-A and the β 2 Complementary Face	25
2.3.3 Cytisine and the β 2 Complementary Face	28
2.3.4 NS9283 and the α 4 Complementary Face.....	31
2.4 Conclusions.....	33

2.5 Methods.....	34
2.5.1 Molecular Biology	34
2.5.2 Oocyte Preparation and Injection.....	35
2.5.3 Chemical Preparation.....	36
2.5.4 Electrophysiology	37
2.5.5 The Hypersensitive Mutation (L9'A)	38
2.6 Acknowledgments.....	39
2.7 References.....	40

Chapter 3: Probing the Non-Canonical Interface for Agonist Interaction with an $\alpha 5$ -Containing Nicotinic Acetylcholine Receptor

3.1 Abstract.....	43
3.2 Introduction.....	44
3.3 Materials and Methods.....	46
3.3.1 Molecular Biology	46
3.3.2 Electrophysiology Studies	47
3.3.2.1 Xenopus Oocyte Preparation and Injection.....	47
3.3.2.2 Chemical Preparation	47
3.3.2.3 Electrophysiology Experimental Protocols	47
3.3.3 Data Analysis.....	48
3.3.3.1 Dose-Response Analysis	48
3.3.3.2 Current-Voltage Analysis.....	48
3.3.3.3 Error Analysis.....	49
3.4 Results.....	49
3.4.1 Expression of an $\alpha 5$ -Containing Receptor.....	49
3.4.2 The $\alpha 5V9'S$ Mutation Confers Distinct Physical Properties Allowing for Definitive Establishment of the Subunit's Incorporation	52
3.4.3 Mutational Analysis of the Aromatic Box at the $\alpha 5$ - $\alpha 4$ Interface Showed No Functional Impact.....	56
3.5 Discussion.....	58

3.6 Acknowledgments.....	62
3.7 References.....	63

Chapter 4: Assay Development for Positive Allosteric Modulator Studies: Identification of Necessary Residues for Potentiation of Type I Modulators in $\alpha 7$ Nicotinic Acetylcholine Receptors67

4.1 Abstract.....	67
4.2 Introduction.....	68
4.3 Results and Discussion	70
4.3.1 Assay Development for PAM Measurements.....	70
4.3.2 Screening for Residues Essential in PAM Potentiation.....	76
4.4 Conclusions.....	83
4.5 Methods.....	84
4.5.1 Molecular Biology and Homology Models	84
4.5.2 Injection of Oocytes and Chemical Preparation	84
4.5.3 Electrophysiology	85
4.6 References.....	87

Chapter 5: An Unaltered Orthosteric Site and a Network of Long-Range Allosteric Interactions for PNU-120596 in $\alpha 7$ Nicotinic Acetylcholine Receptors90

5.1 Abstract.....	90
5.2 Introduction.....	91
5.3 Results	95
5.3.1 Methodology for Interpretation of Functional Coupling Comparisons	95
5.3.2 The Orthosteric Site: Binding Interactions are Unaffected by PNU-120596.....	97
5.3.3 A Double Perturbation Cycle Analysis to Identify Residues Critical to PNU-120596 Function	104

5.3.4 Measuring the Coupling at the Proposed PNU-120596 Binding Site	105
5.3.5 Important Residues in the Gating Interface and the Extracellular Domain	107
5.4 Discussion	109
5.5 Conclusions	112
5.6 Methods	113
5.6.1 Residue Numbering and Protein Modeling	113
5.6.2 Molecular Biology	114
5.6.3 Oocyte Preparation and Injection	114
5.6.4 Chemical Preparation	115
5.6.5 Electrophysiology	115
5.7 Acknowledgments	116
5.8 References	117

Appendix 1: Autosomal Dominant Nocturnal Frontal Lobe Epilepsy Mutation Suppresses Low-Sensitivity ($\alpha 4$)₃($\beta 2$)₂ Nicotinic Acetylcholine Receptor Expression

	121
A1.1 Abstract	121
A1.2 Results and Discussion	122
A1.3 Methods	127
A1.3.1 Molecular Biology	127
A1.3.2 Oocyte Injection	127
A1.3.3 Electrophysiology	128
A1.4 References	129

Appendix 2: Ligand-Gated Ion Channel Screen of Physostigmine Derivatives for Allosteric Modulation and Receptor Agonism

A2.1 Abstract	130
A2.2 Results and Discussion	131

A2.2.1 Screening Compounds for Functional Properties at Various LGICs	131
A2.2.1 Physostigmine Analog Inhibition Characterization	134
A2.3 Conclusions	136
A2.4 Methods	137
A2.5 References	138

Chapter 1

Introduction

1.1 Neuronal Communication

The brain is the most complex organ on earth. There are approximately 10^{11} neurons that can make upwards of 10^4 connections each, comprising a total of perhaps 10^{15} junctions for inter-neuron communication. Neuronal signaling requires propagation of an electrical signal between these individual nerve cells. An action potential (electrical signal) travels through the axon of the nerve cell to the synapse, which is the junction between two neurons. Once the electrical signal reaches the synapse, vesicles containing small molecule neurotransmitters fuse to the cell membrane and release the chemical signaling molecules into the synaptic cleft (space between two nerve cells). Neurotransmitters diffuse across and bind to integral membrane proteins located on the adjacent neuron. The binding of these molecules triggers conformational changes in proteins that allow ions to flow across the membrane and regenerate the electrical signal in the adjacent neuron for further signal propagation (**Figure 1.1**). Synaptic transmission is the basis for neuronal cell communication, which is responsible for a wide array of processing that varies from sensation to learning and memory. When these processes become faulty or even fail, debilitating health disorders can arise that range from chronic pain to neurological disease. In the Dougherty lab, we seek to understand the functional

properties of the proteins responsible for the continuation of the electrical signal at the synapse.

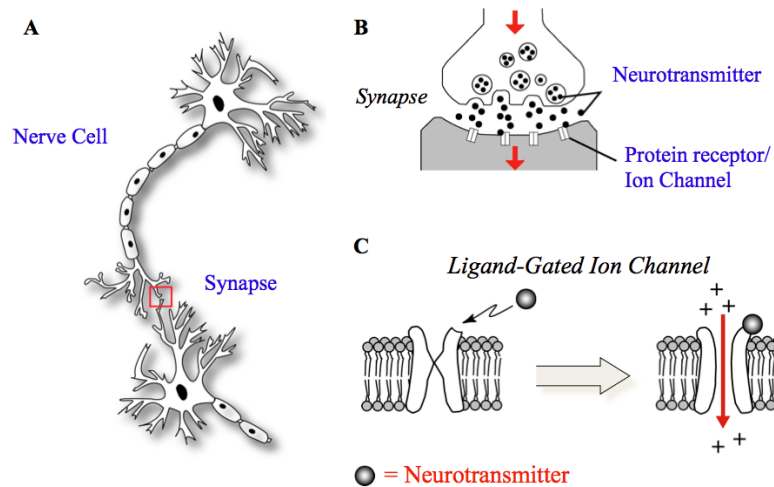


Figure 1.1 Neuronal communication through synaptic transmission. (A) A diagram of two adjacent nerve cells with close physical contact at the synapse. (B) The synapse is the space between neurons where neurotransmitters are released to diffuse across for adjacent receptor activation. (C) LGICs undergo conformational rearrangement upon neurotransmitter binding to allow ions to traverse the membrane.

1.2 Ligand Gated Ion Channels: Nicotinic Acetylcholine Receptors

One class of proteins responsible for neurotransmitter recognition is the ligand gated ion channels (LGICs) or, more specifically for this dissertation, the Cys-loop superfamily of LGICs. The Cys-loop superfamily comprises receptors that are both excitatory and inhibitory. The cation-permeable channels, nicotinic acetylcholine receptors (nAChRs) and serotonin (5-HT_{3A}) receptors, are excitatory and responsible for signal propagation. In contrast are the anion-permeable channels, GABA_A, GABA_C, glycine, and GluCl receptors, which are inhibitory and responsible for signal termination. Cys-loop receptors are comprised of five subunits that can be homomeric (identical) or heteromeric (two to four subunits). Each subunit contains a large extracellular domain, four transmembrane α -helices (M1-M4), and a variable intracellular domain

(**Figure 1.2**). These arrange in a pentameric fashion for ion permeation with the M2 α -helix lining the pore. Neurotransmitters bind at the interface of two subunits and cause a conformational rearrangement approximately 60 Å away at the receptor gate. The “gating region” comprises several residues along the M2 α -helix that are responsible for ion permeation. This dissertation focuses mainly on the nAChRs and their structure-function relationships.

nAChRs are aptly named for both their natural agonist (acetylcholine) and for their sensitivity to nicotine, the main addictive component in cigarettes. These receptors are responsible for synaptic transmission in both the peripheral and central nervous systems (1-3). There are 17 nAChR subunits: α 1- α 10, β 1- β 4, γ , δ , and ϵ . However, α 8 is only found in avian species and the “muscle-type” nAChR (α 1 β 1 γ δ/ϵ) is relegated to

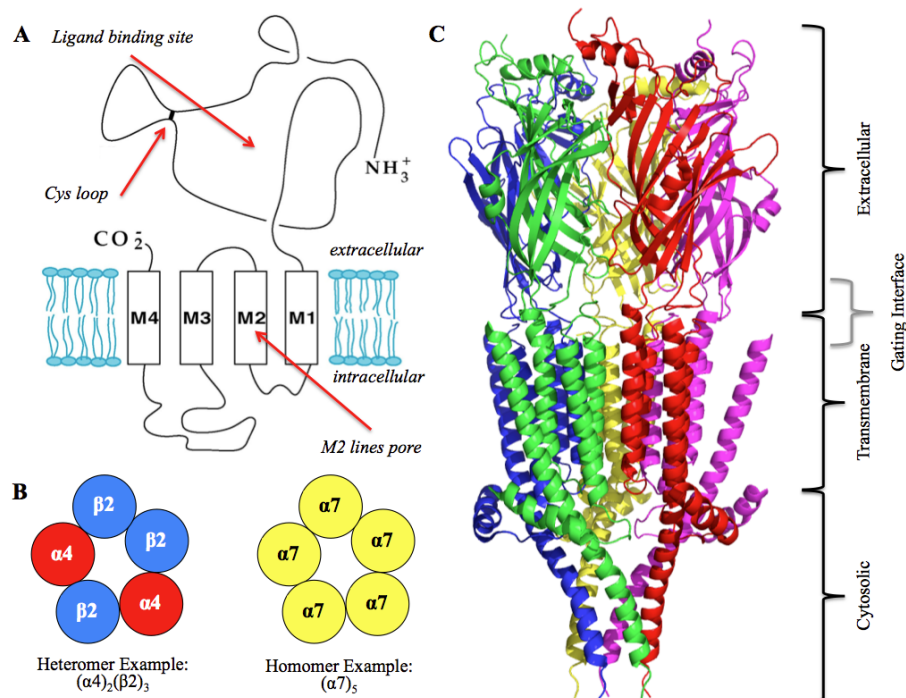


Figure 1.2 Structural arrangements for Cys-loop receptors. (**A**) A representation of a single subunit depicting the homologous regions for the Cys-loop family. (**B**) Examples of hetero- and homo-pentamer arrangements for the nAChR family. (**C**) Crystal structure of the mouse 5HT_{3A} (serotonin) receptor (PDB ID: 4PIR).

only the peripheral system and neuromuscular junctions. $\alpha 2$ - $\alpha 7$, $\alpha 9$, $\alpha 10$, and $\beta 2$ - $\beta 4$ comprise the neuronal nAChR subunits and are prominent throughout the central nervous system in varying assemblies and distributions (**Figure 1.2**) (2,4). Due to their vast presence, nAChRs are crucial in memory and learning and are prominent targets in neurological disorders such as addiction, Alzheimer's disease and Parkinson's disease (2,5-10). The most abundant and widely distributed receptors are the $\alpha 4\beta 2$ and $\alpha 7$ nAChRs (3,4). The $\alpha 4\beta 2$ receptor is a highly sought-after drug target due to its role in nicotine addiction, as seen with Pfizer's engineered smoking cessation drug Chantix® (varenicline) (3,4,11,12). The $\alpha 4\beta 2$ receptor has the ability to assemble into two stoichiometries, the high sensitivity $(\alpha 4\beta 2)_2(\beta 2)$, and low sensitivity $(\alpha 4\beta 2)_2(\alpha 4)$. In addition, association with other subunits, such as $\alpha 5$, has been seen (9,13-15). The accessory subunit (the unpaired 5th subunit) can provide distinct tuning of the receptor's physical properties. The $\alpha 7$ nAChR is a homopentameric channel and also widely distributed throughout the central nervous system. It has been a constant drug target – both in agonist and allosteric modulator development – due to its association with neurological disorders such as schizophrenia and Alzheimer's disease (16-23).

nAChRs are large integral membrane bound proteins, which makes them difficult to crystallize. However, crystallographic success has increased and generated valuable structural information over the years. First, high-resolution crystal structures of a homologous soluble acetylcholine binding protein (AChBP) and a low-resolution cryo-EM structure of an nAChR provide useful information (24-26). Several years later, high-resolution structures of homologous prokaryotic and invertebrate LGICs were obtained and allowed comparisons to be made in what is thought to be the resting

(closed) and conducting (open) form of an ion channel (27-31). In the last year, an exciting breakthrough occurred in that the first set of high-resolution crystal structures of vertebrate Cys-loop receptors (5HT_{3A} and GABA_A) were achieved (**Figure 1.2**) (32,33). Although these advances have influenced our structural knowledge, proteins are inherently dynamic, and static representations may not accurately capture motions associated with activation. Thus, structure-function studies still provide vital information regarding interactions necessary for ligand binding and conformational rearrangements required for receptor activation.

1.3 Non-Canonical Amino Acid Mutagenesis

The goal of the Dougherty lab is to use physical organic chemistry to provide chemical scale structure-function relationships. By identifying distinct non-covalent interactions – cation- π , hydrogen bonding, van der Waals, etc. – we can elucidate contacts that are critical for receptor function, and begin to map important properties to ligand recognition (pharmacophore identification) or functional coupling (conformational motions) on a large and complex protein. We can have a better understanding of neurological diseases and compounds designed for treatment through increased knowledge of the mechanisms associated with receptor activation.

In order to study chemical scale interactions between a ligand and a protein, subtle perturbations must be introduced and the effects must be monitored. Conventional mutagenesis is limited to the 20 naturally occurring amino acids. These provide a good starting point for identifying functionally relevant residues; however the structural changes between the side chain groups are quite large and do not afford the delicate

functional distinctions that we aim to tease out. To work around these limitations, the Dougherty lab has established a working protocol to incorporate non-canonical amino acids that has proven to be a powerful technique in studying structure-function relationships in LGICs (**Figure 1.3**) (34-38). This opens the possibility of probing interactions through the introduction of diverse side chain configurations to study specific interactions of a protein on a chemical scale.

The Dougherty lab has utilized and optimized a method known as *in vivo* nonsense suppression to incorporate non-canonical amino acids (**Figure 1.4**) (35,39-43). This technique allows for site-specific incorporation of a non-canonical amino acid in a relatively quick timeframe. The mRNA codon of the residue to be probed is replaced with a stop or “nonsense” codon (UAG, UGA, or UAA), which is normally used to signify protein synthesis termination. The non-canonical amino acid is chemically

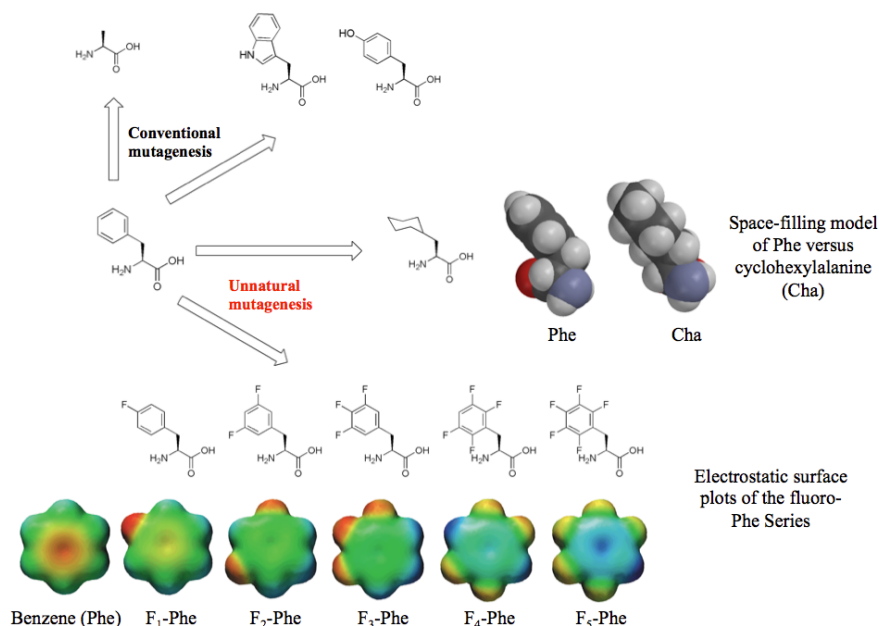


Figure 1.3 The power of non-canonical amino acid mutagenesis. Conventional mutagenesis of phenylalanine (Phe) is limited in structural perturbation and lacks specific control. Non-canonical amino acid allows specific changes in order to answer questions that pertain to steric (cyclohexylalanine) and electrostatic interactions (fluoro-Phe series).

appended to a suppressor tRNA with the appropriate “stop” anticodon. Normally, the nonsense codon generates a truncated protein that is non-functional and is shuttled into degradation pathways. However, in the presence of the chemically ligated suppressor tRNA, protein synthesis continues normally until the full-length protein is generated. Essentially, the ribosome and the remaining machinery of the cell are “hijacked” to synthesize, fold, and post-translationally modify the desired functional protein with a non-canonical amino acid. *Xenopus laevis* oocytes provide an excellent system for this method due to the extremely large (1 mm in diameter) single cells and the minimal expression of endogenous ion channels. The oocytes are large enough to allow direct injection of the suppressor tRNA/mRNA mixture and contain the cell machinery for proper protein synthesis, folding, assembly, and transport to the membrane (**Figure 1.5**). The physiology of the expressed ion channels is nearly identical to that of those expressed in other cell systems or found in native neuronal environments (35).

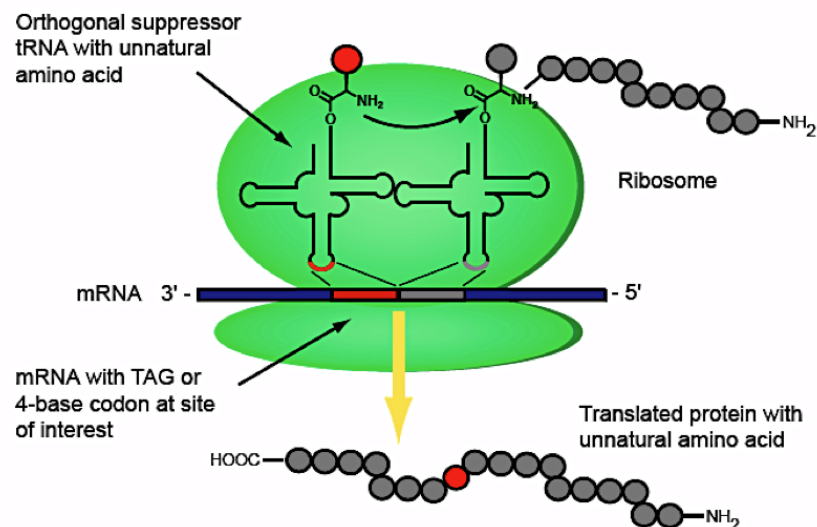


Figure 1.4 Depiction of nonsense suppression methodologies used for site-specific incorporation of non-canonical amino acids.

Since evolution of a tRNA synthetase is not needed in this method, incorporation of new non-canonical amino acids can be immediately swapped to probe a large array of side chains. The downside to the *in vivo* nonsense suppression is the small amount of protein that is actually synthesized. Theoretically, the amount of chemically ligated suppressor tRNA injected translates to the amount of protein synthesized, if efficiency is 100%. Because of reagent limitation and inherent efficiency losses, however, only attomoles of the protein are generated and this is not useful for studying by many of the spectroscopic techniques available. To work around this extremely low yield of protein, we turn to an equally sensitive technique – electrophysiology.

Electrophysiology techniques can be used to indirectly measure receptor-activated currents. Again, the *Xenopus* oocyte provides an ideal system for electrophysiology

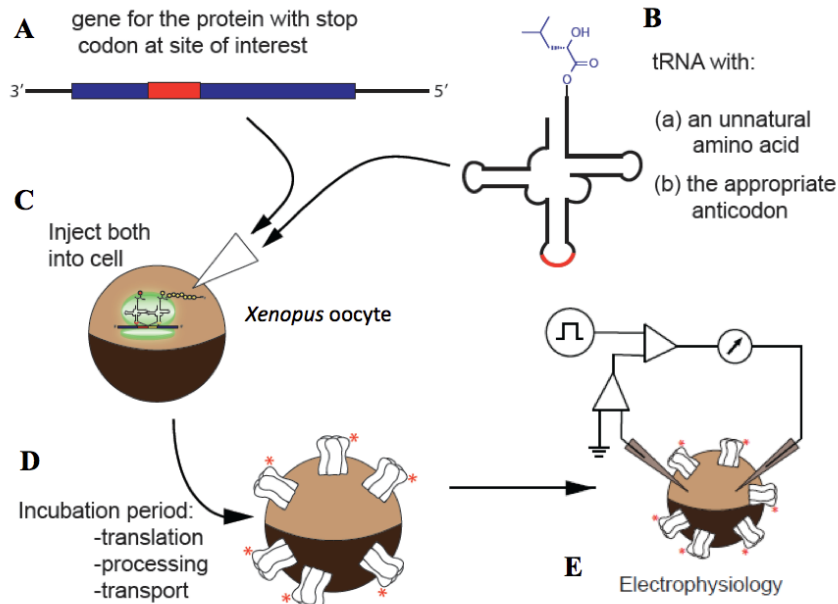


Figure 1.5 Schematic representation of nonsense suppression methodology in *Xenopus* oocytes for non-canonical amino acid incorporation into ion channels. (A) mRNA with incorporated stop codon at site of interest. (B) Chemically appended non-canonical amino acid on orthogonal tRNA with an appropriate anticodon. (C) Physical injection into oocyte cell. (D) Expression of ion channels containing a non-canonical amino acid. (E) Electrophysiology output assay.

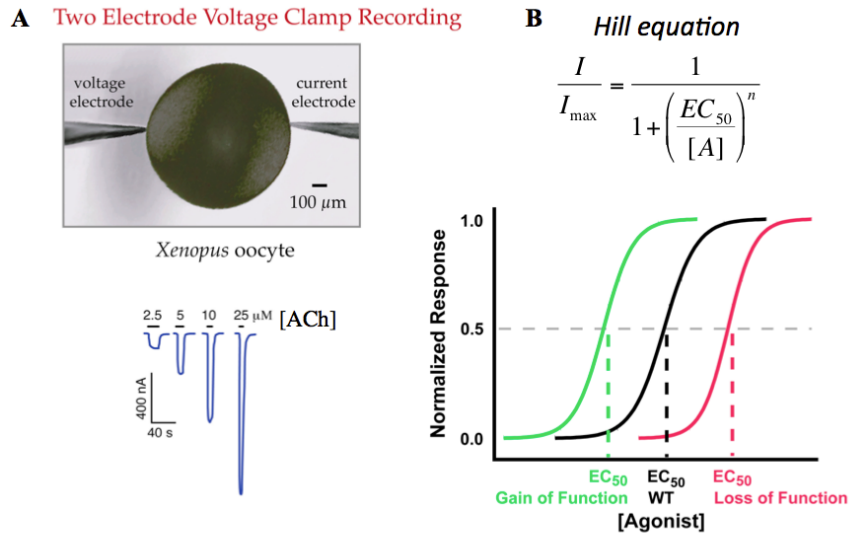


Figure 1.6 The EC_{50} experiment. **(A)** Increasing concentration of an agonist shifts more channels to the open state and creates a larger correction current for the TEVC configuration. **(B)** Responses are normalized to the highest response and plotted against agonist concentration. Fitting the curve to the Hill equation generates a value used for functional comparison of mutated receptors – the EC_{50} . Gain-of-function mutations are depicted as a leftward shift, which decreases the EC_{50} value. Loss-of-function mutations show the opposite trend: a rightward shift represents an increase in EC_{50} value.

studies because its large single cell size allows direct electrode attachments and easy integration into an electrical circuit. The two-electrode voltage clamp (TEVC) method allows measurements of membrane voltage changes induced from the activated receptors (**Figure 1.5 and 1.6**). In this method, the voltage electrode monitors the membrane potential and the current electrode provides current to maintain the desired membrane potential. Upon channel opening, the membrane potential changes and requires additional current to maintain its constant voltage. This injected current is directly related to the sum of the currents passing through all the open ion channels on the cell membrane. The sensitivity of this technique allows current measurements of tens of nA to μA during whole cell recording. Electrophysiology requires only a small amount of protein for signal responses and provides an extremely powerful tool to measure the influences of subtle chemical perturbations on receptor function.

1.4 Electrophysiology Assays: The EC₅₀ and Voltage Jump Experiments

For the purpose of this dissertation, two types of electrophysiology functional assays must be discussed – the EC₅₀ and the voltage jump. The function of the receptor (wild type or mutant) is assayed by applying doses containing increasing concentrations of agonist. For simplicity, receptors are either opened or closed and remain in equilibrium. With addition of agonist, the equilibrium is shifted towards the open state. Thus, higher concentrations of agonist produce a larger population of open receptors and a larger current is measured. At sufficiently high doses, saturation is reached and the response levels off. Measurements are normalized to the max response and plotted in a logarithmic form with agonist concentration. These data are then fit to the Hill equation, which generates an EC₅₀ value and a Hill coefficient (**Figure 1.6**). EC₅₀ is the concentration of agonist needed to elicit half-maximal response from the receptor and the Hill coefficient is a measure of cooperativity. EC₅₀ values are commonly used for functional comparisons: increases in EC₅₀ values correspond to a loss-of-function (more agonist is needed to open the same number of channels) and decreases in EC₅₀ values correspond to a gain-of-function (less agonist is needed to open the same number of channels). The EC₅₀ is a composite measurement of the agonist binding and the channel gating events. Mutations near the agonist binding site are assumed to influence only the binding event, while those close to the pore are thought to mostly influence the gating event; however there are exceptions that are discussed later in this dissertation. For most of the experiments performed here, the EC₅₀ value provides a functional measurement for comparison of the wild type receptor and mutant that is being introduced.

Another electrophysiology test that provides information on receptor properties involves the voltage jump experiment. While the ion channel is open, the negative voltage potential across the membrane drives the flow of cations into the cell. Since we control the membrane potential of the cell, we can vary the voltage by quickly (ms timescale) “jumping” the voltage from large negative potentials to large positive potentials. Switching the membrane potential from negative to positive then drives the flow of ions in the opposite direction – out of the cell. In an idealized pore, plotting voltage vs. current would then provide a linear relationship (**Figure 1.7**). However, not all receptors act as free flowing pores, and they have a unique property of not allowing ions to flow out of the cell, which is termed inward rectification. The degree of inward rectification can vary between receptor types and in some cases can be used to distinguish stoichiometries of specific subtypes (44,45).

1.5 Mutant Cycle Analyses

Proteins are comprised of an array of interactions that work in concert. EC_{50} values are useful in interpreting the influences mutations have on receptor function, but they alone do not identify the strengths associated with these networks of interactions. The mutant cycle analysis provides a quantitative measurement of the energetic coupling of intermolecular and intramolecular interactions occurring in the protein (46). This analysis has been employed in numerous studies of Cys-loop receptors and has provided valuable information about strengths of interactions (47-55). Mutant cycle analyses require three values: a functional output (in this case EC_{50}) of the two single mutations, and the output of the collective double mutant. If the mutations are functionally coupled,

mutating one of the residues will change all or most of the interaction in question and perturbation of the second residue should not cause any additional change in function. Thus, the sum of the functional change of the two individual mutations will be different to the collective double mutation. If the mutations are not functionally coupled and are independent of one another, then the collective double mutant and the sums of the individual residues will be identical. EC_{50} values are used to calculate the coupling coefficient (Ω), which is converted into a free energy value of $\Delta\Delta G$ (**Figure 1.8**) (46). We identify functionally coupled residues or interactions as having values of $\Delta\Delta G$ greater than 0.5 kcal/mol.

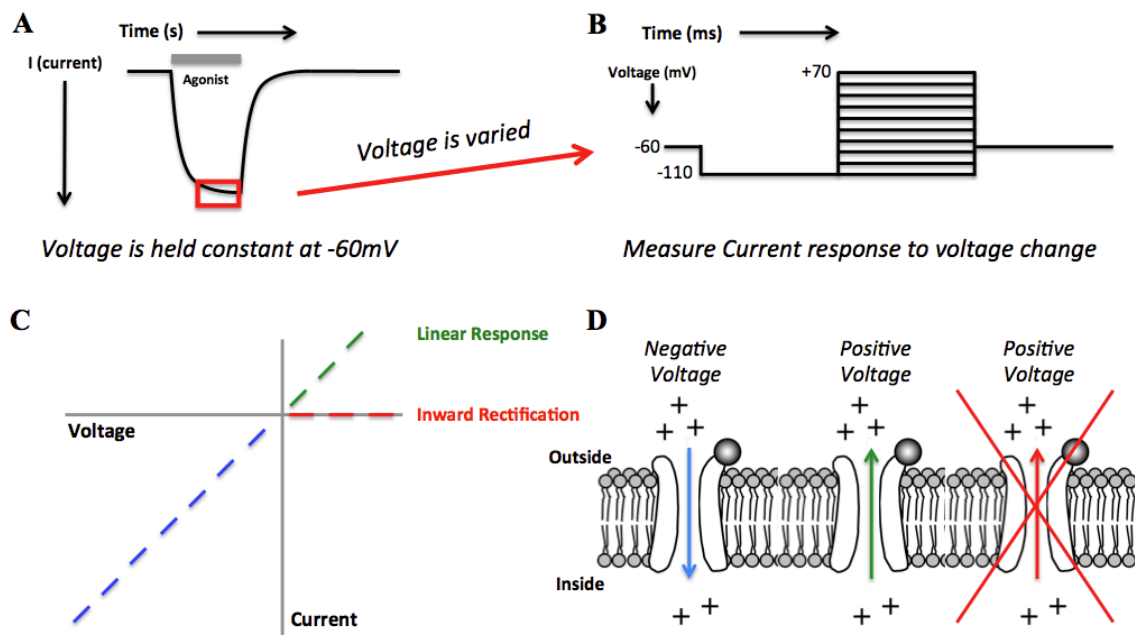


Figure 1.7 The voltage jump experiment. **(A)** An example of a typical timescale and waveform for the EC_{50} experiment. The voltage jump experiment utilizes the activated equilibrium region at the peak of the agonist response. **(B)** Voltage is varied on the millisecond timescale and the current is recorded for each voltage step. **(C)** At negative voltages, the current-voltage relationship responds in linear fashion (blue). At positive voltages, this trend can either continue (green) or be inhibited (red). The phenomenon of current inhibition at positive voltages is called inward rectification. **(D)** A pictorial description of the voltage jump experiment interpretation.

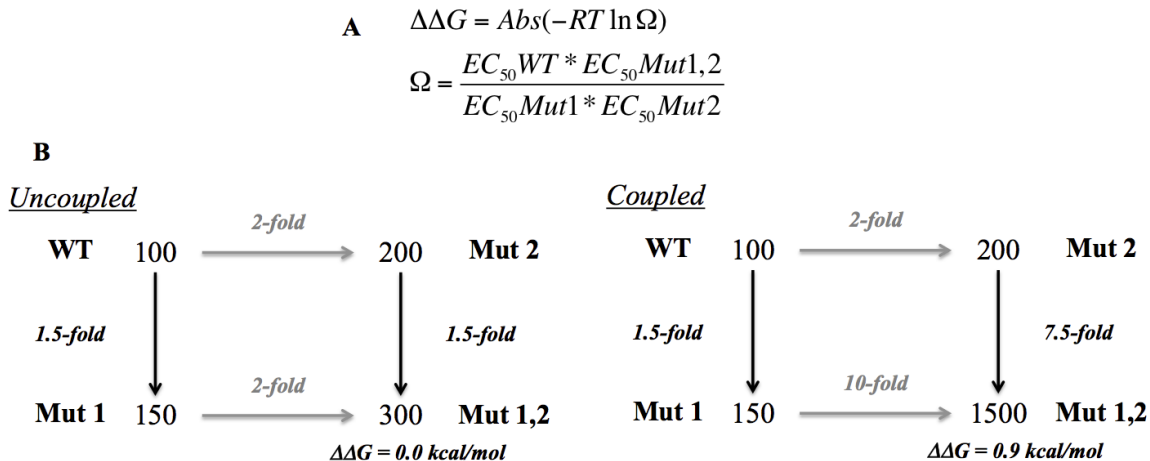


Figure 1.8 The mutant cycle analysis. (A) Equations used to generate coupling coefficients (Ω) and $\Delta\Delta G$ values. (B) Examples of “uncoupled” and “coupled” interactions. R is the ideal gas constant and room temperature (25°C) was used for T.

1.6 Orthosteric vs. Allosteric

Discussions of ion channels so far have revolved around the notion that an agonist binds and then the channel gate opens. The location a ligand can occupy and from which it can cause activation of the protein is termed the orthosteric site. Agonists are a class of ligands that activate the receptor by occupying the orthosteric site, whereas antagonists inhibit receptor function by occupying the same orthosteric site without activation. Research involving the orthosteric site has been crucial in developing agonists and antagonists that are selective and potent for a vast array of targets. However, another class of ligands has been garnering more attention and resources in attempts to develop novel compounds for diseases – allosteric modulators.

Allosteric modulators are ligands that bind at distinct locations away from the orthosteric site in the protein and modulate function without direct activation. The allosteric site can be adjacent to the orthosteric site or tens of angstroms away in the protein. These molecules are analogous to agonists and antagonists in that they can

positively modulate (increase function) or negatively modulate (decrease function) the protein's activity. Allosteric modulator properties are desirable as drug discovery targets because they can have high specificity and activity while minimizing adverse side effects from off-target interactions. Thus, more research has been directed towards the development and understanding of both positive and negative allosteric modulators for disease treatments, including neurological disorders.

1.7 Summary of Dissertation Work

In this dissertation, canonical and non-canonical amino acid mutagenesis was used to study structure-function relationships associated with agonists and allosteric modulators of nAChRs. Group methodology of nonsense suppression in *Xenopus* oocytes, along with electrophysiological assays, was used to assess functional changes associated with receptor mutations. The $\alpha 4\beta 2$ and the $\alpha 4\beta 2\alpha 5$ nAChRs were targeted for agonist selectivity studies. The $\alpha 7$ receptor was used to probe allosteric modulator binding and influence on receptor activation.

Chapter 2 details research investigating the interactions involved in the stoichiometry selective compounds of $\alpha 4\beta 2$ receptors: sazetidine-A, cytisine, and NS9283. Non-canonical amino acid mutagenesis showed that the previously proposed change in hydrogen bonding strengths were not the cause of the selectivity. Instead, the residue composition on the complementary subunit strongly influenced agonist occupation at the binding site. It was concluded that occupation of all primary $\alpha 4$ subunits was needed for full receptor activation and that contemporary binding

models should incorporate the influence of the complementary side for receptor specificity.

Chapter 3 describes the work done towards producing a pure population of the $\alpha 4\beta 2\alpha 5$ receptor and subsequent tests for agonist binding at the $\alpha 5$ - $\alpha 4$ interface. Generation of the $\alpha 4\beta 2\alpha 5$ receptor was aided through the addition of a gain-of-function pore mutation, which also incorporated a handle for identifying assembly through voltage jump experiments. Mutations of the $\alpha 5$ aromatic box residues resulted in no change to receptor function. This suggests agonist occupation at the $\alpha 5$ - $\alpha 4$ interface is not necessary for activation as is seen with the $\alpha 4$ - $\alpha 4$ interface. In addition, this shows that the $\alpha 5$ subunit does not replace $\alpha 4$ or $\beta 2$ subunits and is relegated exclusively to the auxiliary position.

Chapters 4 and 5 are dedicated to studying positive allosteric modulators of $\alpha 7$ receptors. Chapter 4 involves assay development for functional screening of allosteric modulators and adaption of a cooling apparatus for varied temperature control. Chapter 5 revolves around probing the global effects of PNU-120596 on the $\alpha 7$ receptor. It was shown that the higher potency of acetylcholine in the presence of PNU-120596 is not due to an altered agonist binding site. In addition, several residues were identified in the gating interface that are vital to transmitting the effects of PNU-120596. These results suggest a global propagation through several key residues that influence the receptor gating equilibrium while leaving the agonist binding site unperturbed.

Short appendices are included for two additional studies. Appendix 1 involves probing the autosomal dominant nocturnal frontal lobe epilepsy (ADNFLE) mutation located in the $\beta 2$ subunit and its effects on $\alpha 4\beta 2$ and $\alpha 4\beta 2\alpha 5$ nAChRs (in collaboration

with Dr. Weston Nichols of the Lester Group). Appendix 2 comprises a LGIC screen of synthesized physostigmine analogs (in collaboration with Dr. Lindsay Repka of the Reisman Group and Dr. Kristina Daeffler of the Dougherty Group) for agonist or allosteric modulator effects.

1.8 References

1. Corringer, P. J., Novere, N. L., and Changeux, J. P. (2000) Nicotinic Receptors At The Amino Acid Level. *Annual Review of Pharmacology and Toxicology* **40**, 431-458
2. Jensen, A. A., Frolund, B., Lijefors, T., and Krogsgaard-Larsen, P. (2005) Neuronal nicotinic acetylcholine receptors: Structural revelations, target identifications, and therapeutic inspirations. *Journal of Medicinal Chemistry* **48**, 4705-4745
3. Romanelli, M. N., Gratterer, P., Guandalini, L., Martini, E., Bonaccini, C., and Gualtieri, F. (2007) Central nicotinic receptors: structure, function, ligands, and therapeutic potential. *ChemMedChem* **2**, 746-767
4. Gotti, C., Zoli, M., and Clementi, F. (2006) Brain nicotinic acetylcholine receptors: native subtypes and their relevance. *Trends in Pharmacological Sciences* **27**, 482-491
5. Dani, J. A., and Bertrand, D. (2007) Nicotinic acetylcholine receptors and nicotinic cholinergic mechanisms of the central nervous system. *Annual Review of Pharmacology and Toxicology* **47**, 699-729
6. Miwa, J. M., Freedman, R., and Lester, H. A. (2011) Neural systems governed by nicotinic acetylcholine receptors: emerging hypotheses. *Neuron* **70**, 20-33
7. Taly, A., Corringer, P. J., Guedin, D., Lestage, P., and Changeux, J. P. (2009) Nicotinic receptors: allosteric transitions and therapeutic targets in the nervous system. *Nature Reviews. Drug Discovery* **8**, 733-750
8. Albuquerque, E. X., Pereira, E. F., Alkondon, M., and Rogers, S. W. (2009) Mammalian nicotinic acetylcholine receptors: from structure to function. *Physiological Reviews* **89**, 73-120
9. Saccone, N. L., Saccone, S. F., Hinrichs, A. L., Stitzel, J. A., Duan, W., Pergadia, M. L., Agrawal, A., Breslau, N., Grucza, R. A., Hatsukami, D., Johnson, E. O., Madden, P. A. F., Swan, G. E., Wang, J., Goate, A. M., Rice, J. P., and Bierut, L. J. (2009) Multiple Distinct Risk Loci for Nicotinic Dependence Identified by Dense Coverage of the Complete Family of Nicotinic Receptor Subunit (CHRN) Genes. *American Journal of Medical Genetics Neuropsychiatric Genetics*, 453-467
10. Ferini-Strambi, L., Sansoni, V., and Combi, R. (2012) Nocturnal frontal lobe epilepsy and the acetylcholine receptor. *The Neurologist* **18**, 343-349
11. Coe, J. W., Brooks, P. R., Vetelino, M. G., Wirtz, M. C., Arnold, E. P., Huan, J., Sands, S. B., Davis, T. I., Lebel, L. A., Fox, C. B., Shrikhande, A., Heym, J. H., Schaeffer, E., Rollema, H., Lu, Y., Mansbach, R. S., Chambers, L. K., Rovetti, C. C., Schulz, D. W., Tingely III, D., and O'Neil, B. T. (2005) Varenicline: An $\alpha 4\beta 2$ Nicotinic Receptor Partial Agonist for Smoking Cessation. *J Med. Chem.* **48**, 3474-3477
12. Mihalak, K. B., Carroll, F. I., and Luetje, C. W. (2006) Varenicline is a partial agonist at $\alpha 4\beta 2$ and a full agonist at $\alpha 7$ neuronal nicotinic receptors. *Mol Pharmacol* **70**, 801-805
13. Moroni, M., Zwart, R., Sher, E., Cassels, B. K., and Bermudez, I. (2006) $\alpha 4\beta 2$ nicotinic receptors with high and low acetylcholine sensitivity: pharmacology,

- stoichiometry, and sensitivity to long-term exposure to nicotine. *Mol Pharmacol* **70**, 755-768
14. Nelson, M., Kuryatov, A., Choi, C., Zhou, Y., and Lindstrom, J. (2003) Alternate Stoichiometries of the $\alpha 4\beta 2$ Nicotinic Acetylcholine Receptors. *Molecular Pharmacology* **63**, 332-342
 15. Kuryatov, A., Onksen, J., and Lindstrom, J. (2008) Roles of accessory subunits in $\alpha 4\beta 2(*)$ nicotinic receptors. *Molecular Pharmacology* **74**, 132-143
 16. Christopoulos, A. (2002) Allosteric binding sites on cell-surface receptors: novel targets for drug discovery. *Nature Reviews. Drug Discovery* **1**, 198-210
 17. Horenstein, N. A., Leonik, F. M., and Papke, R. L. (2008) Multiple pharmacophores for the selective activation of nicotinic $\alpha 7$ -type acetylcholine receptors. *Mol Pharmacol* **74**, 1496-1511
 18. Narla, S., Klejbor, I., Birkaya, B., Lee, Y. W., Morys, J., Stachowiak, E. K., Terranova, C., Bencherif, M., and Stachowiak, M. K. (2013) $\alpha 7$ nicotinic receptor agonist reactivates neurogenesis in adult brain. *Biochemical Pharmacology* **86**, 1099-1104
 19. Pandya, A. A., and Yakel, J. L. (2013) Effects of neuronal nicotinic acetylcholine receptor allosteric modulators in animal behavior studies. *Biochemical Pharmacology* **86**, 1054-1062
 20. Parri, H. R., Hernandez, C. M., and Dineley, K. T. (2011) Research update: $\alpha 7$ nicotinic acetylcholine receptor mechanisms in Alzheimer's disease. *Biochemical Pharmacology* **82**, 931-942
 21. Tong, M., Arora, K., White, M. M., and Nichols, R. A. (2011) Role of key aromatic residues in the ligand-binding domain of $\alpha 7$ nicotinic receptors in the agonist action of β -amyloid. *The Journal of Biological Chemistry* **286**, 34373-34381
 22. Williams, D. K., Wang, J., and Papke, R. L. (2011) Positive allosteric modulators as an approach to nicotinic acetylcholine receptor-targeted therapeutics: advantages and limitations. *Biochemical Pharmacology* **82**, 915-930
 23. Young, J. W., and Geyer, M. A. (2013) Evaluating the role of the $\alpha 7$ nicotinic acetylcholine receptor in the pathophysiology and treatment of schizophrenia. *Biochemical Pharmacology* **86**, 1122-1132
 24. Brejc, K., van Dijk, W. J., Klaassen, R. V., Schuurmans, M., van der Oost, J., Smit, A. B., and Sixma, T. K. (2001) Crystal structure of an ACh-binding protein reveals the ligand-binding domain of nicotinic receptors. *Nature* **411**, 269-276
 25. Unwin, N. (2005) Refined structure of the nicotinic acetylcholine receptor at 4Å resolution. *J Mol Biol* **346**, 967-989
 26. Miyazawa, A., Fujiyoshi, Y., Stowell, M., and Unwin, N. (1999) Nicotinic Acetylcholine Receptor at 4.6 Å Resolution: Transverse Tunnels in the Channel Wall. *J Mol. Biol.* **288**, 765-786
 27. Bocquet, N., Nury, H., Baaden, M., Le Poupon, C., Changeux, J. P., Delarue, M., and Corringer, P. J. (2009) X-ray structure of a pentameric ligand-gated ion channel in an apparently open conformation. *Nature* **457**, 111-114
 28. Hibbs, R. E., and Gouaux, E. (2011) Principles of activation and permeation in an anion-selective Cys-loop receptor. *Nature* **474**, 54-60

29. Hilf, R. J., and Dutzler, R. (2008) X-ray structure of a prokaryotic pentameric ligand-gated ion channel. *Nature* **452**, 375-379
30. Hilf, R. J., and Dutzler, R. (2009) Structure of a potentially open state of a proton-activated pentameric ligand-gated ion channel. *Nature* **457**, 115-118
31. Nury, H., Van Renterghem, C., Weng, Y., Tran, A., Baaden, M., Dufresne, V., Changeux, J. P., Sonner, J. M., Delarue, M., and Corringer, P. J. (2011) X-ray structures of general anaesthetics bound to a pentameric ligand-gated ion channel. *Nature* **469**, 428-431
32. Hassaine, G., Deluz, C., Grasso, L., Wyss, R., Tol, M. B., Hovius, R., Graff, A., Stahlberg, H., Tomizaki, T., Desmyter, A., Moreau, C., Li, X. D., Poitevin, F., Vogel, H., and Nury, H. (2014) X-ray structure of the mouse serotonin 5-HT₃ receptor. *Nature* **512**, 276-281
33. Miller, P. S., and Aricescu, A. R. (2014) Crystal structure of a human GABA_A receptor. *Nature* **512**, 270-275
34. Dougherty, D. A. (2008) Cys-Loop Neuroreceptors: Structure to the Rescue? *Chemical Reviews* **108**, 1642-1654
35. Dougherty, D. A. (2008) Physical Organic Chemistry on the Brain. *Journal of Organic Chemistry* **73**, 3667-3674
36. Lemoine, D., Jiang, R., Taly, A., Chataigneau, T., Specht, A., and Grutter, T. (2012) Ligand-gated ion channels: new insights into neurological disorders and ligand recognition. *Chem Rev* **112**, 6285-6318
37. Pless, S. A., and Ahern, C. A. (2013) Unnatural amino acids as probes of ligand-receptor interactions and their conformational consequences. *Annual Review of Pharmacology and Toxicology* **53**, 211-229
38. Dougherty, D. A., and Van Arnem, E. B. (2014) In vivo incorporation of non-canonical amino acids by using the chemical aminoacylation strategy: a broadly applicable mechanistic tool. *Chembiochem : a European Journal of Chemical Biology* **15**, 1710-1720
39. Nowak, M., Gallivan, J. P., Silverman, S., Labarca, C. G., Dougherty, D. A., and Lester, H. A. (1998) In Vivo Incorporation of Unnatural Amino Acids into Ion Channels in Xenopus Oocyte Expression System. *Methods Enzymol* **293**, 504-530
40. Rodriguez, E. A., Lester, H. A., and Dougherty, D. A. (2007) Improved amber and opal suppressor tRNAs for incorporation of unnatural amino acids in vivo. Part 2: evaluating suppression efficiency. *RNA* **13**, 1715-1722
41. Rodriguez, E. A., Lester, H. A., and Dougherty, D. A. (2007) Improved amber and opal suppressor tRNAs for incorporation of unnatural amino acids in vivo. Part 1: minimizing misacylation. *RNA* **13**, 1703-1714
42. Rodriguez, E. A., Lester, H. A., and Dougherty, D. A. (2006) In vivo incorporation of multiple unnatural amino acids through nonsense and frameshift suppression. *Proceedings of the National Academy of Sciences of the United States of America* **103**, 8650-8655
43. Nowak, M., Kearney, P. C., Sampson, J. R., Saks, M. E., Labarca, C. G., Silverman, S., Zhong, W., Thorson, J., Abelson, J. N., Davidson, N., Schultz, P. G., Dougherty, D. A., and Lester, H. A. (1995) Nicotinic Receptor Binding Site Probed with Unnatural Amino Acid Incorporation in Intact Cells. *Science* **268**, 439-442

44. Marotta, C. B., Dilworth, C. N., Lester, H. A., and Dougherty, D. A. (2013) Probing the non-canonical interface for agonist interaction with an $\alpha 5$ containing nicotinic acetylcholine receptor. *Neuropharmacology* **77C**, 342-349
45. Xiu, X., Puskar, N. L., Shanata, J. A., Lester, H. A., and Dougherty, D. A. (2009) Nicotine binding to brain receptors requires a strong cation- π interaction. *Nature* **458**, 534-537
46. Horovitz, A. (1996) Double-mutant cycles: a powerful tool for analyzing protein structure and function. *Folding and Design* **1**, R121-R126
47. Blum, A. P., Gleitsman, K. R., Lester, H. A., and Dougherty, D. A. (2011) Evidence for an extended hydrogen bond network in the binding site of the nicotinic receptor: role of the vicinal disulfide of the $\alpha 1$ subunit. *The Journal of Biological Chemistry* **286**, 32251-32258
48. Blum, A. P., Lester, H. A., and Dougherty, D. A. (2010) Nicotinic pharmacophore: the pyridine N of nicotine and carbonyl of acetylcholine hydrogen bond across a subunit interface to a backbone NH. *Proceedings of the National Academy of Sciences of the United States of America* **107**, 13206-13211
49. Gleitsman, K. R., Kedrowski, S. M., Lester, H. A., and Dougherty, D. A. (2008) An intersubunit hydrogen bond in the nicotinic acetylcholine receptor that contributes to channel gating. *The Journal of Biological Chemistry* **283**, 35638-35643
50. Gleitsman, K. R., Shanata, J. A., Frazier, S. J., Lester, H. A., and Dougherty, D. A. (2009) Long-range coupling in an allosteric receptor revealed by mutant cycle analysis. *Biophysical Journal* **96**, 3168-3178
51. Kash, T. L., Jenkins, A., Kelly, J. C., Trudell, J. R., and Harrison, N. L. (2003) Coupling of agonist binding to channel gating in the GABAA receptor. *Nature* **421**, 272-275
52. Price, K. L., Millen, K. S., and Lummis, S. C. (2007) Transducing agonist binding to channel gating involves different interactions in 5-HT3 and GABAC receptors. *The Journal of Biological Chemistry* **282**, 25623-25630
53. Venkatachalan, S. P., and Czajkowski, C. (2008) A conserved salt bridge critical for GABA(A) receptor function and loop C dynamics. *Proceedings of the National Academy of Sciences of the United States of America* **105**, 13604-13609
54. Daeffler, K. N., Lester, H. A., and Dougherty, D. A. (2012) Functionally important aromatic-aromatic and sulfur- π interactions in the D2 dopamine receptor. *Journal of the American Chemical Society* **134**, 14890-14896
55. Miles, T. F., Bower, K. S., Lester, H. A., and Dougherty, D. A. (2012) A coupled array of noncovalent interactions impacts the function of the 5-HT3A serotonin receptor in an agonist-specific way. *ACS Chemical Neuroscience* **3**, 753-760

Chapter 2

*Selective Ligand Behaviors Provide New Insights into Agonist Activation of Nicotinic Acetylcholine Receptors**

**Reproduced with permission from: (DOI: 10.1021/cb400937d) Christopher B. Marotta, Iva Rreza, Henry A. Lester, and Dennis A. Dougherty. Selective ligand behaviors provide new insights into agonist activation of nicotinic acetylcholine receptors. ACS Chem. Biol., 2014, 9 (5), pp 1153-1159. Copyright 2014 American Chemical Society. The work described in this chapter was done in collaboration with Iva Rreza.*

Link to article: 10.1021/cb400937d

2.1 Abstract

Nicotinic acetylcholine receptors are a diverse set of ion channels that are essential to everyday brain function. Contemporary research studies selective activation of individual subtypes of receptors, with the hope of increasing our understanding of behavioral responses and neurodegenerative diseases. Here, we aim to expand current binding models to help explain the specificity seen among three activators of $\alpha 4\beta 2$ receptors: sazetidine-A, cytisine, and NS9283. Through mutational analysis, we can interchange the activation profiles of the stoichiometry-selective compounds sazetidine-A and cytisine. In addition, mutations render NS9283 – currently identified as a positive allosteric modulator – into an agonist. These results lead to two conclusions: (1) occupation at each primary face of an α subunit is needed to activate the channel and (2) the complementary face of the adjacent subunit dictates the binding ability of the agonist.

2.2 Introduction

Nicotinic acetylcholine receptors (nAChRs) are a diverse family of the larger Cys-loop superfamily of ligand gated ion channels (LGICs). These channels are found throughout the brain and CNS and play vital roles in the chemical and electrical communication between neurons, contributing to memory, learning, and other neural functions (1-3). Because of their diverse properties and widespread distribution throughout the brain, these LGICs are prominent targets in neurological disorders, such as drug addiction, Alzheimer's disease, and Parkinson's disease (4,5).

Neuronal nAChRs have been extensively studied, and much is known about their assembly and structure (2,6-8). There are two classes of subunits, identified as $\alpha 2 - \alpha 9$ and $\beta 2 - \beta 4$, which assemble into homomeric (α only) or heteromeric (α and β) channels consisting of five subunits in total (9). For each subunit, there is a main agonist binding pocket, denoted as the primary (+) face, which includes four of the five residues that make up the canonical "aromatic box" (10). The fifth aromatic box residue and other key binding residues, including backbone contacts, are found on the complementary (–) face of the adjacent subunit (10). The five subunits then arrange in an alternating + and – fashion to form a functional receptor (**Figure 2.1**). For decades it has been assumed that the (+) face of the agonist binding site is provided by α subunits and the (–) face by β subunits. However, recent evidence establishes the ability of α subunits to also contribute to the (–) face.

The core pharmacophore of a cationic nitrogen and a hydrogen bond acceptor for agonists of the nAChR was first introduced in 1970 (11). Since then, the binding model has evolved to consist of three specific interactions that include a cation- π interaction on

the primary subunit, along with hydrogen bonding interactions on both the primary and complementary subunits (12,13). Based on this model, a number of studies have aimed to explain the efficacies and selectivities of agonists to different nAChRs of varying subunits and stoichiometries (12-14).

Here, we studied the activation profiles of $\alpha 4\beta 2$ receptors and their responses to mutations for the following compounds: sazetidine-A, cytisine, and NS9283 (**Figure 2.1**). Our conclusions lead us to propose an expansion of the published structural models (10,12,15,16). We establish that: (1) the selectivity of drug binding at subunit interfaces is largely controlled by a pocket on the complementary subunit that is

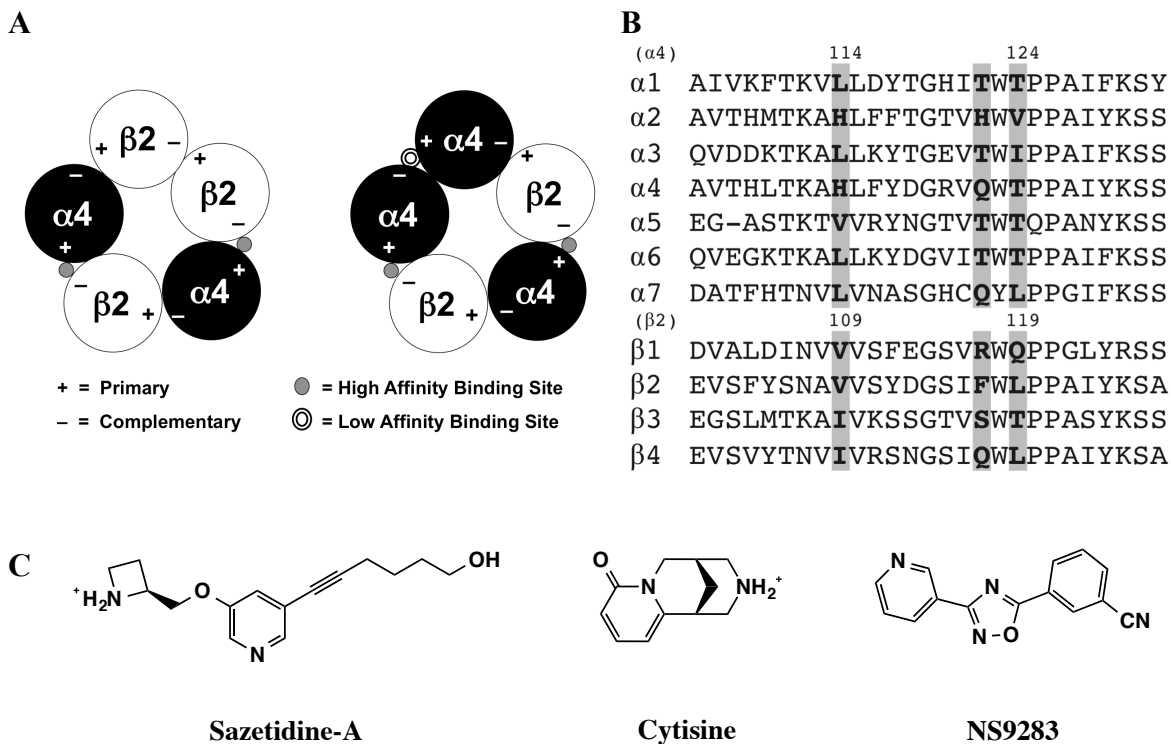


Figure 2.1 (A) View from the extracellular side of the high affinity (A2B3) and low affinity (A3B2) $\alpha 4\beta 2$ receptors. Agonist binding locations are indicated by smaller circles at the interfaces of $\alpha 4$ - $\beta 2$ subunits and $\alpha 4$ - $\alpha 4$ subunits. (B) Sequence alignment of the rat muscle and neuronal nAChR subunits. The three residues that greatly influence agonist affinity are highlighted in gray. (C) Structures of sazetidine-A, cytisine, and NS9283.

hydrophobic in some subunits and hydrophilic in others and (2) an agonist must be bound at all α subunits in a given receptor to favor the activated channel. This expansion aids in our understanding of subunit- and stoichiometry-selective agents and can provide valuable insight for further development and application towards therapeutic strategies.







2.3 Results and Discussion

2.3.1 Hydrogen Bonding: Non-Canonical Amino Acid Analysis

Sazetidine-A has a unique activation profile, in that it selectively activates the $(\alpha 4)_2(\beta 2)_3$ stoichiometry over the $(\alpha 4)_3(\beta 2)_2$; these stoichiometries will be abbreviated A2B3 and A3B2, respectively (17). Unnatural amino acids are useful tools used to parse out specific chemical interactions between ligand and receptor. Previous structure-function studies of cytosine, an agonist that has the opposite activation profile for $\alpha 4\beta 2$ receptors, showed that the active drug-receptor combination (A3B2) favored the hydrogen bond to the TrpB backbone CO (“donor”), while the inactive form favored the hydrogen bond to the backbone NH on the complementary face (“acceptor”) (**Table 2.1, Figure 2.2**) (12). We proposed that this difference could explain the stoichiometric selectivity of the drug. Through unnatural amino acid incorporation, we were able to characterize the cation- π binding, hydrogen-bond donating, and hydrogen-bond accepting properties of sazetidine-A and compare the results to those previously measured for cytosine. We now find, however, that the opposite hydrogen bonding pattern is not seen for sazetidine-A and that the pattern roughly follows the one observed for cytosine: a larger affect for the hydrogen-bonding acceptor in the A2B3 stoichiometry and a larger affect for the hydrogen-bonding donor in the A3B2 stoichiometry (**Table 2.1,**

Figure 2.2). This pattern suggests an alternative explanation is needed to identify the properties of stoichiometry selective agonists.

Table 2.1 Agonist Binding Model Comparison

Stoichiometry	Compound	Wild Type EC ₅₀ (μM) ^a	Relative Efficacy (%) ^b	TrpB Cation-π ^c	H-Bond Donor ^d	H-Bond Acceptor ^e
	Acetylcholine ^f	4.0	[100]	69	1.1	6.8
	Cytisine ^f	0.066	0	31	8.8	62
	Sazetidine-A	0.0046	80	22	5.7	10
	Acetylcholine ^f	87	[100]	540	1.1	8.5
	Cytisine ^f	15	7	30	27	14
	Sazetidine-A	0.14	0	58	11	5.0

^a See methods for wild type EC₅₀ corrections. ^b Ratio of *I*_{max} of compound divided by *I*_{max} of acetylcholine.

^c Ratio of EC₅₀ values for 4,5,6,7-tetrafluoro-Trp and Trp incorporation at α4 W154 (Fig. 2A). ^d Ratio of EC₅₀ values for Thr-α-hydroxy and Thr incorporation at α4 T155 (Fig. 2A). ^e Ratio of EC₅₀ values for Leu α-hydroxy and Leu incorporation at β2 L119 (Fig. 2A). ^f Previously reported values from Tavares et al. (12). Measured EC₅₀ values reported in Table 2.2.

2.3.2 Sazetidine-A and the β2 Complementary Face

It has been shown that the unique hydrophobic appendage off of the pyridine ring of sazetidine-A gives the compound its subunit and receptor selectivity, and that the alcohol group at the end of the appendage does not play a significant role (15,18,19). Because this aliphatic adjunct interacts mostly with the complementary side, we began by focusing on the known differences between α4 and β2 subunits in this region (16). Previous investigations identified an α4-α4 binding site and suggested the differences between the “high” affinity (α4-β2) and “low” affinity (α4-α4) binding pockets are due to three key residues that reside on the complementary face (20-22). The β2(–) face residues (V109, F117, and L119) generate a hydrophobic pocket for the high affinity case, while the aligning α4(–) face residues (H114, Q122, and T124) create a hydrophilic, low affinity pocket (**Figure 2.1, Figure 2.2**). We have evaluated the triple mutant of the α4(–) face by swapping these three residues (H114V, Q122F, and T124L)

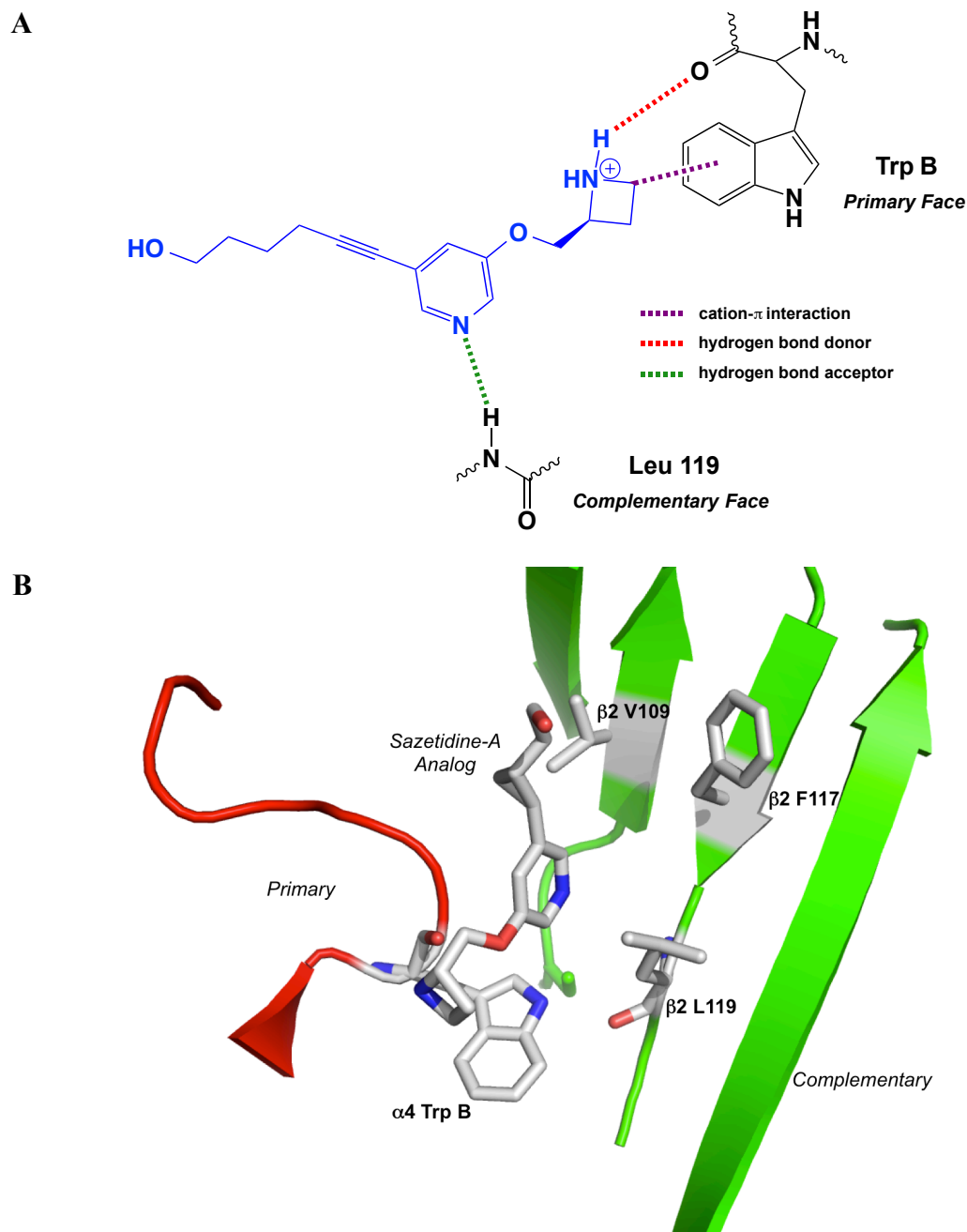


Figure 2.2 Binding models of sazetidine-A and analogs. **(A)** Binding model for sazetidine-A based on established interactions seen with nicotine (12). The cation- π interaction is in purple, the hydrogen bond donor is in red, and the hydrogen bond acceptor is in green. **(B)** Crystal structure showing a sazetidine-A analog bound to Ct-AChBP (PDB: 4B5D) (15). The three key residues identified for the hydrophobic pocket associated with the β 2 subunit (V109, F117, & L119) are shown, as is the TrpB residue from the α 4 subunit. These residues were mutated into the crystal structure to show general spatial locations (no residue minimizations calculated).

Table 2.2

Mutation	$(\alpha 4 \text{ L9'A})_2(\beta 2)_3$			$(\alpha 4 \text{ L9'A})_3(\beta 2)_2$			Fold Shift			Fold Shift			I_{\max} (μA)
	EC_{50} (nM)	Hill	n	EC_{50} (nM)	Hill	n	EC_{50} (nM)	Hill	n	EC_{50} (nM)	Hill	n	I_{\max} (μA)
WT	1.1 ± 0.04	2.3 ± 0.2	21	–	–	–	$3.3 - 35$	1.8 ± 0.8	21	0.32 ± 0.09	1.8 ± 0.8	21	$0.95 - 13$
$\beta 2\text{Leu119}$	0.80 ± 0.04	1.9 ± 0.2	11	0.7	–	–	$4.3 - 30$	1.9 ± 0.4	9	0.20 ± 0.03	1.9 ± 0.4	9	$0.45 - 12$
Lah	8.5 ± 0.2	1.4 ± 0.04	14	10	1.4 ± 0.04	14	$0.49 - 22$	1.8 ± 0.1	12	0.99 ± 0.03	1.8 ± 0.1	12	$0.24 - 55$
$\alpha 4\text{Thr155}$	0.65 ± 0.07	1.7 ± 0.3	13	0.6	1.7 ± 0.3	13	$1.9 - 6.4$	2.4 ± 0.4	14	0.16 ± 0.02	2.4 ± 0.4	14	$0.79 - 5.8$
Tah	3.7 ± 0.2	1.6 ± 0.1	12	5.7	1.6 ± 0.1	12	$0.52 - 8.6$	1.4 ± 0.1	14	1.8 ± 0.1	1.4 ± 0.1	14	$0.43 - 12$
$\alpha 4\text{Trp154}$	0.46 ± 0.03	1.8 ± 0.2	16	0.42	1.8 ± 0.2	16	$0.25 - 2.4$	1.7 ± 0.2	8	0.19 ± 0.02	1.7 ± 0.2	8	$0.47 - 11$
Trp-F1	0.78 ± 0.06	1.6 ± 0.2	18	1.7	1.6 ± 0.2	18	$0.089 - 0.93$	1.7 ± 0.2	8	0.38 ± 0.03	1.7 ± 0.2	8	$1.1 - 8.1$
Trp-Br	0.87 ± 0.06	1.8 ± 0.2	14	1.9	1.8 ± 0.2	14	$0.25 - 1.8$	–	–	–	–	–	–
Trp-F2	1.4 ± 0.1	1.4 ± 0.1	20	3.1	1.4 ± 0.1	20	$0.049 - 0.74$	1.9 ± 0.2	8	0.70 ± 0.04	1.9 ± 0.2	8	$11 - 34$
Trp-CN	2.2 ± 0.1	1.7 ± 0.1	4	4.8	1.7 ± 0.1	4	$0.21 - 0.40$	–	–	–	–	–	–
Trp-F3	3.5 ± 0.3	1.2 ± 0.1	11	7.6	1.2 ± 0.1	11	$0.27 - 1.3$	1.1 ± 0.1	8	4.6 ± 0.4	1.1 ± 0.1	8	$0.30 - 1.1$
Trp-F4	10.0 ± 0.7	1.1 ± 0.06	12	22	1.1 ± 0.06	12	$0.042 - 1.2$	0.89 ± 0.05	7	11 ± 1	0.89 ± 0.05	7	$0.66 - 3.0$

Agonist = Sazetidine-A. WT = wild type. Leu, Thr, Trp = wild type recovery control (nonsense suppression method with the wild type amino acid).

Lah = leucine- α -hydroxy. Tah = threonine- α -hydroxy. Trp-F1 = 5-flouro-tryptophan. Trp-Br = 5-bromo-tryptophan. Trp-F2 = 5,7-diflouro-tryptophan. Trp-CN = 5-cyano-tryptophan. Trp-F3 = 5,6,7-triflouro-tryptophan. Trp-F4 = 4,5,6,7-tetraflouro-tryptophan.

to make them resemble the $\beta 2(-)$ face. We were able to generate receptor responses and measure an EC_{50} curve for sazetidine-A in the A3B2 receptor, which was not possible with the wild type $\alpha 4$ subunit (**Table 2.3, Figure 2.3**). The EC_{50} value for the triple mutant was about five-fold larger than the wild type A2B3 response, a small difference compared to having zero response in the wild type A3B2 receptor. Single mutations at the $\alpha 4$ subunit did not give rise to sazetidine-A response at low μM doses (**Table 2.4**). Combinations of double mutations saw some response towards low μM doses of sazetidine-A (**Table 2.4**). Mutations to make the β subunit more like the α subunit resulted in a large loss of function for sazetidine-A (**Table 2.5**).

Table 2.3 Sazetidine-A EC_{50} (nM) Values

Receptor	EC_{50} (nM)	Hill	n	I_{max} (μA)
$(\alpha 4)_2(\beta 2)_3$	1.9 ± 0.1	2.0 ± 0.2	14	$0.059 - 0.26$
$(\alpha 4)_3(\beta 2)_2$	NR	—	—	—
$(\alpha 4)_2(\beta 2)_3 + 10 \mu M$ NS9283	2.0 ± 0.2	1.7 ± 0.2	13	$0.067 - 1.6$
$(\alpha 4)_3(\beta 2)_2 + 10 \mu M$ NS9283	1.1 ± 0.1	2.0 ± 0.2	14	$0.4 - 7.2$
$(\alpha 4 \text{ H114V, Q122F, T124L})_2(\beta 2)_3$	4.8 ± 0.3	1.8 ± 0.2	13	$0.18 - 1.3$
$(\alpha 4 \text{ H114V, Q122F, T124L})_3(\beta 2)_2$	9 ± 1	2.3 ± 0.6	14	$0.71 - 6.2$

Agonist = Sazetidine-A

NR = No Response

2.3.3 Cytisine and the $\beta 2$ Complementary Face

Since these three residues had a large affect on receptor agonist selectivity and activation for sazetidine-A, we considered cytosine in an attempt to explain its selectivity for A3B2 over A2B3 receptors. Early chimera analysis showed that cytosine selectivity for human $\beta 4$ over $\beta 2$ subunits is strongly influenced by the extracellular region (23), and more recent analyses provide further details (24). Sequence alignment shows that of the three residues considered here, the only difference lies in the 117 position – $\beta 2$ F117 and

$\beta 4$ L117 for the human subunits. For the rodent subunits considered here, $\beta 4$ is Q117, which is identical to the $\alpha 4$ residue at this same position (**Figure 2.1**). In the rodent wild type $\alpha 4\beta 2$ receptors, cytosine is a partial agonist with a biphasic response for the A3B2 receptor. No response is observed for the A2B3 receptor (**Table 2.6**), although signal can be obtained in receptors with hypersensitive mutations (see **2.5 Methods**). However, with the single mutation of F117Q in the $\beta 2$ subunit, cytosine generated a sizable response for the A2B3 receptor. The mutation also raised the efficacy of the A3B2 receptor compared to the wild type response (**Table 2.6**).

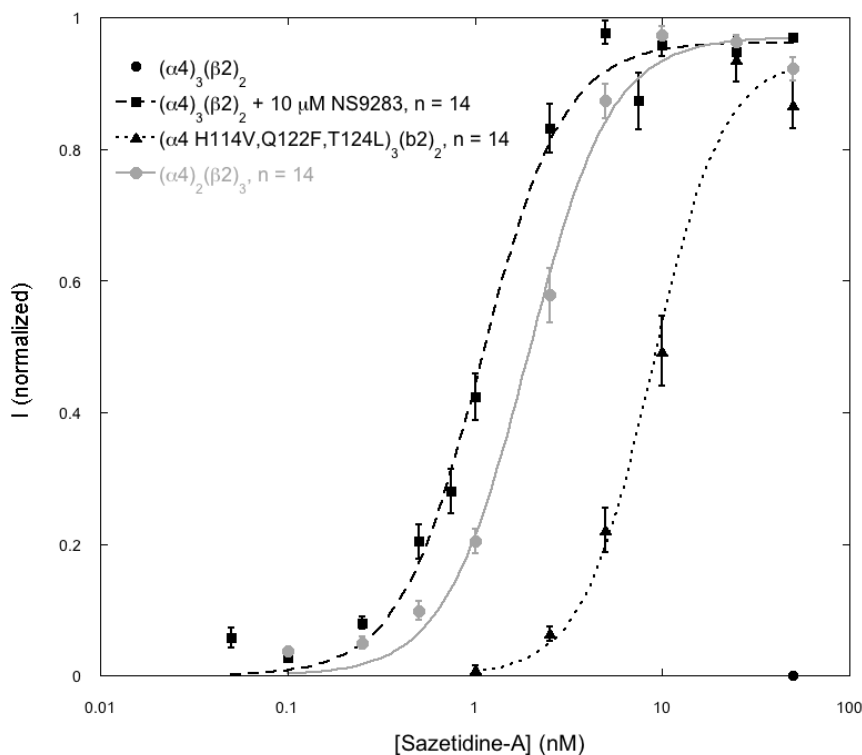


Figure 2.3 Sazetidine-A EC₅₀ curves. $(\alpha 4)_3(\beta 2)_2$ cannot be activated by sazetidine-A. Responses can be obtained by mutating the complementary side of the $\alpha 4$ subunit to resemble the $\beta 2$ subunit as seen with $(\alpha 4 \text{ H114V, Q122F, T124L})_3(\beta 2)_2$ receptor. Also shown is wild type $(\alpha 4)_3(\beta 2)_2$ receptor exposed to a combination of sazetidine-A and NS9283.

Table 2.4

Acetylcholine					Sazetidine-A						
Receptor	EC ₅₀ (μM) [1]	Hill [1]	EC ₅₀ (μM) [2]	Hill [2]	% [1]	n	I _{max} (μA)	EC ₅₀ (nM)	Hill	n	I _{max} (μA)
(α4) ₂ (β2) ₃	0.78 ± 0.02	1.1 ± 0.02	–	–	–	16	0.15–2.4	1.9 ± 0.1	2.0 ± 0.2	14	0.059–0.26
(α4) ₃ (β2) ₂	2.7 ± 9	0.69 ± 0.54	100 ± 11	1.6 ± 0.3	17	8	9.8–27	NR			
(α4 H114V) ₃ (β2) ₂	44 ± 80	1.1 ± 0.5	240 ± 50	2.6 ± 2	47	11	0.29–12	NR			
(α4 Q122F) ₃ (β2) ₂	2.1 ± 3	0.64 ± 0.3	190 ± 20	1.8 ± 0.3	23	15	0.31–12	NR			
(α4 T124L) ₃ (β2) ₂	4.8 ± 14	0.92 ± 0.5	33 ± 9	1.8 ± 0.8	37	7	1.0–4.8	NR			
(α4 H114V, Q122F) ₃ (β2) ₂	34 ± 60	1.0 ± 0.6	260 ± 40	4.0 ± 5	51	19	0.59–15	>2000	0.90 ± 0.1	17	1.1–13
(α4 H114V, T124L) ₃ (β2) ₂	11 ± 20	1.1 ± 0.4	66 ± 22	2.0 ± 1	46	17	0.52–11	>2000	0.94 ± 0.1	16	0.072–2.8
(α4 Q122F, T124L) ₃ (β2) ₂	0.74 ± 0.1	0.96 ± 0.1	–	–	–	10	0.067–0.22	NR			
(α4 H114V, Q122F, T124L) ₃ (β2) ₂	2.7 ± 0.2	0.81 ± 0.03	–	–	–	16	0.89–18	9 ± 1	2.3 ± 0.6	14	0.71–6.2

NR = No Response

Table 2.5 (α4 L9'A)₂(β2)₃

Mutation	Acetylcholine				Sazetidine-A					
	EC ₅₀ (μM)	Hill	n	Fold Shift	I _{max} (μA)	EC ₅₀ (nM)	Hill	n	Fold Shift	I _{max} (μA)
WT	0.34 ± 0.01	1.2 ± 0.02	15	–	0.88 – 15	0.66 ± 0.04	2.1 ± 0.2	14	–	0.69 – 8.1
β2 V109H	1.3 ± 0.03	1.3 ± 0.03	15	3.8	1.5 – 13	7.7 ± 0.4	1.4 ± 0.1	12	12	1.2 – 5.2
β2 F117Q	1.1 ± 0.01	1.2 ± 0.01	14	3.2	0.53 – 10.	510 ± 30	1.4 ± 0.1	12	770	0.74 – 5.8
β2 L119T	20 ± 0.7	1.3 ± 0.05	14	59	1.7 – 12	180 ± 6	1.2 ± 0.04	14	270	0.87 – 12

WT = wild type

2.3.4 NS9283 and the $\alpha 4$ Complementary Face

We next considered NS9283, which has a binding preference for the $\alpha 4$ - $\alpha 4$ interface (25). This compound has been previously characterized as a benzodiazepine-like positive allosteric modulator (PAM) for only the A3B2 stoichiometry of receptors containing either $\alpha 2$ or $\alpha 4$ subunits (25,26). In addition, its effects are lost when the $\alpha 4(-)$ face is mutated to resemble the $\beta 2(-)$ face in the region of the classical agonist binding site (27). Since we have molecules that selectively associate with $\alpha 4$ - $\alpha 4$ (NS9283) and $\alpha 4$ - $\beta 2$ (sazetidine-A) interfaces, co-application should generate an A3B2 receptor response. As shown in **Figures 2.3, 2.4 and Table 2.3**, we find that individual applications of NS9283 and sazetidine-A show essentially no activation of wild type A3B2 receptors. However, co-application generates full activation of the receptor, compared to acetylcholine. The A3B2 $\alpha 4$ triple mutant (H114V, Q122F, T124L) was then exposed to similar conditions. The sazetidine-A response for the mutant was preserved, but the effect of NS9283 was completely lost (**Table 2.3, Figure 2.4**). The mutations eliminate the ability of NS9283 to bind at the $\alpha 4$ - $\alpha 4$ interface and allow sazetidine-A to replace it in binding. These data suggest that occupation of an agonist at each α subunit is necessary for a receptor response. We generated the A3B2 $\beta 2$ triple mutant (V109H, F117Q, L119T) to test if NS9283 could alone activate the channel. A response was seen in a dose dependent manner, suggesting the drug is a partial agonist, albeit, not potent or highly efficacious (**Figure 2.4**). Because NS9283 is sparingly soluble, a full EC₅₀ curve could not be obtained. Nevertheless, we were able to transform a compound once designated as a PAM into an agonist, suggesting it could be binding to the canonical aromatic binding site. Also, due to its low potency and lower receptor

expression, the corresponding A2B3 $\beta 2$ triple mutant (V109H, F117Q, L119T) was inconclusive with regard to activation via NS9283.

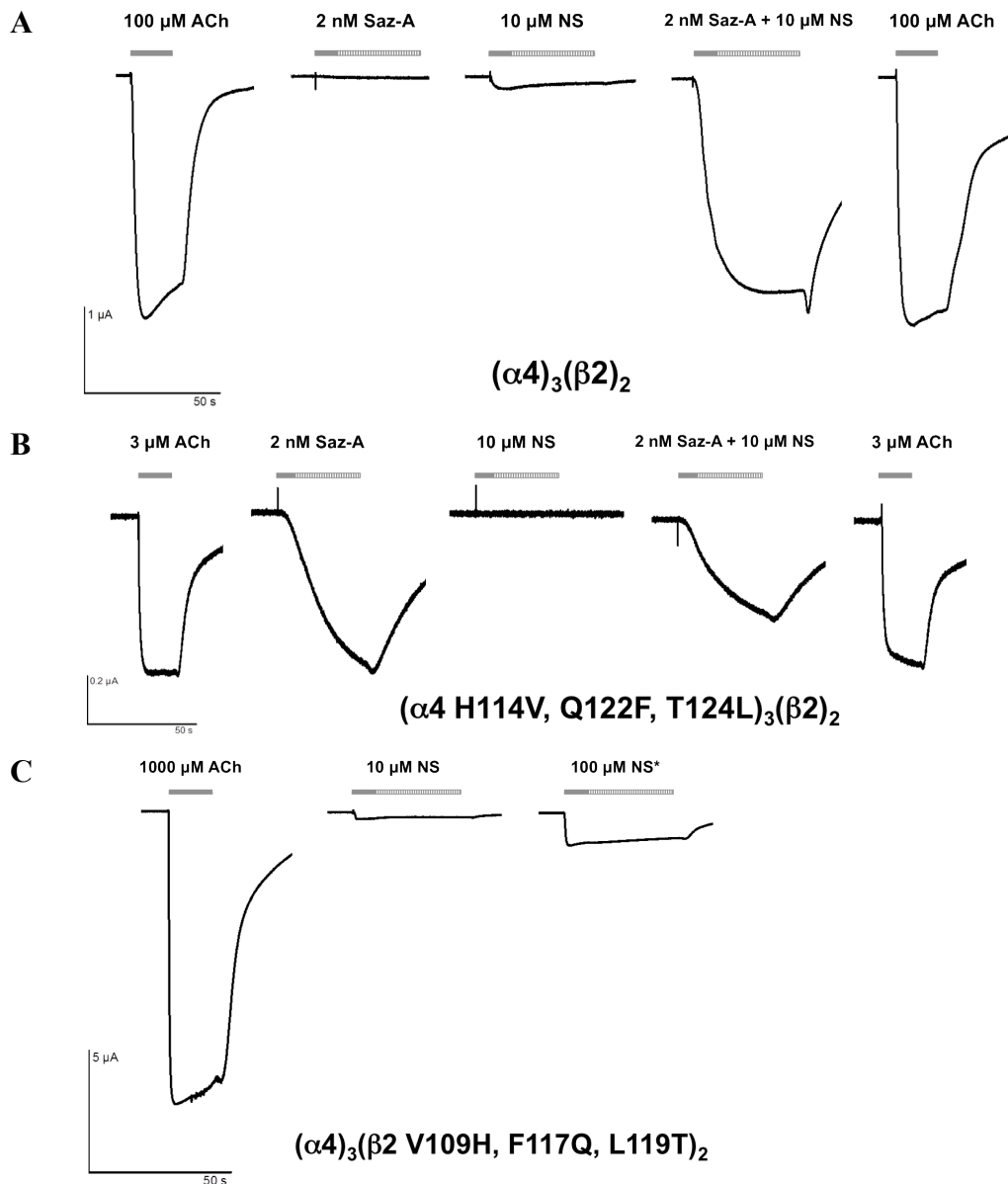


Figure 2.4 Sample traces of responses to acetylcholine (ACh), sazetidine-A (Saz-A), and NS9283 (NS) to A3B2 receptors. Solid gray bars indicate drug application and dashed bars indicate a pause where drug remains present but the buffer wash has not started. Gaps between traces indicate buffer washes (see methods for duration of drug application and buffer washes). (A) Activation of wild type receptor by ACh at its EC_{50} value, and Saz-A and NS at the concentrations shown. (B) Activation of $(\alpha 4 \text{ H114V, Q122F, T124L})_3(\beta 2)_2$. (C) Application of I_{max} concentrations of acetylcholine and two concentrations of NS to $(\alpha 4)_3(\beta 2 \text{ V109H, F117Q, L119T})_2$. The * indicates a 1% by volume DMSO drug solution

2.4 Conclusions

The present work confirms and expands upon recent studies on the (–), complementary face of the agonist binding site of nAChRs. In particular, the long-held belief that agonist binding sites are formed only at $\alpha(+)/\beta(-)$ interfaces has been challenged by increasing evidence for a viable agonist binding site at $\alpha(+)/\alpha(-)$ interfaces. Here we use several drugs that show some subtype specificity to probe this issue. The novel agonist sazetidine-A can only activate $\alpha 4\beta 2$ receptors with an A2B3 stoichiometry. In the alternative A3B2 stoichiometry, an $\alpha(+)/\alpha(-)$ interface exists. The (–) face of such an interface is relatively polar, and evidently it is incompatible with the hydrophobic side chain of sazetidine-A that is expected to project into this region (recall that the OH group of sazetidine-A is not necessary for function). By mutating three residues in this region to be more hydrophobic and thus more like a $\beta 2(-)$ face, we can prepare A3B2 receptors that are quite responsive to sazetidine-A (**Table 2.3**).

In a complementary series of experiments, we considered the drug NS9283, which binds only to $\alpha(+)/\alpha(-)$ interfaces. It is unable to activate the receptor on its own, and it is thus an allosteric modulator. We reasoned that a combination of NS9283 and sazetidine-A would activate A3B2 receptors, with the former binding to the $\alpha(+)/\alpha(-)$ interface and the latter to the $\alpha(+)/\beta(-)$ interfaces. Indeed, a mixture of NS9283 and sazetidine-A is quite potent at A3B2 receptors, while neither compound alone can activate the receptor. Taking this one step further, by mutating all interfaces so they resemble $\alpha(+)/\alpha(-)$ interfaces, NS9283 becomes an agonist, rather than the allosteric modulator it is for the wild type receptor.

We also applied this interface concept to cytosine, which has the reverse activation profile of sazetidine-A, in that it cannot activate the A2B3 receptor. By mutating one residue of the $\beta 2$ subunit to that of the $\alpha 4$ subunit, we find that cytosine can activate the A2B3 receptor. In addition, this same mutation increased efficacy of cytosine for the A3B2 receptor from 7% to 16% (**Table 2.6**).

In sum, this work shows the relevance of the $\alpha(+)/\alpha(-)$ interface of nAChRs to achieving full receptor activation. This knowledge could be of great value to efforts to develop selective agonists for specific nAChR subtypes.

Table 2.6 Cytosine-A EC_{50} (μM) Values

Receptor	EC_{50} (μM) [1]	Hill [1]	EC_{50} (μM) [2]	Hill [2]	% [1]	n	Cyt I_{max} (μA)	ACh I_{max} (μA)	Efficacy
$(\alpha 4)_2(\beta 2)_3$	NR	—	—	—	—	—	—	0.15 - 2.4	—
$(\alpha 4)_3(\beta 2)_2$	0.047 ± 0.005	1.8 ± 0.3	6.0 ± 0.3	1.3 ± 0.1	22	16	0.052 - 2.9	0.94 - 33	$7 \pm 0.1 \%$
$(\alpha 4)_2(\beta 2 \text{ F117Q})_3$	0.019 ± 0.001	1.6 ± 0.1	—	—	—	11	0.026 - 0.10	0.084 - 2.5	$22 \pm 0.1 \%$
$(\alpha 4)_3(\beta 2 \text{ F117Q})_2$	0.03 ± 0.01	1.0 ± 0.3	3.3 ± 0.7	1.1 ± 0.2	33	17	0.055 - 4.0	0.51 - 20	$16 \pm 0.3 \%$

Agonist = Cytosine

NR = No Response

2.5 Methods

2.5.1 Molecular Biology

Rat nAChR $\alpha 4$ and $\beta 2$ subunits were in pAMV (unnatural mutagenesis) and pGEMhe (natural mutagenesis) vectors. Site-directed mutagenesis was performed using the QuikChange protocol (Stratagene). Circular DNA of $\alpha 4$ and $\beta 2$ in pAMV was linearized with the NotI restriction enzyme and the plasmids in pGEMhe were linearized with the SbfI restriction enzyme. After purification (Qiagen), the T7 mMessage Machine kit (Ambion) was used to *in vitro* transcribe mRNA from linearized DNA templates.

QIAGEN's RNeasy RNA purification kit was used to isolate the transcribed mRNA product.

For unnatural amino acid incorporation, the amber (UAG) stop codon was used for all $\alpha 4$ subunit incorporation and the opal (UGA) stop codon was used for the $\beta 2$ subunit incorporation. 74-nucleotide THG73 tRNA (for UAG) and 74-nucleotide TQOpS' tRNA (for UGA) were *in vitro* transcribed using the MEGAshortscript T7 (Ambion) kit and isolated using Chroma Spin DEPC-H₂O columns (Clontech). Synthesized unnatural amino acids coupled to the dinucleotide dCA were enzymatically ligated to the appropriate 74-nucleotide tRNA as previously described (13,28).

2.5.2 Oocyte Preparation and Injection

Xenopus laevis stage V and VI oocytes were harvested via standard protocols (28). For unnatural amino acid incorporation to the α subunit, the $\alpha 4$ and $\beta 2$ mRNAs were mixed in a 3:1 ratio by mass to obtain the A2B3 receptor, and in a 100:1 ratio to obtain the A3B2 receptor. Unnatural amino acid incorporation to the β subunit used $\alpha 4$ and $\beta 2$ mRNA ratios of 1:20 and 10:1 to obtain the A2B3 and A3B2 receptors, respectively. mRNA mixtures and deprotected (photolysis) tRNA were mixed in a 1:1 volume ratio, and 50 nL were injected into each oocyte. After injection, the oocytes were incubated at 18° C in ND96+ medium for 24 h. For the unnatural amino acids with reduced cation- π binding ability, a second round of injections following the same procedure was performed followed by incubation for an additional 24 h. The reliability of the unnatural amino acid incorporation was confirmed through read-through/reaminoacylation tests as previously performed (12).

For the natural mutagenesis experiments, the $\alpha 4$ and $\beta 2$ mRNAs were mixed in 1:2 or 10:1 ratios by mass to obtain the A2B3 and A3B2 receptors, respectively (29). A total of 50 nL were injected to each oocyte, delivering an mRNA mass total of 25 ng. Oocytes were incubated at 18° C in ND96+ medium for 24-72 h.

2.5.3 Chemical Preparation

Acetylcholine chloride was purchased from Sigma-Aldrich and dissolved to 1 M stock solutions in ND96 Ca^{2+} free buffer (96 mM NaCl, 2 mM KCl, 1 mM MgCl_2 , 5 mM HEPES at pH 7.5). Sazetidine-A dihydrochloride and (-)-cytisine were purchased from Tocris Bioscience and dissolved to 10 mM stock solutions in ND96 Ca^{2+} free buffer.

NS9283 was synthesized following a patented protocol (30). 3-pyridylamidoxime and 3-cyanobenzoyl chloride were purchased from Sigma-Aldrich. 0.5 g of 3-pyridylamidoxime was dissolved in 5.4 mL of pyridine. Then 0.6 g of 3-cyanobenzoyl chloride was added while stirring. The mixture was heated at reflux for 90 min and then cooled to room temperature. 200 mL of water was added and the white powder was filtered with two subsequent washes with water. The resulting powder was lyophilized overnight to remove the excess water. The reaction resulted in 60% yield, and the product was pure by LC-MS and NMR. ^1H NMR (300 MHz, $\text{DMSO}-d_6$) δ 9.26 (dd, $J = 2.2, 0.9$ Hz, 1H), 8.82 (dd, $J = 4.8, 1.6$ Hz, 1H), 8.64 (td, $J = 1.7, 0.7$ Hz, 1H), 8.50 (ddd, $J = 8.0, 1.9, 1.1$ Hz, 1H), 8.47 (dt, $J = 6.0, 2.1$ Hz, 1H), 8.22 (dt, $J = 7.9, 1.4$ Hz, 1H), 7.88 (td, $J = 7.9, 0.7$ Hz, 1H), 7.65 (ddd, $J = 7.9, 4.8, 0.9$ Hz, 1H); MS (+ES-API) m/z 249 ($\text{M}+\text{H}$) $^+$.

The purified compound, NS9283, was then dissolved to a 10 mM stock solution in DMSO. All drug solutions containing NS9283 were 0.1% DMSO (v/v) with the

exception of the 100 mM dose, which had 1% DMSO (v/v). Appropriate controls of 1% DMSO (v/v) in ND96 Ca^{2+} free buffer only were applied to expressing cells to show no receptor response to the higher DMSO concentration.

2.5.4 Electrophysiology

The OpusXpress 6000A (Axon Instruments) in two-electrode voltage clamp mode was used for all electrophysiological recordings. The holding potential was set to -60 mV and the running buffer used was ND96 Ca^{2+} free solution for all experiments. All acetylcholine drug applications used 1 mL of drug solution applied over 15 s followed by a 2.5 min buffer wash at a rate of 3 mL min⁻¹. All sazetidine-A, cytisine, NS9283, and co-applications used 1 mL of drug solution applied over 8 s with a 30 s pause before a 5 min buffer wash at a rate of 3 mL min⁻¹. Dose-response measurements utilized a series of approximately three-fold concentration steps, spanning several orders of magnitude, for a total of eight to eighteen doses. Data were sampled at 50 Hz and then low-pass filtered at 5 Hz. Experiments testing activity of compounds involved two to three acetylcholine doses of either EC₅₀ or I_{max} values, followed by the test doses of compounds being probed, followed by one to two doses of the previous acetylcholine concentrations.

Averaged and normalized data were fit to one or two Hill terms to generate EC₅₀ and Hill coefficient (nH) values. All currents for the activity testing were normalized to the highest acetylcholine dose applied pre-compound testing. The efficacy of compounds was measured as the ratio of the I_{max} of the compound divided by the I_{max} of acetylcholine. All acetylcholine EC₅₀ values for the conventional mutations made in

pGEMhe are reported in (Table 2.7). Error bars represent standard error of the mean (SEM) values.

Table 2.7

Receptor	EC ₅₀ (μM) [1]	Hill [1]	EC ₅₀ (μM) [2]	Hill [2]	% [1]	n	I _{max} (μA)
(α4) ₂ (β2) ₃	0.78 ± 0.02	1.1 ± 0.02	–	–	–	16	0.15 – 2.4
(α4) ₃ (β2) ₂	7.2 ± 23	0.7 ± 0.4	106 ± 13	1.7 ± 0.5	26	15	1.7 – 31
(α4) ₂ (β2) ₃ + 10 μM NS9283	0.48 ± 0.02	1.1 ± 0.05	–	–	–	12	0.095 – 7.2
(α4) ₃ (β2) ₂ + 10 μM NS9283	0.15 ± 0.004	1.07 ± 0.03	–	–	–	14	0.42 – 42
(α4) ₂ (β2 F117Q) ₃	1.6 ± 0.1	1.6 ± 0.1	–	–	–	15	0.033 – 0.28
(α4) ₃ (β2 F117Q) ₂	9 ± 15	0.9 ± 0.4	134 ± 22	1.6 ± 0.3	25	14	1.5 – 15
(α4) ₂ (β2 V109H, F117Q, L119T) ₃	35 ± 1	1.5 ± 0.04	–	–	–	14	2.0 – 28
(α4) ₃ (β2 V109H, F117Q, L119T) ₂	180 ± 10	1.6 ± 0.1	–	–	–	12	0.16 – 6.3
(α4 H114V, Q122F, T124L) ₂ (β2) ₃	1.0 ± 0.03	1.1 ± 0.03	–	–	–	22	0.11 – 4.2
(α4 H114V, Q122F, T124L) ₃ (β2) ₂	2.7 ± 0.2	0.81 ± 0.03	–	–	–	16	0.89 – 18

Agonist = Acetylcholine

2.5.5 The Hypersensitive Mutation (L9'A)

In the case of unnatural amino acid incorporation and mutagenesis scanning, EC₅₀ values were obtained using a hypersensitive mutation in the α4 subunit (L9'A). This mutation serves two purposes in the experimental setup: (1) the gain of function mutation gives a larger concentration window to probe effects of introduced mutations and (2) the pore mutation causes differences in rectification between the two stoichiometries, which can be probed via voltage jump experiments to confirm which stoichiometry is being observed (13,31). Since the EC₅₀ is shifted from true wild type, a correction factor was applied according to the procedure of Moroni *et al.* to obtain the wild type EC₅₀ value (32).

2.6 Acknowledgments

We would like to thank the NIH (NS034407, DA017279, DA280382), NIH/NRSA (GM07616), and the California Tobacco-Related Disease Research Program from the University of California (19XT-0102) for support of this work.

2.7 References

1. Miwa, J. M., Freedman, R., and Lester, H. A. (2011) Neural systems governed by nicotinic acetylcholine receptors: emerging hypotheses. *Neuron* **70**, 20-33
2. Albuquerque, E. X., Pereira, E. F., Alkondon, M., and Rogers, S. W. (2009) Mammalian nicotinic acetylcholine receptors: from structure to function. *Physiological Reviews* **89**, 73-120
3. Dani, J. A., and Bertrand, D. (2007) Nicotinic acetylcholine receptors and nicotinic cholinergic mechanisms of the central nervous system. *Annual Review of Pharmacology and Toxicology* **47**, 699-729
4. Jensen, A. A., Frolund, B., Lijefors, T., and Krogsgaard-Larsen, P. (2005) Neuronal nicotinic acetylcholine receptors: Structural revelations, target identifications, and therapeutic inspirations. *Journal of Medicinal Chemistry* **48**, 4705-4745
5. Taly, A., Corringer, P. J., Guedin, D., Lestage, P., and Changeux, J. P. (2009) Nicotinic receptors: allosteric transitions and therapeutic targets in the nervous system. *Nature Reviews. Drug Discovery* **8**, 733-750
6. Dougherty, D. A. (2008) Cys-Loop Neuroreceptors: Structure to the Rescue? *Chemical Reviews* **108**, 1642-1654
7. Dougherty, D. A. (2008) Physical Organic Chemistry on the Brain. *Journal of Organic Chemistry* **73**, 3667-3674
8. Unwin, N. (2005) Refined structure of the nicotinic acetylcholine receptor at 4Å resolution. *J Mol Biol* **346**, 967-989
9. Gotti, C., Zoli, M., and Clementi, F. (2006) Brain nicotinic acetylcholine receptors: native subtypes and their relevance. *Trends in Pharmacological Sciences* **27**, 482-491
10. Brejc, K., van Dijk, W. J., Klaassen, R. V., Schuurmans, M., van der Oost, J., Smit, A. B., and Sixma, T. K. (2001) Crystal structure of an ACh-binding protein reveals the ligand-binding domain of nicotinic receptors. *Nature* **411**, 269-276
11. Beers, W. H., and Reich, E. (1970) Structure And Activity Of Acetylcholine. *Nature* **228**, 917-922
12. Tavares Xda, S., Blum, A. P., Nakamura, D. T., Puskar, N. L., Shanata, J. A., Lester, H. A., and Dougherty, D. A. (2012) Variations in binding among several agonists at two stoichiometries of the neuronal, $\alpha 4\beta 2$ nicotinic receptor. *Journal of the American Chemical Society* **134**, 11474-11480
13. Xiu, X., Puskar, N. L., Shanata, J. A., Lester, H. A., and Dougherty, D. A. (2009) Nicotine binding to brain receptors requires a strong cation- π interaction. *Nature* **458**, 534-537
14. Puskar, N. L., Xiu, X., Lester, H. A., and Dougherty, D. A. (2011) Two neuronal nicotinic acetylcholine receptors, $\alpha 4\beta 4$ and $\alpha 7$, show differential agonist binding modes. *The Journal of Biological Chemistry* **286**, 14618-14627
15. Zhang, H. K., Eaton, J. B., Yu, L. F., Nys, M., Mazzolari, A., van Elk, R., Smit, A. B., Alexandrov, V., Hanania, T., Sabath, E., Fedolak, A., Brunner, D., Lukas, R. J., Vistoli, G., Ulens, C., and Kozikowski, A. P. (2012) Insights into the structural determinants required for high-affinity binding of chiral cyclopropane-

- containing ligands to $\alpha 4\beta 2$ -nicotinic acetylcholine receptors: an integrated approach to behaviorally active nicotinic ligands. *J Med Chem* **55**, 8028-8037
16. Billen, B., Spurny, R., Brams, M., van Elk, R., Valera-Kummer, S., Yakel, J. L., Voets, T., Bertrand, D., Smit, A. B., and Ulens, C. (2012) Molecular actions of smoking cessation drugs at $\alpha 4\beta 2$ nicotinic receptors defined in crystal structures of a homologous binding protein. *Proc. Natl. Acad. Sci. U. S. A.* **109**, 9173-9178
 17. Zwart, R., Carbone, A. L., Moroni, M., Bermudez, I., Mogg, A. J., Folly, E. A., Broad, L. M., Williams, A. C., Zhang, D., Ding, C., Heinz, B. A., and Sher, E. (2008) Sazetidine-A is a potent and selective agonist at native and recombinant $\alpha 4\beta 2$ nicotinic acetylcholine receptors. *Molecular Pharmacology* **73**, 1838-1843
 18. Liu, Y., Richardson, J., Tran, T., Al-Muhtasib, N., Xie, T., Yenugonda, V. M., Sexton, H. G., Rezvani, A. H., Levin, E. D., Sahibzada, N., Kellar, K. J., Brown, M. L., Xiao, Y., and Paige, M. (2013) Chemistry and pharmacological studies of 3-alkoxy-2,5-disubstituted-pyridinyl compounds as novel selective $\alpha 4\beta 2$ nicotinic acetylcholine receptor ligands that reduce alcohol intake in rats. *J Med Chem* **56**, 3000-3011
 19. Liu, J., Yu, L. F., Eaton, J. B., Caldarone, B., Cavino, K., Ruiz, C., Terry, M., Fedolak, A., Wang, D., Ghavami, A., Lowe, D. A., Brunner, D., Lukas, R. J., and Kozikowski, A. P. (2011) Discovery of isoxazole analogues of sazetidine-A as selective $\alpha 4\beta 2$ -nicotinic acetylcholine receptor partial agonists for the treatment of depression. *J Med Chem* **54**, 7280-7288
 20. Eaton, J. B., Lucero, L. M., Stratton, H., Chang, Y., Cooper, J. F., Lindstrom, J. M., Lukas, R. J., and Whiteaker, P. (2014) The unique $\alpha 4(+)/(-)\alpha 4$ agonist binding site in $(\alpha 4)3(\beta)2$ subtype nicotinic acetylcholine receptors permits differential agonist desensitization pharmacology vs. the $(\alpha 4)2(\beta 2)3$ subtype. *The Journal of Pharmacology and Experimental Therapeutics* **348**, 46-58
 21. Mazzaferro, S., Benallegue, N., Carbone, A., Gasparri, F., Vijayan, R., Biggin, P. C., Moroni, M., and Bermudez, I. (2011) Additional acetylcholine (ACh) binding site at $\alpha 4/\alpha 4$ interface of $(\alpha 4\beta 2)2\alpha 4$ nicotinic receptor influences agonist sensitivity. *The Journal of Biological Chemistry* **286**, 31043-31054
 22. Harpsoe, K., Ahring, P. K., Christensen, J. K., Jensen, M. L., Peters, D., and Balle, T. (2011) Unraveling the high- and low-sensitivity agonist responses of nicotinic acetylcholine receptors. *The Journal of Neuroscience: the Official Journal of the Society for Neuroscience* **31**, 10759-10766
 23. Figl, A., Cohen, B. N., Quick, M. W., Davidson, N., and Lester, H. A. (1992) Regions of $\beta 4$ - $\beta 2$ subunit chimeras that contribute to the agonist selectivity of neuronal nicotinic receptors. *FEBS letters* **308**, 245-248
 24. Harpsoe, K., Hald, H., Timmermann, D. B., Jensen, M. L., Dyhring, T., Nielsen, E. O., Peters, D., Balle, T., Gajhede, M., Kastrup, J. S., and Ahring, P. K. (2013) Molecular determinants of subtype-selective efficacies of cytisine and the novel compound NS3861 at heteromeric nicotinic acetylcholine receptors. *The Journal of Biological Chemistry* **288**, 2559-2570
 25. Timmermann, D. B., Sandager-Nielsen, K., Dyhring, T., Smith, M., Jacobsen, A. M., Nielsen, E. O., Grunnet, M., Christensen, J. K., Peters, D., Kohlhaas, K., Olsen, G. M., and Ahring, P. K. (2012) Augmentation of cognitive function by NS9283, a stoichiometry-dependent positive allosteric modulator of $\alpha 2$ - and $\alpha 4$ -

- containing nicotinic acetylcholine receptors. *British Journal of Pharmacology* **167**, 164-182
26. Grupe, M., Jensen, A. A., Ahring, P. K., Christensen, J. K., and Grunnet, M. (2013) Unravelling the mechanism of action of NS9283, a positive allosteric modulator of $(\alpha 4)\beta 2$ nicotinic ACh receptors. *British Journal of Pharmacology* **168**, 2000-2010
 27. Olsen, J. A., Kastrup, J. S., Peters, D., Gajhede, M., Balle, T., and Ahring, P. K. (2013) Two Distinct Allosteric Binding Sites at $\alpha 4\beta 2$ Nicotinic Acetylcholine Receptors Revealed by NS206 and NS9283 Give Unique Insights to Binding-Activity Associated Linkage at Cys-Loop Receptors. *The Journal of Biological Chemistry* **288**, 35997-36006
 28. Nowak, M., Gallivan, J. P., Silverman, S., Labarca, C. G., Dougherty, D. A., and Lester, H. A. (1998) In Vivo Incorporation of Unnatural Amino Acids into Ion Channels in Xenopus Oocyte Expression System. *Methods Enzymol* **293**, 26
 29. Nelson, M., Kuryatov, A., Choi, C., Zhou, Y., and Lindstrom, J. (2003) Alternate Stoichiometries of the $\alpha 4\beta 2$ Nicotinic Acetylcholine Receptors. *Molecular Pharmacology* **63**, 332-342
 30. Ji, J., Lee, C.-H., Sippy, K. B., Li, T., and Gopalakrishnan, M. (2009) Novel [1,2,4]oxadiazole compounds as $\alpha 4\beta 2$ positive allosteric modulators and their preparation and use in the treatment of diseases. (Laboratories, A. ed., USA)
 31. Marotta, C. B., Dilworth, C. N., Lester, H. A., and Dougherty, D. A. (2013) Probing the non-canonical interface for agonist interaction with an $\alpha 5$ containing nicotinic acetylcholine receptor. *Neuropharmacology* **77C**, 342-349
 32. Moroni, M., Zwart, R., Sher, E., Cassels, B. K., and Bermudez, I. (2006) $\alpha 4\beta 2$ nicotinic receptors with high and low acetylcholine sensitivity: pharmacology, stoichiometry, and sensitivity to long-term exposure to nicotine. *Molecular Pharmacology* **70**, 755-768

Chapter 3

*Probing the Non-Canonical Interface for Agonist Interaction with an $\alpha 5$ Containing Nicotinic Acetylcholine Receptor**

This chapter is adapted from: Christopher B. Marotta, Crystal N. Dilworth, Henry A. Lester, and Dennis A. Dougherty. Probing the Non-Canonical Interface for Agonist Interaction with an $\alpha 5$ Containing Nicotinic Acetylcholine Receptor. *Neuropharmacology*, **2014, 77, pages 342-349. Copyright 2013 Elsevier Ltd. *The work described in this chapter was done in collaboration with Dr. Crystal N. Dilworth.**

Link to article: doi:10.1016/j.neuropharm.2013.09.028

3.1 Abstract

Nicotinic acetylcholine receptors (nAChRs) containing the $\alpha 5$ subunit are of interest because genome-wide association studies and candidate gene studies have identified polymorphisms in the $\alpha 5$ gene that are linked to an increased risk for nicotine dependence, lung cancer, and/or alcohol addiction. To probe the functional impact of an $\alpha 5$ subunit on nAChRs, a method to prepare a homogeneous population of $\alpha 5$ -containing receptors must be developed. Here we use a gain of function (9') mutation to isolate populations of $\alpha 5$ -containing nAChRs for characterization by electrophysiology. We find that the $\alpha 5$ subunit modulates nAChR rectification when co-assembled with $\alpha 4$ and $\beta 2$ subunits. We also probe the $\alpha 5$ – $\alpha 4$ interface for possible ligand binding interactions. We find that mutations expected to ablate an agonist binding site involving the $\alpha 5$ subunit have no impact on receptor function. The most straightforward interpretation of this observation is that agonists do not bind at the $\alpha 5$ – $\alpha 4$ interface, in contrast to what has recently been demonstrated for the $\alpha 4$ – $\alpha 4$ interface in related receptors. In addition, our

mutational results suggest that the $\alpha 5$ subunit does not replace the $\alpha 4$ or $\beta 2$ subunits and is relegated to occupying only the auxiliary position of the pentameric receptor.

3.2 Introduction

Nicotinic acetylcholine receptors (nAChRs) are widespread in the peripheral and central nervous systems. Because these receptors can be activated by nicotine as well as their native ligand acetylcholine, they have been associated with several health-related phenomena. Nicotine is the major addictive component of tobacco, and chronic tobacco use (smoking) has been implicated in many types of cancer as well as heart disease. Other related phenomena include an inverse correlation between smoking and Parkinson's disease and the observation that patients with autosomal dominant nocturnal frontal lobe epilepsy who smoke have fewer seizures (1).

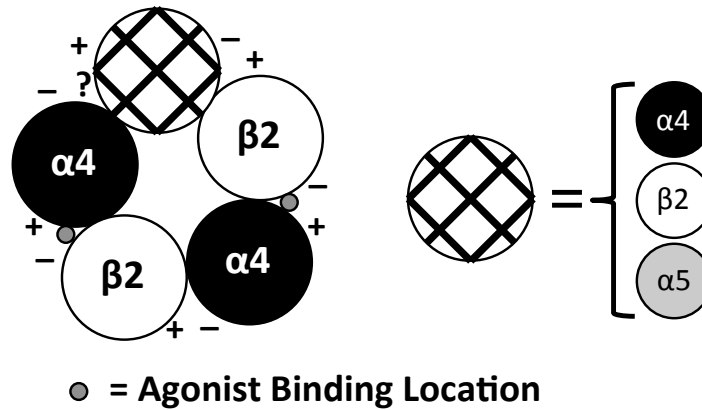
nAChRs belong to the Cys-loop family of ionotropic receptors, which share a pentameric architecture arranged around a central ion-permeable pore. Many diverse subunit combinations can form functional receptors, and these combinations have distinct pharmacologies concerning responses to acute applications and chronic or repeated applications of nicotinic drugs. Neuronal nAChRs are composed of $\alpha 2$ - $\alpha 11$ and $\beta 2$ - $\beta 4$ subunits and assemble as α plus β or α -only pentamers. The neuronal $\alpha 4\beta 2$ receptor subtype is one of the two most abundant nAChRs in the central nervous system (CNS). Two $\alpha 4\beta 2$ pentameric stoichiometries are known: $(\alpha 4\beta 2)_2(\beta 2)$ and $(\alpha 4\beta 2)_2(\alpha 4)$, which shall be referred to as A2B3 and A3B2, respectively (2). Subunit stoichiometry of nAChRs is important in determining pharmacology, stability, and subcellular location.

The A2B3 stoichiometry displays higher sensitivity to nicotine and has been proposed to play an especially prominent role in nicotine addiction.

Several brain regions express receptors that contain an $\alpha 5$ subunit ($\alpha 5^*$ receptors), including the substantia nigra pars compacta, subthalamic nucleus, medial habenula, prefrontal cortex, and hippocampus. Receptors containing $\alpha 5$ play a part in nicotine self-administration and nicotine withdrawal (3). These receptors are also important for dopamine release and attention tasks (4-6). The $\alpha 4\beta 2\alpha 5$ receptors are more permeable to Ca^{2+} than $\alpha 4\beta 2$ receptors and have a higher sensitivity to nicotine (7). The $\alpha 5$ subunit has been assumed to occupy the fifth “auxiliary” position in pentameric receptors, and it has not previously been thought to participate in forming a functional agonist binding site. However, recent studies have proposed that a low affinity binding site exists in the A3B2 $\alpha 4\beta 2$ receptor at the $\alpha 4$ – $\alpha 4$ interface (**Fig. 3.1**) (8-10), in addition to the higher affinity binding sites at the $\alpha 4$ – $\beta 2$ interface. This new binding location utilizes an auxiliary subunit interface, leading to questions as to whether $\alpha 5$ can participate in a similar motif.

Given the precise localization and unique functional properties of $\alpha 5^*$ receptors, $\alpha 5$ presents itself as a valuable therapeutic target. However, currently there are no pharmacological ligands that can functionally isolate $\alpha 5^*$ receptors. If $\alpha 5$ does participate in a ligand-binding site at the $\alpha 5$ – $\alpha 4$ interface, this interaction would be a vital target for selective ligand development.

A



B

	TrpD		TyrA		TrpB		TyrC1		TyrC2
	98		136		191		232		237
Mouse $\alpha 5$	NVWLK	...	VLFDN	...	GSWTY	...	RTDSCC	--	WYPC
Mouse $\alpha 4$	NVWVK	...	VLINN	...	GSWTY	...	RKYECCA	EI	YPD
Mouse $\beta 2$	NVWLT	...	VLINN	...	RSWTY	...	NPDDST	---	YVD

Fig. 3.1 (A) View of nAChRs from the extracellular solution. The $\alpha 4\beta 2$ receptor has two $\alpha 4$ subunits, two $\beta 2$ subunits, and two conventional antagonist/agonist binding sites, at $\alpha 4$ – $\beta 2$ interfaces. The fifth subunit is the “accessory” subunit, and in this study three possibilities are the $\alpha 4$, $\alpha 5$ or $\beta 2$ subunits. The accessory subunit may also contribute to a binding interface, shown by “?” **(B)** Sequence alignment of the mouse nAChR subunits highlighting the aromatic box residue locations on loops D, A, B, and C (in sequence). The residues shown are identical to their human sequence except the final residue (Cys) in the mouse $\alpha 5$ subunit is a tyrosine (Tyr, Y) in the human subunit. Note that TrpD is on the “complementary” face of a subunit, and so it is not expected to contribute to an $\alpha 5$ – $\alpha 4$ interface.

3.3 Materials and Methods

3.3.1 Molecular Biology

Mouse nAChR $\alpha 5$ wt, $\alpha 5$ -GFP, $\alpha 4$, and $\beta 2$ subunits were in pGEMhe. The QuikChange protocol (Stratagene) was used for site-directed mutagenesis. Circular DNA for $\alpha 5$, $\alpha 4$, and $\beta 2$ was linearized as follows: *SphI* restriction enzyme for $\alpha 5$ plasmids and *SbfI* restriction enzyme for the $\alpha 4$ and $\beta 2$ plasmids. After purification (Qiagen), mRNA was synthesized from linearized DNA template through run-off transcription by

using the T7 mMessage Machine kit (Ambion). Purification of mRNA was performed using QIAGEN's RNeasy RNA purification kit.

3.3.2 Electrophysiology Studies

3.3.2.1 Xenopus Oocyte Preparation and Injection

Xenopus laevis stage V and VI oocytes were harvested via standard protocols (11). The $\alpha 5$ mRNA was mixed with $\alpha 4$ and $\beta 2$ mRNA in a 10:1:1 ratio by mass and 50 nl were injected into the oocytes delivering 40 ng of total mRNA. After injection, oocytes were incubated at 18° C in ND96+ medium for 24-96 h. The control experiments of only $\alpha 4$ and $\beta 2$ mRNA with ratios of 1:1, 1:2, and 10:1 had total mRNA amounts of 6.67 ng, 20 ng and 21 ng, respectively.

3.3.2.2 Chemical Preparation

Acetylcholine chloride, (-)-nicotine tartrate, and mecamylamine hydrochloride were purchased from Sigma-Aldrich and dissolved to 1 M and 0.25 M stock solutions in ND96 Ca^{2+} free buffer (96 mM NaCl, 2 mM KCl, 1 mM MgCl_2 , 5 mM HEPES at pH 7.5), respectively.

3.3.2.3 Electrophysiological Experimental Protocols

Electrophysiological recordings were performed using the two electrode voltage clamp mode with the OpusXpress 6000A (Axon Instruments). The holding potential was -60 mV. All recordings involving $\alpha 5^*$ receptors and $\alpha 4\beta 2$ receptors used the ND96 Ca^{2+} free solution as the running buffer. All measurements used 1 mL of drug

solution applied during 15 s (except 25 s for current-voltage experiments) followed by a 2 min buffer wash except for nicotine application which received a 5 min buffer wash. Dose-response measurements utilized a series of approximately three-fold concentration steps, spanning several orders of magnitude, for a total of eight to eighteen doses. Data were low-passed filtered at 5 Hz and digitized at 125 Hz.

Mecamylamine experiments involved three acetylcholine doses, followed by two co-application doses of acetylcholine and mecamylamine, followed by two doses of acetylcholine only. Before each co-application, there was a 30 s pre-incubation of mecamylamine only.

3.3.3 Data Analysis

3.3.3.1 Dose-Response Analysis

Averaged and normalized data were fit to one or two Hill terms to generate EC_{50} and Hill coefficient (nH) values. All currents for the mecamylamine experiment were normalized to the highest current response pre-mecamylamine addition. The percentage recovery was calculated by comparing pre- and post-mecamylamine applications.

3.3.3.2 Current-Voltage Analysis

I-V relations were generated from 400 ms test pulses, applied at intervals of 500 ms, ranging from -110 mV to +70 mV in 20 mV increments. To minimize distortions from desensitization or ion accumulation, the increments proceeded in both depolarizing and hyperpolarizing directions during each drug application, and averaged data were analyzed. To isolate agonist-induced currents, we subtracted records taken in buffer only.

The current was averaged during 200 to 400 ms after the jump, and then normalized to the value at -110 mV.

3.3.3.3 Error Analysis

Error bars on dose-response curves represent standard error of the mean (SEM) values. Maximal current values (wild type vs. V9'S $\alpha 5$ subunit) and voltage jump comparisons (at +70 mV) were subjected to Student t Test analysis and gave t probabilities < 0.001.

3.4 Results

3.4.1 Expression of an $\alpha 5$ -Containing Receptor

Accurate interpretation of structure-function relationships from electrophysiological responses requires expression of a homogeneous receptor population. As such, a method to prepare and confirm a homogenous population of $\alpha 5^*$ receptors must first be established before we can begin to interpret results from mutational analysis of the putative $\alpha 5$ - $\alpha 4$ interface. $\alpha 5$ presents a unique challenge because of its role as an accessory subunit. When $\alpha 5$ is co-expressed with $\alpha 4$ and $\beta 2$ subunits, we consider the possibility of three different receptor populations on the cell surface: $(\alpha 4\beta 2)_2(\beta 2)$, $(\alpha 4\beta 2)_2(\alpha 4)$, and $(\alpha 4\beta 2)_2(\alpha 5)$. The assumption that $\alpha 4\beta 2\alpha 5$ receptors have an $(\alpha 4\beta 2)_2(\alpha 5)$ stoichiometry is partly based on analogy to the muscle-type receptor, which contains two conventional binding interfaces ($\alpha/\gamma(\epsilon)$ and α/δ) and then a single auxiliary subunit, β . Previously, differences in EC_{50} values and rectification

behaviors allowed a distinction to be made between the two $\alpha 4\beta 2$ receptor stoichiometries (12). Here, we apply similar strategies to evaluate $\alpha 5^*$ receptors.

Varying mRNA injection ratios in oocytes can bias assembly to a specific receptor stoichiometry (2,12,13). Specifically, using excess of $\alpha 5$ mRNA compared to $\alpha 4$ and $\beta 2$ mRNA promotes preferential assembly with an $\alpha 5$ subunit (14). A ratio of 10:1:1 of $\alpha 5:\alpha 4:\beta 2$ mRNA was used to bias the system toward incorporation of the $\alpha 5$ subunit. As seen in (**Fig. 3.2**), injection of a 1:1 ratio of $\alpha 4:\beta 2$ mRNA produces a biphasic dose-response relation, reflecting the presence of A2B3 (high affinity) and A3B2 (low affinity) forms of the $\alpha 4\beta 2$ receptor. However, a monophasic dose-response relation is clearly seen upon the addition of the $\alpha 5$ mRNA (14). mRNA injections of 1:2 of $\alpha 4:\beta 2$ (resulting in A2B3 receptors) and 10:1 of $\alpha 4:\beta 2$ (resulting in A3B2 receptors) were performed in order to compare EC_{50} values of the two $\alpha 4\beta 2$ receptor stoichiometries with the new value obtained from introducing the $\alpha 5$ mRNA (**Fig. 3.2, Table 3.1**). We find that the EC_{50} value resulting from 10:1:1 $\alpha 5:\alpha 4:\beta 2$ mRNA injection is nearly identical to that for the A2B3 receptor. This could indicate that $\alpha 5$ -containing receptors coincidentally have nearly the same EC_{50} as A2B3 $\alpha 4\beta 2$ receptors, or that the addition of the $\alpha 5$ mRNA is attenuating the expression of the A3B2 receptor, resulting in a single population of A2B3 receptors at the surface. An additional challenge to evaluating these putative $\alpha 4\beta 2\alpha 5$ receptors was the low agonist-induced current (tens to hundreds of nA) seen in these experiments.

To address the first issue, we tested the response to voltage-jump protocols that we had previously used to distinguish A2B3 and A3B2 $\alpha 4\beta 2$ receptors (12). **Figure 3.3**

shows that there is a distinct loss of rectification for receptors prepared by a 10:1:1 $\alpha 5:\alpha 4:\beta 2$ mRNA injection compared to A2B3 and A3B2 receptors. This result suggests that we have $\alpha 5^*$ receptors on the surface of the oocyte.

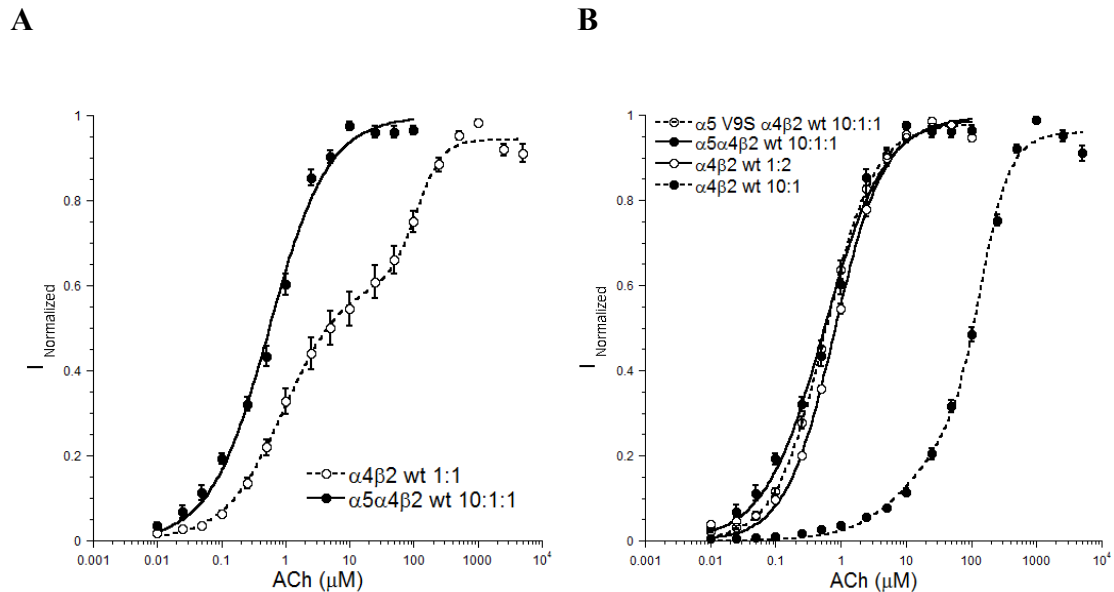


Fig. 3.2 (A) Dose response relations for the mouse $\alpha 4\beta 2$ receptor with a 1:1 injection ratio, and for the mouse $(\alpha 4\beta 2)_2(\alpha 5)$ receptor with a 10:1:1 $\alpha 5:\alpha 4:\beta 2$ mRNA injection ratio. (B) Comparison of dose-response relations for the two stoichiometries of the mouse $\alpha 4\beta 2$ receptors (A2B3 and A3B2) and the mouse $(\alpha 4\beta 2)_2(\alpha 5)$ receptor with and without the $\alpha 5V9'S$ mutation.

To overcome the small currents that were hampering our efforts to fully characterize these channels, we introduced an often-used reporter mutation at the 9' position of the pore lining M2 helix (15-18). Mutations in this region frequently result in increased expression levels. In addition, 9' mutations typically cause a gain of function in the receptor, evidenced by a reduction in EC_{50} values and due to an altered P_{open} , without affecting the ligand-binding domain (19). Most subunits of nAChRs have a conserved Leu at the 9' position, but the accessory subunits $\alpha 5$ and $\beta 3$ contain a Val in that position. The V9'T (20) or V9'S (21) mutation has been employed to study $\alpha 3\beta 4\alpha 5$ nAChRs, but not $\alpha 4\beta 2\alpha 5$ nAChRs. In the present work a V9'S mutation was introduced into the $\alpha 5$

subunit, and the above experiments were repeated with the $\alpha 5V9'S$ subunit. Interestingly, we observe nearly identical EC_{50} values for $(\alpha 4\beta 2)_2(\alpha 5)$ and $(\alpha 4\beta 2)_2(\alpha 5V9'S)$ as shown in (**Fig. 3.2**). However, a substantial increase in agonist-induced current was observed (**Table 3.1**), and more consistent responses among batches of oocytes were noted. These observations further support the notion that the $\alpha 5$ subunit has been incorporated, since the only change between the experiments was the mutation in the $\alpha 5$ subunit.

Table 3.1

Receptor (Ratio)	EC_{50} (μM)	Hill	n	Current Range (μA)
$\alpha 4$ wt $\beta 2$ wt (1:1)	0.9 ± 0.2 (low)	0.9 ± 0.1 (low)	25	-0.14 to -7.0
	110 ± 15 (high)	2.1 ± 0.5 (high)	-	-
$\alpha 4$ wt $\beta 2$ wt (1:2)	0.80 ± 0.05	1.15 ± 0.7	13	-0.15 to -0.97
$\alpha 4$ wt $\beta 2$ wt (10:1)	141 ± 27	2.0 ± 0.7	17	-1.5 to -16
$\alpha 4L9'A$ $\beta 2$ wt (1:10)	0.39 ± 0.02	1.25 ± 0.7	13	-0.31 to -7.2
$\alpha 4L9'A$ $\beta 2$ wt (10:1)	0.046 ± 0.001	1.27 ± 0.04	13	-4.1 to -22
$\alpha 5$ wt $\alpha 4$ wt $\beta 2$ wt (10:1:1)	0.55 ± 0.05	0.95 ± 0.1	12	-0.027 to -0.20
$\alpha 5V9'S$ $\alpha 4$ wt $\beta 2$ wt (10:1:1)	0.57 ± 0.01	1.14 ± 0.01	26	-0.38 to -5.7
$\alpha 5V9'S$ GFP $\alpha 4$ wt $\beta 2$ wt (10:1:1)	0.76 ± 0.02	1.07 ± 0.03	17	-0.34 to -7.2

Agonist = Acetylcholine

3.4.2 The $\alpha 5V9'S$ Mutation Confers Distinct Physical Properties Allowing for Definitive Establishment of the Subunit's Incorporation

The two stoichiometries of the $\alpha 4\beta 2$ receptor are distinguishable by their distinct EC_{50} values. However, their rectification properties are similar (**Fig. 3.2, 3.3 and Table 3.1, 3.2**). Previous studies have shown that introduction of an L9'A mutation in the $\alpha 4$ subunit changes the rectification behavior of $\alpha 4\beta 2$ receptors (12). Xiu *et al.* report that the A2B3 receptor rectifies much more markedly than the A3B2 when the $\alpha 4$ L9'A mutation is present (12). Similarly, we find that introduction of the V9'S mutation to the $\alpha 5$ subunit produces a more marked loss of rectification compared to the wild type $\alpha 5$ subunit (**Fig. 3.3**). In anticipation of future studies on receptor trafficking and

localization, we prepared receptors with the V9'S mutation and meGFP inserted in the M3-M4 loop of the $\alpha 5$ subunit. This receptor also gives a wild type EC_{50} and a loss of rectification (**Table 3.1, 3.2**).

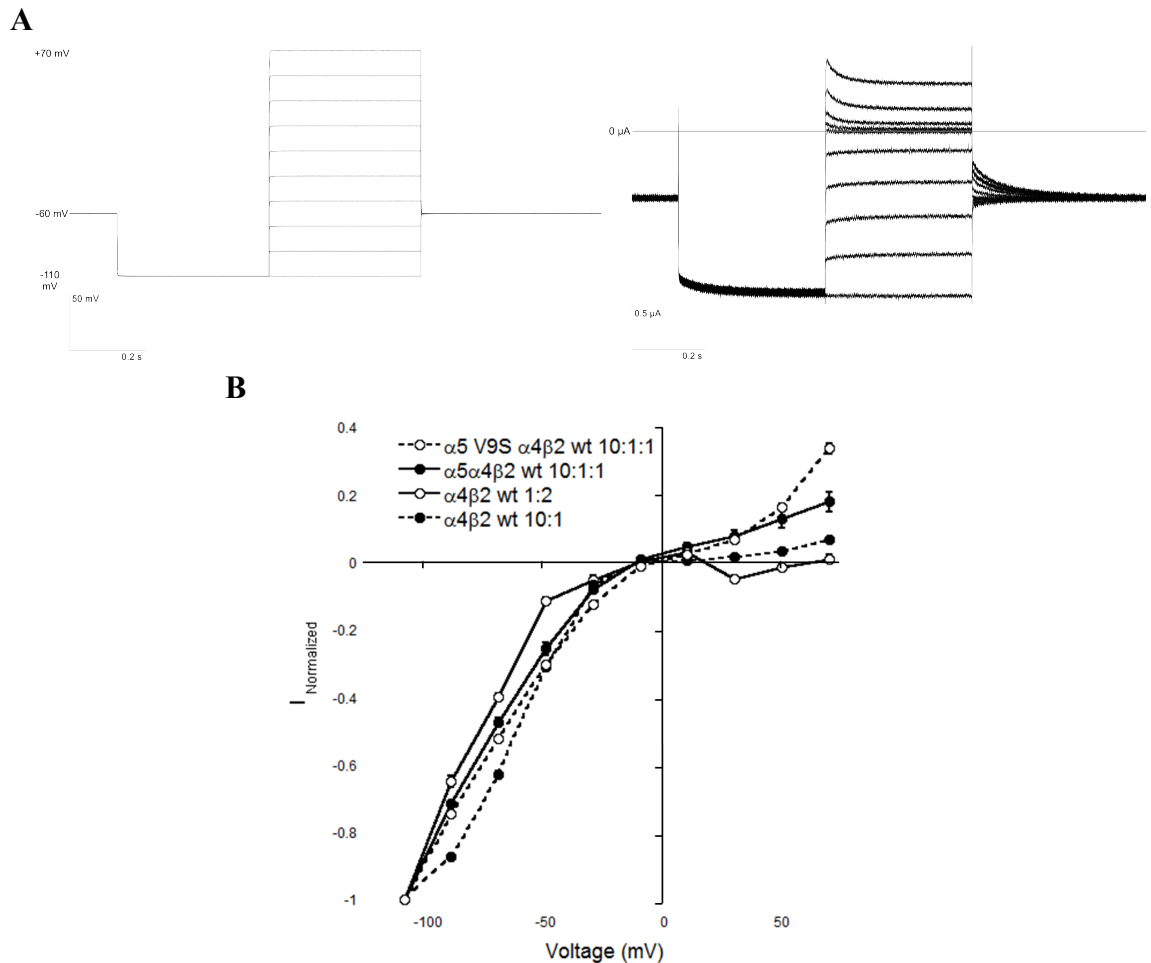


Fig. 3.3 Summary of rectification analysis. **(A)** Sample traces of the voltage jump experiment. The superimposed command voltage sweeps (left) and the ACh-induced currents (right) for the $(\alpha 4\beta 2)_2(\alpha 5V9'S)$ receptor are shown. **(B)** Comparison of current-voltage relations for the two stoichiometries of the mouse $\alpha 4\beta 2$ receptors (A2B3 and A3B2) and the mouse $(\alpha 4\beta 2)_2(\alpha 5)$ receptor with and without the 9' mutation.

In addition to the EC_{50} and rectification data, we also sought to more fully characterize the $(\alpha 4\beta 2)_2(\alpha 5V9'S)$ receptor. Mecamylamine has been extensively characterized as an open channel blocker with a slow wash off time for the $\alpha 4\beta 2$ receptor (22). A distinctive property of this open channel blocker is its “trapping”

Table 3.2

Receptor (Ratio)	ACh Induced Current at +70 mV (Normalized)	Current Range (μ A) at -110mV	Current Range (μ A) at +70mV	n
$\alpha 4$ wt $\beta 2$ wt (1:1*)	0.01 ± 0.01	-0.35 to -1.8	-0.02 to 0.11	34
$\alpha 4$ wt $\beta 2$ wt (1:2)	0.01 ± 0.01	-0.10 to -1.4	-0.03 to 0.09	34
$\alpha 4$ wt $\beta 2$ wt (10:1)	0.067 ± 0.008	-1.7 to -24	0.08 to 2.0	60
$\alpha 4$ L9'A $\beta 2$ wt (1:10)	0.054 ± 0.005	-0.23 to -5.0	-0.006 to 0.25	28
$\alpha 4$ L9'A $\beta 2$ wt (10:1)	0.34 ± 0.01	-1.0 to -18	0.39 to 6.4	31
$\alpha 5$ wt $\alpha 4$ wt $\beta 2$ wt (10:1:1)	0.10 ± 0.03	-0.073 to -0.14	-0.013 to 0.027	6
$\alpha 5$ V9'S $\alpha 4$ wt $\beta 2$ wt (10:1:1)	0.34 ± 0.02	-0.56 to -2.5	0.15 to 1.2	34
$\alpha 5$ V9'S GFP $\alpha 4$ wt $\beta 2$ wt (10:1:1)	0.33 ± 0.02	-0.71 to -1.9	0.27 to 0.5	12

ACh doses were the corresponding receptor's EC50 value for the voltage jump experiments

**The smaller of the two EC50 values was used for this measurement*

behavior: it associates and disassociates preferentially from the open pore of the receptor (23). Because of the prolonged wash-off time, subsequent applications of an agonist are generally needed to dissociate the molecule from the pore.

The results in **Figure 3.4** show a dramatic difference between the $(\alpha 4\beta 2)_2(\alpha 5V9'S)$ receptor and the $\alpha 4\beta 2$ receptor. When the $\alpha 5V9'S$ subunit is present, mecamylamine washes off the receptor completely within 120 s. We also find that introducing an L9'A mutation into the $\alpha 4$ subunit results in mecamylamine successfully washing out of both the A2B3 and A3B2 receptors (**Table 3.3**). This suggests that the observed results with the $\alpha 5V9'S$ subunit are due to the 9' mutation rather than an intrinsic property of the subunit. However, this still generates an important observation for this system. For studies of the $(\alpha 4\beta 2)_2(\alpha 5V9'S)$ receptor, the observation of nearly complete response recovery within 120 s indicates that we have prepared a receptor population on the plasma membrane that is highly enriched in $\alpha 5^*$ receptors, if not completely homogeneous. If a more mixed population containing both $\alpha 5^*$ and $\alpha 4\beta 2$ receptors was being expressed, the response would have recovered less fully. Results

from the rectification and open channel blocker experiments strongly indicate that we are able to express on the oocyte surface an $\alpha 5^*$ receptor population that is homogeneous or very nearly so. With this, we can now begin to investigate the $\alpha 5$ – $\alpha 4$ interface, knowing that responses from introduced mutations are directly due to changes in the $(\alpha 4\beta 2)_2(\alpha 5V9'S)$ receptor.

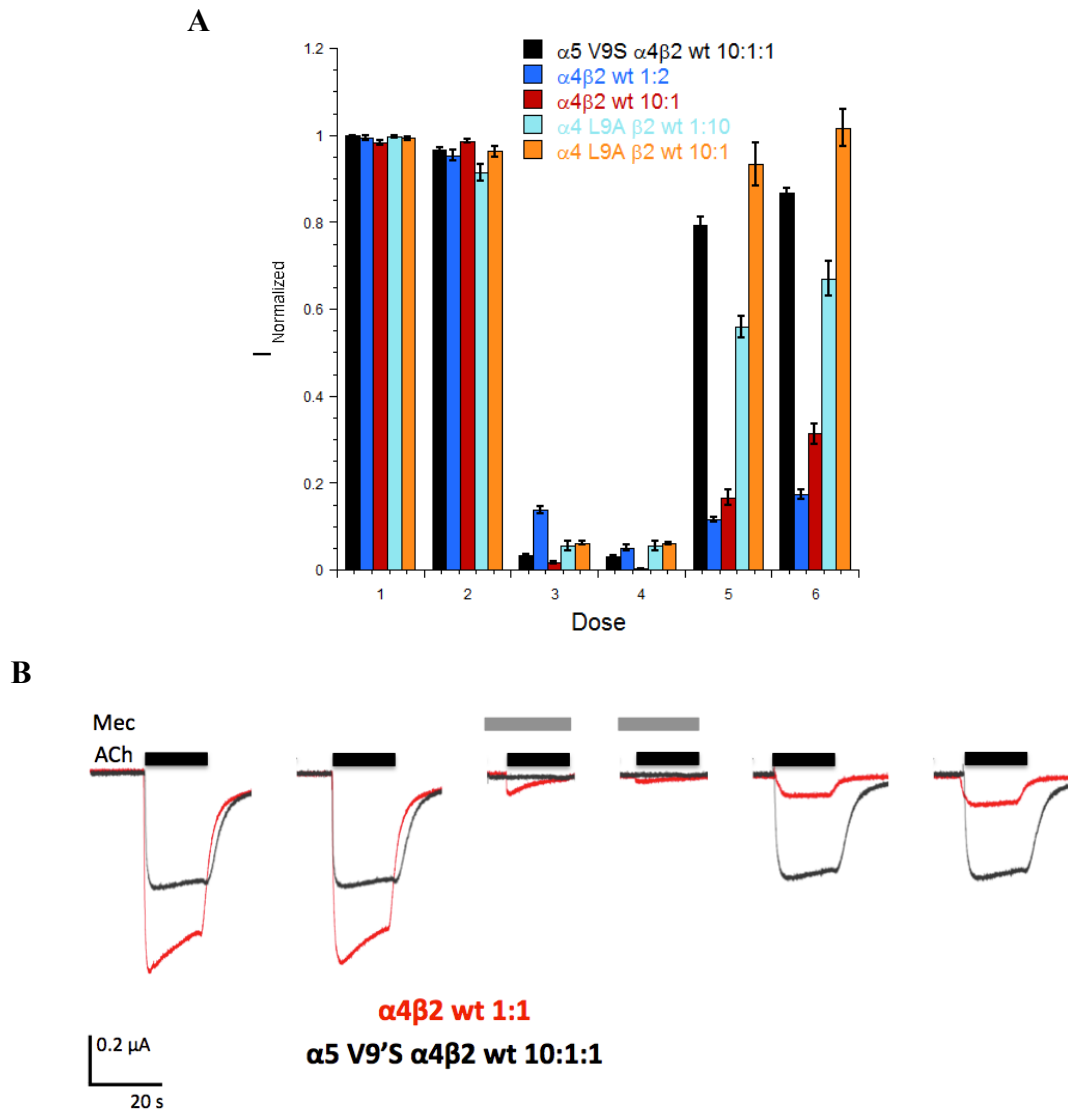


Fig. 3.4 (A) Response recovery following co-application of acetylcholine and mecamylamine following the protocol in part B. (B) A sample current trace of a single oocyte recording for each of the subunit combinations indicated. The $\alpha 4\beta 2$ nAChR is in red and the $(\alpha 4\beta 2)_2(\alpha 5V9'S)$ nAChR is in black. A 120 s wash period occurred between each dose.

Table 3.3

Receptor (Ratio)	Signal Recovery	Current Range (μ A)	n
α 5V9'S α 4 wt β 2 wt (10:1:1)	80 ± 2 %	-0.46 to -1.0	14
α 4 wt β 2 wt (1:2)	12 ± 1 %	-0.16 to -1.5	13
α 4 wt β 2 wt (10:1)	17 ± 2 %	-1.3 to -22	16
α 4L9'A β 2 wt (1:10)	56 ± 2 %	-0.08 to -0.84	15
α 4L9'A β 2 wt (10:1)	93 ± 5 %	-1.3 to -20	14

ACh doses were 10 times the corresponding receptor's EC₅₀ value for the mecamylamine experiments. Mecamylamine was kept at constant 100 μ M value to ensure full channel block

3.4.3 Mutational Analysis of the Aromatic Box at the α 5– α 4 Interface Showed No Functional Impact

The aromatic box of nAChR agonist binding sites is highly conserved and has been extensively characterized (24-28). The aromatic box mediates an essential cation- π interaction between the positively charged portion of the ligand and one (or occasionally two) of the five aromatic residues (A, B, C1, C2, and D) of the aromatic box. In fact, this aromatic box structure has been seen in a wide range of binding sites for cationic structures (29). The sequence alignment in **Figure 3.1** highlights the residues of interest for studying the α 5 subunit. Residues TrpB, TyrC2, and TyrA have previously been shown to be involved in cation- π interactions in other receptors, and these residues would be part of the principal component of an aromatic box contributed by α 5 if an α 5– α 4 binding site exists. The TrpD residue of the α 5 subunit was also investigated to probe the possibility of agonist binding at the β 2– α 5 interface. In addition, this mutation can subsequently probe the possibility that α 5 subunits were replacing β 2 subunits that would normally participate in the α 4– β 2 binding site. Interestingly, the C1 residue of the aromatic box that is typically a Tyr in α subunits is an Asp in the α 5 subunit.

An alanine scan of the aromatic residues of α 5 was performed. As shown in **Tables 3.4, 3.5**, negligible changes in EC₅₀ were seen in all cases for both ACh and

nicotine as agonists. Since the C1 site is not aromatic in the $\alpha 5$ subunit, an Asp-to-Tyr mutation was introduced. Again, no change in EC_{50} was seen. Current-voltage relations confirmed the inclusion of the $\alpha 5$ subunit for all the mutations (**Table 3.6**).

Table 3.4

Receptor (Ratio)	<i>Acetylcholine</i>			Fold Shift	Current Range (μA)
	EC ₅₀ (μM)	Hill	n		
$\alpha 4$ wt $\beta 2$ wt (1:2)	0.80 ± 0.05	1.2 ± 0.1	13	-	0.15 - 0.97
$\alpha 4$ wt $\beta 2$ wt (10:1)	140 ± 30	2.0 ± 0.7	17	-	1.5 - 16
$\alpha 5V9'S$ $\alpha 4$ wt $\beta 2$ wt (10:1:1)	0.57 ± 0.01	1.1 ± 0.01	26	-	0.38 - 5.7
$\alpha 5V9'S$ W98A (Trp D)	1.1 ± 0.08	1.1 ± 0.07	10	1.9	0.038 - 1.5
$\alpha 5V9'S$ F136A (Tyr A)	0.66 ± 0.02	1.2 ± 0.04	10	1.2	0.21 - 0.54
$\alpha 5V9'S$ W191A (Trp B)	0.55 ± 0.03	1.2 ± 0.08	19	1	0.068 - 0.67
$\alpha 5V9'S$ D232Y (Tyr C1)	0.60 ± 0.02	1.3 ± 0.04	13	1	0.20 - 1.2
$\alpha 5V9'S$ Y237A (Tyr C2)	0.82 ± 0.03	1.2 ± 0.05	16	1.4	0.067 - 0.41

Table 3.5

Receptor (Ratio)	<i>Nicotine</i>			Fold Shift	Current Range (μA)
	EC ₅₀ (μM)	Hill	n		
$\alpha 4$ wt $\beta 2$ wt (1:2)	0.17 ± 0.01	1.4 ± 0.1	15	-	0.07 - 0.45
$\alpha 4$ wt $\beta 2$ wt (10:1)	6.7 ± 1	0.86 ± 0.1	12	-	0.39 - 3.3
$\alpha 5V9'S$ $\alpha 4$ wt $\beta 2$ wt (10:1:1)	0.19 ± 0.02	1.4 ± 0.2	34	-	0.11 - 1.4
$\alpha 5V9'S$ W98A (Trp D)	0.27 ± 0.02	1.4 ± 0.1	15	1.4	0.030 - 0.65
$\alpha 5V9'S$ F136A (Tyr A)	0.16 ± 0.02	1.3 ± 0.2	12	0.8	0.095 - 0.30
$\alpha 5V9'S$ W191A (Trp B)	0.16 ± 0.01	1.4 ± 0.1	13	0.8	0.092 - 1.8
$\alpha 5V9'S$ D232Y (Tyr C1)	0.19 ± 0.02	1.4 ± 0.2	12	1	0.56 - 3.3
$\alpha 5V9'S$ Y237A (Tyr C2)	0.17 ± 0.01	1.3 ± 0.1	10	0.9	0.41 - 3.1

Table 3.6

Receptor (Ratio)	ACh Induced Current at +70 mV (Normalized)	Current Range (μA) at -110mV	Current Range (μA) at +70mV	n
$\alpha 5V9'S$ $\alpha 4$ wt $\beta 2$ wt (10:1:1)	0.34 ± 0.02	-0.56 to -2.5	0.15 to 1.2	34
$\alpha 5$ V9'S W98A (Trp D)	0.35 ± 0.03	-0.13 to -1.4	0.056 to 0.39	16
$\alpha 5$ V9'S F136A (Tyr A)	0.39 ± 0.03	-0.13 to -0.68	0.040 to 0.43	16
$\alpha 5$ V9'S W191A (Trp B)	0.43 ± 0.03	-0.18 to -3.2	0.064 to 1.2	18
$\alpha 5$ V9'S D232Y (Tyr C1)	0.37 ± 0.41	-0.34 to -6.1	0.10 to 1.7	14
$\alpha 5$ V9'S Y237A (Tyr C2)	0.38 ± 0.03	-0.12 to -6.0	0.080 to 1.4	15

ACh doses were the corresponding receptor's EC_{50} value for the voltage jump experiments

3.5 Discussion

Accessory subunits play important roles in nAChR function, because they confer unique properties to their parent receptors. Not surprisingly, expression of these subunits is highly regulated and restricted to specific brain regions (5,30). Some examples of this region specificity are found in the cerebral cortex, where $\alpha 5^*$ receptors are expressed only in layer VI, and in the striatum, where $\alpha 5$ may be expressed only in the dopaminergic neurons of the caudatoputamen, but not in the nucleus accumbens region (31-33). $\alpha 5$ is of particular interest because well-replicated human genome-wide association studies have identified a single nucleotide polymorphism that affects the risk for nicotine dependence, lung cancer, and alcohol dependence (34-36). This mutation, encoding Asn at position 398 in the coding region of the *CHRNA5* gene, also affects nicotine self-administration in mice (3,37). Thus, it would be beneficial to be able to probe functional differences of $\alpha 5^*$ receptors using pharmacological agents *in vivo*.

Here we aimed to elucidate possible ligand binding motifs involving the $\alpha 5$ subunit in the $(\alpha 4\beta 2)_2(\alpha 5)$ receptor. The α designation for $\alpha 5$ arose from the existence of adjacent Cys residues in the C loop (**Fig. 3.1B**), although other aspects of the C loop, such as replacement of conserved TyrC1 and residue deletions, are more β -like. Also, $\alpha 5$ is unable to form functional receptors unless other α subunits are also expressed. As such, $\alpha 5$ is generally considered to be an accessory subunit. However, the discovery of an $\alpha 4$ – $\alpha 4$ binding interface in A3B2 $\alpha 4\beta 2$ receptors suggests the possibility of an unusual binding site at the $\alpha 5$ – $\alpha 4$ binding interface (8).

To address this question, we first optimized our expression system to ensure a homogeneous, or at least very highly enriched, population of receptors. Early studies on

wild type receptors in oocytes suggested that biasing mRNA injection ratios strongly toward $\alpha 5$ would produce a homogeneous population of $\alpha 5$ -containing receptors. However, expression levels were low, making thorough characterization challenging. Introducing a V9'S mutation into the $\alpha 5$ subunit resulted in increased agonist responses, allowing greater consistency and reproducibility between experiments.

We have two lines of evidence to support the argument that $\alpha 5$ is incorporated into the receptor and that the population of receptors on the oocyte plasma membrane is homogeneous or very nearly so. First, we see altered rectification behavior for channels with $\alpha 5$ vs. pure $\alpha 4\beta 2$ receptors (**Fig. 3.3**). The effect is evident in fully wild type receptors, but is more apparent for the $\alpha 5V9'S$ receptors. This is the second system for which we have observed that a 9' mutation can markedly affect channel rectification properties. A single 9' mutation in the accessory subunit location – $\alpha 5V9'S$ in this case – is sufficient to alter the rectification properties of the receptor. In the $\alpha 4\beta 2$ receptor, the A3B2 receptor with the L9'A mutation in the $\alpha 4$ subunit shows a marked loss of rectification, but replacing the third $\alpha 4L9'A$ subunit with a $\beta 2$ subunit (A2B3) restores rectification (**Table 3.2**) (12).

The second argument for incorporation of $\alpha 5$ into our expressed receptors is based on altered behavior by the channel blocker mecamylamine. For $\alpha 4\beta 2$ receptors, mecamylamine blockade washes out very slowly, and most efficiently when agonist is also added (**Fig. 3.4B**). When the $\alpha 5V9'S$ subunit is included, mecamylamine blockade washes out readily. Note that the washout is essentially complete, arguing that all, or very nearly all, receptors contain the $\alpha 5$ subunit. Any population of $\alpha 4\beta 2$ receptors would have led to residual mecamylamine block. The alteration of mecamylamine block is only

seen when the V9'S mutation is present in $\alpha 5$. An $\alpha 4$ L9'A mutation also impacts mecamylamine block, indicating that it is the pore mutation that is affecting block, not the intrinsic properties of the $\alpha 5$ subunit. Presumably, mecamylamine binds within the pore near the 9' residue.

Having established that $\alpha 5$ is incorporated into the receptors, we can comment on its impact on receptor function. It is interesting that the $\alpha 4\beta 2\alpha 5$ receptor has essentially the same EC_{50} as the $(\alpha 4\beta 2)_2(\beta 2)$ receptor. This strongly suggests that the $\alpha 5$ subunit is not displacing an $\alpha 4$ subunit that contributes to an agonist binding site, as this should produce an EC_{50} change, especially since any mutation of TyrC1 in nAChR agonist binding sites shifts EC_{50} strongly, and $\alpha 5$ is mutated at that site. The same argument could be made that $\alpha 5$ does not replace a $\beta 2$ subunit that contributes to the agonist binding site, although perhaps less forcefully since the two have similar sequences in loop D. Note that if two (or more) $\alpha 5$ subunits were incorporated, then one of the canonical $\alpha 4/\beta 2$ interfaces would disappear, and again it is difficult to imagine that happening without EC_{50} being impacted. It is surprising that the V9'S mutation in $\alpha 5$ does not shift EC_{50} . Typically, introducing a polar substituent at any 9' position of a nAChR leads to a drop in EC_{50} . In other cases the wild type 9' residue is Leu not Val, but it is not obvious why that would lead to a change in behavior

To probe for the existence of an agonist binding site at the $\alpha 5$ – $\alpha 4$ interface, we mutated the conserved residues in $\alpha 5$ that would contribute to the aromatic box of such a binding site (TyrA, TrpB, TyrC1, and TyrC2). Converting an aromatic to an Ala or converting the Asp that aligns with TyrC1 to Tyr did not have a marked effect on agonist responses. These are fairly dramatic mutations that would produce very substantial shifts

in EC₅₀ in established agonist binding sites. We also mutated TrpD of $\alpha 5$ to Ala, to probe whether $\alpha 5$ replaces a $\beta 2$ subunit and contributes a complementary face, interacting with an $\alpha 4$ subunit. Again, no meaningful impact on receptor function was seen.

The most straightforward interpretation of these results is that there is no ACh or nicotine binding site at the $\alpha 5$ – $\alpha 4$ interface, and so mutation of key residues has no functional impact. We cannot rule out the possibility that ACh binds to the $\alpha 5$ – $\alpha 4$ interface, but that the binding does not meaningfully impact receptor function. Also, our assay precludes the application of drugs at concentrations greater than 100 μ M for $\alpha 5^*$ receptors, and so it is possible that there is a very low affinity binding site (dissociation constant on the order of mM). However, the biological implications of such a site seem negligible. Also, it is possible that other drugs could bind at the $\alpha 5$ – $\alpha 4$ interface, and that binding at the $\alpha 5$ – $\alpha 4$ interface could have a functional consequence in receptors in which the conventional, $\alpha 4$ – $\beta 2$ interfaces have in some way been compromised.

Although it does not contribute an ACh binding site in the nAChRs studied here, the $\alpha 5$ subunit can play other important roles. The $\alpha 5$ subunit also co-assembles with $\alpha 3$ and $\beta 4$ subunits to form functional nAChRs, especially in peripheral ganglia and in the medial habenula-interpeduncular nucleus pathway (3), and it has been shown to modulate expression levels of these receptors (38). Also, the $\alpha 5$ subunit could impart pore-related differences such as Ca²⁺ permeability (7), and intracellular loop-related differences such as endoplasmic reticulum exit and synaptic targeting (39).

In conclusion, we have developed a protocol for preparing highly enriched populations of ($\alpha 4\beta 2$)₂($\alpha 5$) nAChRs, and we have shown that mutations that would be expected to disrupt an $\alpha 5$ – $\alpha 4$ interfacial binding site do not affect receptor function. In

addition, we have shown that $\alpha 5$ subunits only occupy the auxiliary position when co-assembled with $\alpha 4$ and $\beta 2$ subunits. Further studies will be required to develop a strategy for selectively probing $\alpha 5^*$ receptors with pharmacological agents.

3.6 Acknowledgments

We thank Bruce N. Cohen for help with data interpretation. This work was supported by grants from the NIH (NS034407, DA017279, DA280382), NIH/NRSA (GM07616), and the California Tobacco-Related Disease Research Program from the University of California (19XT-0102).

3.7 References

1. Brodtkorb, E., and Picard, F. (2006) Tobacco habits modulate autosomal dominant nocturnal frontal lobe epilepsy. *Epilepsy and Behavior* **9**, 515-521
2. Nelson, M., Kuryatov, A., Choi, C., Zhou, Y., and Lindstrom, J. (2003) Alternate Stoichiometries of the $\alpha 4\beta 2$ Nicotinic Acetylcholine Receptors. *Molecular Pharmacology* **63**, 332-342
3. Fowler, C. D., Lu, Q., Johnson, P. M., Marks, M. J., and Kenny, P. J. (2011) Habenular $\alpha 5$ nicotinic receptor subunit signalling controls nicotine intake. *Nature* **471**, 597-601
4. Salminen, O., Murphy, K. L., McIntosh, J. M., Drago, J., Marks, M. J., Collins, A. C., and Grady, S. R. (2004) Subunit Composition and Pharmacology of Two Classes of Striatal Presynaptic Nicotinic Acetylcholine Receptors Mediating Dopamine Release in Mice. *Molecular Pharmacology* **65**, 1526-1536
5. Gotti, C., Zoli, M., and Clementi, F. (2006) Brain nicotinic acetylcholine receptors: native subtypes and their relevance. *Trends Pharmacol Sci* **27**, 482-491
6. Bailey, C. D., De Biasi, M., Fletcher, P. J., and Lambe, E. K. (2010) The nicotinic acetylcholine receptor $\alpha 5$ subunit plays a key role in attention circuitry and accuracy. *J Neurosci* **30**, 9241-9252
7. Kuryatov, A., Onksen, J., and Lindstrom, J. (2008) Roles of accessory subunits in $\alpha 4\beta 2(*)$ nicotinic receptors. *Molecular Pharmacology* **74**, 132-143
8. Mazzaferro, S., Benallegue, N., Carbone, A., Gasparri, F., Vijayan, R., Biggin, P. C., Moroni, M., and Bermudez, I. (2011) Additional acetylcholine (ACh) binding site at $\alpha 4/\alpha 4$ interface of $(\alpha 4\beta 2)_2\alpha 4$ nicotinic receptor influences agonist sensitivity. *J Biol Chem* **286**, 31043-31054
9. Rohde, L. A., Ahring, P. K., Jensen, M. L., Nielsen, E. O., Peters, D., Helgstrand, C., Krintel, C., Harpsoe, K., Gajhede, M., Kastrup, J. S., and Balle, T. (2012) Intersubunit bridge formation governs agonist efficacy at nicotinic acetylcholine $\alpha 4\beta 2$ receptors: unique role of halogen bonding revealed. *J Biol Chem* **287**, 4248-4259
10. Harpsoe, K., Ahring, P. K., Christensen, J. K., Jensen, M. L., Peters, D., and Balle, T. (2011) Unraveling the high- and low-sensitivity agonist responses of nicotinic acetylcholine receptors. *J Neurosci* **31**, 10759-10766
11. Nowak, M., Gallivan, J. P., Silverman, S., Labarca, C. G., Dougherty, D. A., and Lester, H. A. (1998) In Vivo Incorporation of Unnatural Amino Acids into Ion Channels in Xenopus Oocyte Expression System. *Methods Enzymol* **293**, 504-530
12. Xiu, X., Puskar, N. L., Shanata, J. A., Lester, H. A., and Dougherty, D. A. (2009) Nicotine binding to brain receptors requires a strong cation- π interaction. *Nature* **458**, 534-537
13. Moroni, M., Zwart, R., Sher, E., Cassels, B. K., and Bermudez, I. (2006) $\alpha 4\beta 2$ nicotinic receptors with high and low acetylcholine sensitivity: pharmacology, stoichiometry, and sensitivity to long-term exposure to nicotine. *Molecular Pharmacology* **70**, 755-768
14. Ramirez-Latorre, J., Yu, C. R., Qu, X., Perin, F., Karlin, A., and Role, L. (1996) Functional contributions of $\alpha 5$ subunit to neuronal acetylcholine receptor channels. *Nature* **380**, 347-352

15. Filatov, G. N., and White, M. M. (1995) The Role Of Conserved Leucines In The M2 Domain Of The Acetylcholine-Receptor In Channel Gating. *Molecular Pharmacology* **48**, 379-384
16. Kearney, P. C., Zhang, H., Zhong, W., Dougherty, D. A., and Lester, H. A. (1996) Determinants of nicotinic receptor gating in natural and unnatural side chain structures at the M2 9' position. *Neuron* **17**, 1221-1229
17. Labarca, C., Nowak, M. W., Zhang, H. Y., Tang, L. X., Deshpande, P., and Lester, H. A. (1995) Channel Gating Governed Symmetrically By Conserved Leucine Residues In The M2 Domain Of Nicotinic Receptors. *Nature* **376**, 514-516
18. Zhong, W., Gallivan, J. P., Zhang, Y., Li, L., Lester, H. A., and Dougherty, D. A. (1998) From *ab initio* Quantum Mechanics to Molecular Neurobiology: A Cation- π Binding Site in the Nicotinic Receptor. *Proc. Natl. Acad. Sci. (USA)* **95**, 12088-12093
19. Gleitsman, K. R., Shanata, J. A., Frazier, S. J., Lester, H. A., and Dougherty, D. A. (2009) Long-range coupling in an allosteric receptor revealed by mutant cycle analysis. *Biophys J* **96**, 3168-3178
20. Groot-Kormelink, P. J., Boorman, J. P., and Sivilotti, L. G. (2001) Formation of functional $\alpha 3\beta 4\alpha 5$ human neuronal nicotinic receptors in *Xenopus* oocytes: a reporter mutation approach. *British Journal of Pharmacology* **134**, 789-797
21. Li, P., McCollum, M., Bracamontes, J., Steinbach, J. H., and Akk, G. (2011) Functional characterization of the $\alpha 5$ (Asn398) variant associated with risk for nicotine dependence in the $\alpha 3\beta 4\alpha 5$ nicotinic receptor. *Molecular Pharmacology* **80**, 818-827
22. Papke, R. L., Sanberg, P. R., and Shytle, R. D. (2001) Analysis of Mecamylamine Stereoisomers on Human Nicotinic Receptor Subtypes. *Journal of Pharmacology and Experimental Therapeutics* **297**, 646-657
23. Lester, H. A. (1992) The Permiation Pathway of Neurotransmitter-Gated Ion Channels. *Annual Review of Biophysics* **21**, 267-293
24. Mu, T., Lester, H. A., and Dougherty, D. A. (2003) Different Binding Orientations for the Same Agonist at Homologous Receptors: A Lock and Key or a Simple Wedge? *Journal of the American Chemical Society* **125**, 6850-6852
25. Cashin, A. L., Petersson, E. J., Lester, H. A., and Dougherty, D. A. (2005) Using Physical Chemistry To Differentiate Nicotinic from Cholinergic Agonists at the Nicotinic Acetylcholine Receptor. *Journal of the American Chemical Society* **127**, 350-357
26. Dougherty, D. A. (2008) Cys-Loop Neuroreceptors: Structure to the Rescue? *Chemical Reviews* **108**, 1642-1654
27. Puskar, N. L., Xiu, X., Lester, H. A., and Dougherty, D. A. (2011) Two Neuronal Nicotinic Acetylcholine Receptors, $\alpha 4\beta 4$ and $\alpha 7$, Show Differential Agonist Binding Modes. *Journal of Biological Chemistry* **286**, 14618-14627
28. Tavares, X. D., Blum, A. P., Nakamura, D. T., Puskar, N. L., Shanata, J. A., Lester, H. A., and Dougherty, D. A. (2012) Variations in binding among several agonists at two stoichiometries of the neuronal, $\alpha 4\beta 2$ nicotinic receptor. *Journal of the American Chemical Society* **134**, 11474-11480

29. Dougherty, D. A. (2013) The Cation- π Interaction. *Accounts of Chemical Research* **46**, 885-893
30. Miwa, J. M., Freedman, R., and Lester, H. A. (2011) Neural systems governed by nicotinic acetylcholine receptors: emerging hypotheses. *Neuron* **70**, 20-33
31. Salas, R., Orr-Urtreger, A., Broide, R. S., Beaudet, A., Paylor, R., and De Biasi, M. (2003) The Nicotinic Acetylcholine Receptor Subunit $\alpha 5$ Mediates Short-Term Effects of Nicotine in Vivo. *Molecular Pharmacology* **63**, 1059-1067
32. Wada, E., McKinnon, D., Heinemann, S., Patrick, J., and Swanson, L. W. (1990) The distribution of mRNA encoded by a new member of the neuronal nicotinic acetylcholine receptor gene family ($\alpha 5$) in the rat central nervous system. *Brain Research* **526**, 45-54
33. Exley, R., McIntosh, J. M., Marks, M. J., Maskos, U., and Cragg, S. J. (2012) Striatal $\alpha 5$ nicotinic receptor subunit regulates dopamine transmission in dorsal striatum. *J Neurosci* **32**, 2352-2356
34. Saccone, N. L., Saccone, S. F., Hinrichs, A. L., Stitzel, J. A., Duan, W., Pergadia, M. L., Agrawal, A., Breslau, N., Grucza, R. A., Hatsukami, D., Johnson, E. O., Madden, P. A. F., Swan, G. E., Wang, J., Goate, A. M., Rice, J. P., and Bierut, L. J. (2009) Multiple Distinct Risk Loci for Nicotinic Dependence Identified by Dense Coverage of the Complete Family of Nicotinic Receptor Subunit (CHRNA5) Genes. *American Journal of Medical Genetics Neuropsychiatric Genetics*, 453-467
35. Bierut, L. J. (2010) Convergence of genetic findings for nicotine dependence and smoking related diseases with chromosome 15q24-25. *Trends Pharmacol Sci* **31**, 46-51
36. Hartz, S. M., Short, S. E., Saccone, N. L., Culverhouse, R., Chen, L., Schwantes-An, T. H., Coon, H., Han, Y., Stephens, S. H., Sun, J., Chen, X., Ducci, F., Dueker, N., Franceschini, N., Frank, J., Geller, F., Gubjartsson, D., Hansel, N. N., Jiang, C., Keskitalo-Vuokko, K., Liu, Z., Lyytikainen, L. P., Michel, M., Rawal, R., Rosenberger, A., Scheet, P., Shaffer, J. R., Teumer, A., Thompson, J. R., Vink, J. M., Vogelzangs, N., Wenzlaff, A. S., Wheeler, W., Xiao, X., Yang, B. Z., Aggen, S. H., Balmforth, A. J., Baumeister, S. E., Beaty, T., Bennett, S., Bergen, A. W., Boyd, H. A., Broms, U., Campbell, H., Chatterjee, N., Chen, J., Cheng, Y. C., Cichon, S., Couper, D., Cucca, F., Dick, D. M., Foroud, T., Furberg, H., Giegling, I., Gu, F., Hall, A. S., Hallfors, J., Han, S., Hartmann, A. M., Hayward, C., Heikkila, K., Hewitt, J. K., Hottenga, J. J., Jensen, M. K., Jousilahti, P., Kaakinen, M., Kittner, S. J., Konte, B., Korhonen, T., Landi, M. T., Laatikainen, T., Leppert, M., Levy, S. M., Mathias, R. A., McNeil, D. W., Medland, S. E., Montgomery, G. W., Muley, T., Murray, T., Nauck, M., North, K., Pergadia, M., Polasek, O., Ramos, E. M., Ripatti, S., Risch, A., Ruczinski, I., Rudan, I., Salomaa, V., Schlessinger, D., Styrkarsdottir, U., Terracciano, A., Uda, M., Willemsen, G., Wu, X., Abecasis, G., Barnes, K., Bickel, H., Boerwinkle, E., Boomsma, D. I., Caporaso, N., Duan, J., Edenberg, H. J., Francks, C., Gejman, P. V., Gelernter, J., Grabe, H. J., Hops, H., Jarvelin, M. R., Viikari, J., Kahonen, M., Kendler, K. S., Lehtimäki, T., Levinson, D. F., Marazita, M. L., Marchini, J., Melbye, M., Mitchell, B. D., Murray, J. C., Nothen, M. M., Penninx, B. W., Raitakari, O., Rietschel, M., Rujescu, D., Samani, N. J., Sanders, A. R., Schwartz,

- A. G., Shete, S., Shi, J., Spitz, M., Stefansson, K., Swan, G. E., Thorgeirsson, T., Volzke, H., Wei, Q., Wichmann, H. E., Amos, C. I., Breslau, N., Cannon, D. S., Ehringer, M., Grucza, R., Hatsukami, D., Heath, A., Johnson, E. O., Kaprio, J., Madden, P., Martin, N. G., Stevens, V. L., Stitzel, J. A., Weiss, R. B., Kraft, P., and Bierut, L. J. (2012) Increased Genetic Vulnerability to Smoking at CHRNA5 in Early-Onset Smokers. *Archives of General Psychiatry* **69**, 854-861
37. Frahm, S., Šlimak, Marta A., Ferrarese, L., Santos-Torres, J., Antolin-Fontes, B., Auer, S., Filkin, S., Pons, S., Fontaine, J.-F., Tsetlin, V., Maskos, U., and Ibañez-Tallon, I. (2011) Aversion to Nicotine Is Regulated by the Balanced Activity of $\beta 4$ and $\alpha 5$ Nicotinic Receptor Subunits in the Medial Habenula. *Neuron* **70**, 522-535
38. George, A. A., Lucero, L. M., Damaj, M. I., Lukas, R. J., Chen, X., and Whiteaker, P. (2012) Function of human $\alpha 3\beta 4\alpha 5$ nicotinic acetylcholine receptors is reduced by the $\alpha 5$ (D398N) variant. *J Biol Chem* **287**, 25151-25162
39. Gotti, C., Moretti, M., Zanardi, A., Gaimarri, A., Champtiaux, N., Changeux, J. P., Whiteaker, P., Marks, M. J., Clementi, F., and Zoli, M. (2005) Heterogeneity and selective targeting of neuronal nicotinic acetylcholine receptor (nAChR) subtypes expressed on retinal afferents of the superior colliculus and lateral geniculate nucleus: Identification of a new native nAChR subtype $\alpha 3\beta 2(\alpha 5$ or $\beta 3)$ enriched in retinocollicular afferents. *Molecular Pharmacology* **68**, 1162-1171

Chapter 4

Assay Development for Positive Allosteric Modulator Studies: Identification of Necessary Residues for Potentiation of Type I Modulators in $\alpha 7$ Nicotinic Acetylcholine Receptors

4.1 Abstract

Nicotinic acetylcholine receptors (nAChRs) play vital roles in neuronal communication and are targets for neurological disorders. The $\alpha 7$ nAChR has been tied to schizophrenia and Alzheimer's disease, which has resulted in a vast array of selective agonists. Over the last decade, research has increased on another class of compounds, positive allosteric modulators (PAMs). Allosteric modulators can influence physiological responses of the receptor when the natural neurotransmitter is present. However, our understanding of distinct structure-function relationships for these compounds is minimal.

This report involves modification of experimental methods for PAM potentiation measurements by introducing a temperature-controlling apparatus and using a new analysis method, charge integration, for the $\alpha 7$ receptor. This new assay was used to monitor mutagenesis effects on PAM potentiation. It was found that gain-of-function pore mutations greatly attenuate Type I PAM potentiation and that mutations in the transmembrane domain can reduce or eliminate these effects. These results suggest a different region, adjacent to Type II PAM binding, that is vital in Type I potentiation in

the $\alpha 7$ receptor. Further research can provide mechanistic insight to the residues responsible for Type I and Type II PAM physiological differentiation.

4.2 Introduction

Neuronal nicotinic acetylcholine receptors (nAChRs) are a class of membrane proteins that belong to the Cys-loop superfamily of ligand-gated ion channels (LGICs). These receptors are composed of five subunits ($\alpha 2$ - $\alpha 7$, $\alpha 9$, $\alpha 10$, or $\beta 2$ - $\beta 4$) that can assemble homo- or heteromerically to form a pore that, when activated, allows cations to pass across the membrane (1-4). Ion permeability permits these receptors to play a large role in neuronal communication in the central nervous system (CNS). The diversity in receptor function and CNS distribution ties nAChRs to vital functions like memory and learning but also implicates them in neurological disorders such as addiction, Alzheimer's disease, and Parkinson's disease (2,4-8).

The $\alpha 7$ nAChR is a unique homopentamer that is widely distributed throughout the brain and has been associated with neurological disorders such as schizophrenia and Alzheimer's disease (9-16). In the case of Alzheimer's disease, there are studies suggesting direct inhibition of function when associated with aggregated amyloid- β peptides (11,12). Discovering agonists that selectively activate the $\alpha 7$ receptor may be insufficient to reverse some of the effects associated with Alzheimer's disease. In the last decade, more research has been dedicated to studying compounds that are positive allosteric modulators (PAMs) of $\alpha 7$ and other nAChRs (7,9,13,15,17-25). Allosteric modulators are compounds that bind to the protein at locations that are distant from the normal agonist binding pocket and change the receptor's function without directly

activating the receptor. The “positive” notion indicates a beneficial cooperativity in receptor function when a PAM and agonist are co-applied. Generally, an increase in current is observed upon co-application of a PAM with an agonist compared to the agonist alone. This can be represented by two functional changes: a decrease in EC_{50} values (gain-of-function) and/or a larger signal for all the doses of the original EC_{50} experiment (**Figure 4.1**). These two cases are not exclusive and both tend to affect EC_{50} curves (9,18,21,22).

PAMs have received more attention as pharmaceutical targets because they have the potential to modulate receptor response without direct activation of the receptor. In addition, they have the potential to be more specific to receptor association, thus lowering side effects (9). Because of their potential in disease treatment, understanding where they bind and how they generate their effects is vital for further rational drug design.

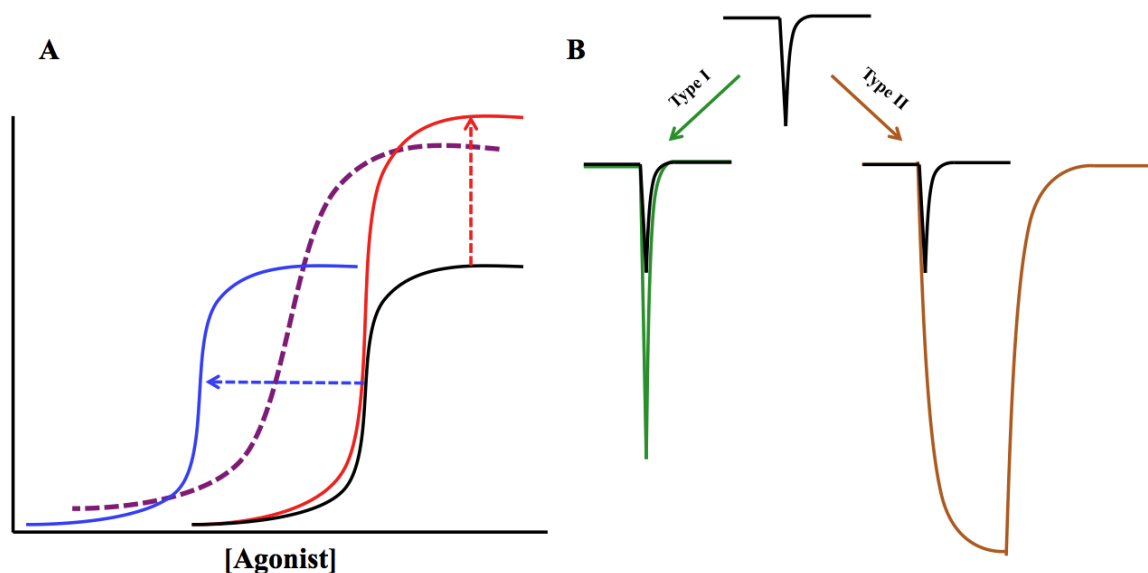


Figure 4.1 (A) Effects of PAMs on EC_{50} curves. There can be a gain-of-function (blue) or an increase in signal (red) relative to agonist alone (black). However most cases involve both changes and a hybrid curve is seen (purple). (B) Two classes of PAMs for $\alpha 7$ nAChRs. Type I (green) elicit only a change in peak height. Type II (brown) affect peak height, closure rates, and can reactivate the desensitized state.

Currently, PAMs exist in two classes – Type I and Type II – and are separated according to the response they generate. Type I PAMs solely increase the peak current response, while Type II PAMs increase peak current response, drastically slow receptor closure rates, and can reactivate the desensitized state (**Figure 4.1**) (21). Numerous Type I and Type II PAMs have been developed for the $\alpha 7$ receptor. Probing for differences in structure-function relationships of the two types of PAMs would provide mechanistic insight to the distinct pharmacologies.

This report focuses on assay development and subsequent investigation of Type I PAMs for the $\alpha 7$ receptor. Experimental protocols and data analysis were adapted and expanded upon by inclusion of a temperature control system and peak integration measurements. Conventional amino acid mutagenesis was employed to identify residues needed for PAM potentiation. These results show that gain-of-function pore mutations severely attenuate Type I PAM properties and can convert PAMs into negative allosteric modulators (NAMs). In addition, several new residues studied here showed reduction or elimination of Type I PAM potentiation.

4.3 Results and Discussion

4.3.1 Assay Development for PAM Measurements

The first part of the report focuses on assay modification for consistent PAM signal potentiation. Type I PAMs have a singular effect in that they increase the signal response relative to the native agonist-only dose. These values are reported as a percent increase in peak height at a given agonist concentration. For these studies, we chose to use 100 μ M acetylcholine (ACh) since it was close to most EC_{50} values for mutations.

Table 4.1 PAM Potentiation Protocol

Applications	Notes	Future Studies Adaptations
100 μ M ACh	<i>Ignore</i>	EC50
100 μ M ACh	<i>Average together</i>	EC50
100 μ M ACh		EC50
100 μ M ACh and PAM	<i>60 s pre-incubation, co-application, and average together</i>	EC50 + PAM
100 μ M ACh and PAM		EC50 + PAM
100 μ M ACh	<i>Average together</i>	EC50
100 μ M ACh		EC50

This allowed for ample baseline signal while allowing room for signal to be potentiated. PAMs may decrease the barrier to reach the open-state equilibrium rather than change the equilibrium (or conductance) of open receptors at max concentrations. A shift in EC50 without an increase in max signal when comparing the agonist alone vs. agonist/PAM co-application experiments would represent this phenomenon (**Figure 4.1**).

The protocol outlined in **Table 4.1** was the experimental procedure designed to measure percent change in peak height for PAMs (*see 4.4.3 Methods for further information on experimental parameters regarding application durations and calculations*). The first dose is ignored because the initial fluidics of the experiment can have a significant effect on receptor response. The initial dose allows the system to come to equilibrium in regards to small movements during the first drug application and buffer wash. Repetitive doses allow for averaging of both the agonist-only and agonist/PAM co-application signals. In addition, abnormal receptor responses can be identified and eliminated from analysis. Pre-incubation of the PAM prior to the agonist/PAM co-application permits the PAM to come to binding equilibrium to ensure maximal response measurements and serves as an internal control to ensure introduced mutations do change the compound's profile from a PAM to an allosteric agonist (26,27). Subsequent doses of agonist only provide insight into the receptor's ability to return to

pre-PAM applications and give a qualitative assessment of removal of the PAM compound from the oocyte.

In the Dougherty lab, previous studies of the $\alpha 7$ receptor included a pore point mutation (T6'S) that slowed activation closure rates and desensitization. However, this mutation has large effects on PAM function (see **section 4.3.2** below for discussion) and cannot be used for these studies. Removal of the T6'S mutation from the $\alpha 7$ receptor makes electrophysiological recording more challenging because of the dramatic increase in closure rates of activated receptors. Maximum peak current response can be variable because the electrophysiological recordings cannot reliably record the closure rates. Papke *et al.* has introduced a way to reduce this variability by integrating the current response over the drug application time period for a total charge value instead of a peak height measurement (28). As seen in **Table 4.2**, introduction of the integration analysis has reduced the relative percent error in the receptor responses. When applied to the dose response curves, a decrease in the EC_{50} value to values near the T6'S mutation values are observed (see **Figure 4.2**). This analysis retains the gain-of-function property of the T6'S and provides a way to compare waveform anomalies that sometimes occur during repetitive dosing (**Figure 4.2**). Due to the lack of literature for interpretation of total charge analysis from peak integration, comparisons of PAM potentiation will involve both peak height measurements and integration analysis in some cases.

Table 4.2 Peak Height vs. Integration for PAM Potentiation					
		5-HI	<i>Relative Error</i>	5-MI	<i>Relative Error</i>
$\alpha 7$WT:hRic3	<i>Max Peak</i>	300 \pm 40	13%	760 \pm 100	13%
	<i>Integration</i>	450 \pm 30	7%	2600 \pm 100	4%
$\alpha 7$ WT	<i>Max Peak</i>	380 \pm 40	11%	600 \pm 60	10%
	<i>Integration</i>	480 \pm 40	8%	2400 \pm 150	6%

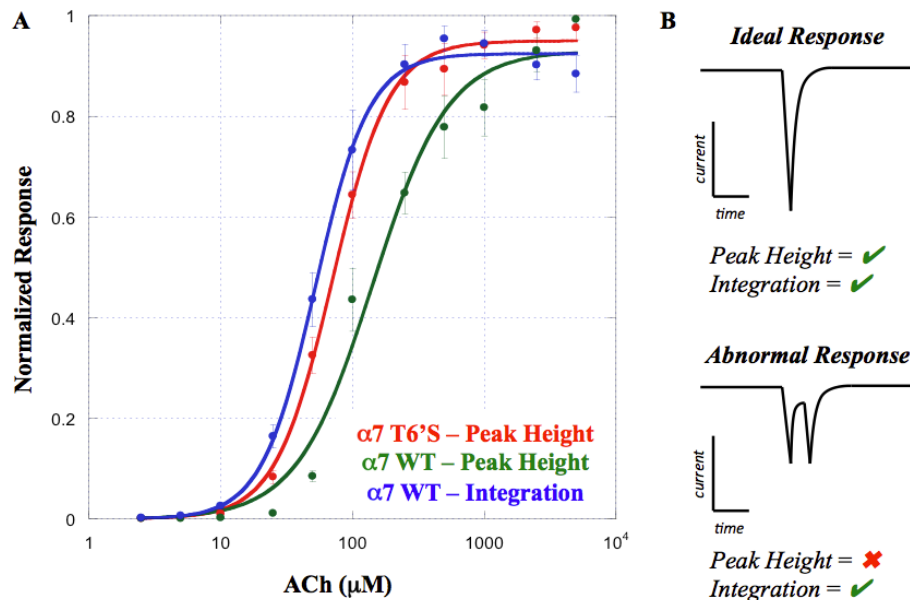


Figure 4.2 (A) Dose response curves for $\alpha 7$ T6'S:hRic3 and $\alpha 7$ WT:hRic3 using max peak current analysis and peak integration analysis. Integration of the peak response shifted the wild type (WT) receptor EC₅₀ to a value comparable to the T6'S receptor. The variability between cell measurements that arises due to the fast desensitization of the receptor is reduced through this method of analysis. (B) Examples of ideal and abnormal $\alpha 7$ WT responses. The closure rate is extremely fast, and the electronics have issues measuring large current changes. These generate unusable waveforms for peak height analysis. However, integration can recover these waveforms since the total charge is being calculated.

During experimental runs using the protocol outline in **Table 4.1**, an issue arose involving the measurements of receptor response to consecutive agonist-only doses. Comparing the signal response to identical agonist applications pre- and post-exposure to the PAM showed a steady increase in receptor response. In addition, replacing all steps with agonist only (and buffer for pre-incubation steps) showed a steady increase in signal despite the agonist applications being made of the same stock. The experiments were repeated at cooler temperatures (13-16°C) as opposed to room temperature (20°C) to solve the consistent signal increase. To achieve temperature control, a cooling unit (*MGW Lauda-Brinkmann rm3*) was adapted to the electrophysiology rig (See **Figure 4.3**). Roughly two feet of buffer lines were submerged in a second line containing salt/water

mixture, which was subsequently submerged into the cooling unit containing 100% isopropanol at a temperature of -4°C to -6°C . Depending on flow rates, the buffer entered the oocyte chamber in the range of $13\text{--}16^{\circ}\text{C}$. Drug plates were kept on ice during washing steps to ensure an application temperature less than 15°C . These were more variable and ranged from $9\text{--}14^{\circ}\text{C}$, but the main goal of sub- 15°C was consistently achieved. Temperature was monitored through a temperature-sensing adaptor for a multimeter (*Fluke 116 HVAC Multimeter*). Reduction of the experimental temperature can affect the two main sources of variability in these measurements: (1) the extremely fast desensitization of the receptor and (2) the steady increase in peak current over application of a constant concentration of agonist. Since the rates of conformational conversions are correlated with temperature, performing these experiments in a chilled buffer solution can slow conformational rearrangements and reduce some of the variability in the electrophysiological measurements. The steady signal increase can be attributed to the release of more vesicles containing receptors to the surface, which can

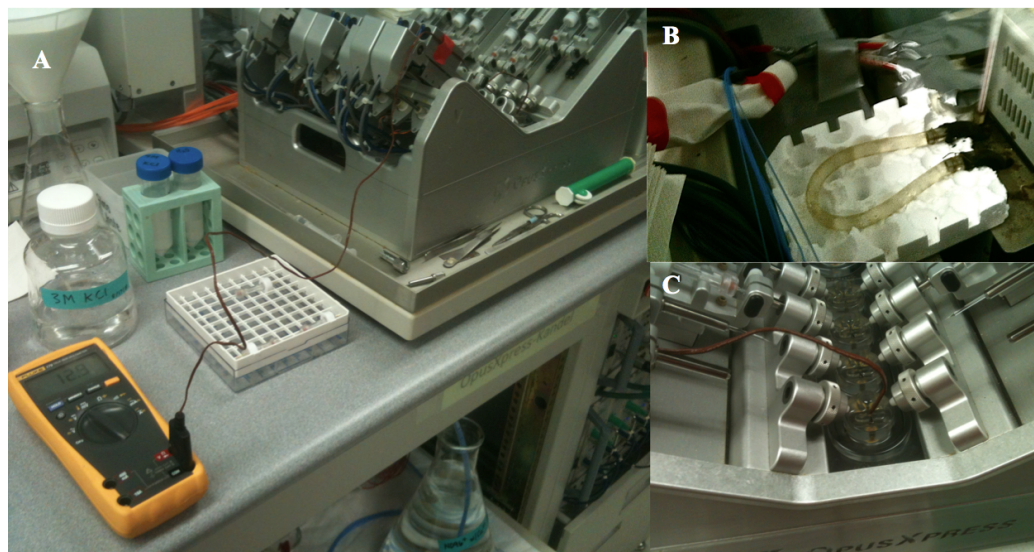


Figure 4.3 Attached cooling unit. (A) Temperature measuring multimeter. (B) Cooling unit with submerged tubing. (C) Multimeter sensor in recording chamber.

Table 4.3 Extracellular Mutations and Temperature Effects On Genistein

Receptor w/ <i>hRic3</i>	Room Temperature (19-20°C)			Cold Buffer Application (11-16°C)		
	EC ₅₀ (μM)	Hill	% PAM Inc.	EC ₅₀ (μM)	Hill	% PAM Inc.
α7 WT	52 ± 2	2.1 ± 0.2	950 ± 260	32 ± 1	3.2 ± 0.2	120 ± 14
α7 P83G	94 ± 3	1.9 ± 0.1	1400 ± 330	57 ± 6	3.0 ± 0.6	430 ± 30
α7 K89A	40 ± 1	1.7 ± 0.1	1400 ± 300	24 ± 0.5	3.6 ± 0.3	320 ± 40
α7 H107A	24 ± 2	1.6 ± 0.2	610 ± 80	15 ± 1	2.5 ± 0.2	290 ± 30
α7 F126A	—	—	—	5.5 ± 0.3	3.4 ± 0.5	130 ± 20
α7 K127A	—	—	—	15 ± 1	3.1 ± 0.5	230 ± 20
α7 Y153A	70 ± 5	1.4 ± 0.1	1000 ± 160	32 ± 3	2.0 ± 0.3	240 ± 30
α7 N173A	—	—	—	62 ± 6	2.4 ± 0.5	200 ± 20
α7 T201A	—	—	—	164 ± 6	4.6 ± 0.4	730 ± 180

Genistein = 10μM, All values are from integration data (no peak height analysis)

Green = Arias et al. (33), Blue = Ludwig et al. (32)

skew the data by causing a non-level baseline. Vesicle trafficking can be slowed and even halted by cooling the oocyte temperature to or below 15°C (29). An example comparing the effects of experiments performed at cooler temperatures can be seen in **Table 4.3**. There is a collective gain-of-function in regards to EC₅₀ values. In addition, there is dampening of the percent PAM increases and reduction in relative percent error.

The adaptations to the protocol and data analysis outline here greatly reduced the variability originally seen in initial measurements and provided reproducible measurements between repeated experiments. These PAM guidelines were used to further study mutational effects on a series of Type I PAMs outlined in the next section. PAM experiments in the future that utilize this protocol (**Table 4.1**) should change the concentration of agonist used for experiments. These studies used a single concentration of agonist (100 μM ACh) but use of the EC₅₀ value for the mutation being probed would be more appropriate. This would provide a better comparison of PAM potentiation across mutations. Despite this observation, the experiments here still provide useful starting points and conclusions regarding Type I effects on the α7 receptor. The temperature-controlling unit was a novel attachment to the electrophysiology rig and

provided the first series of controlled temperature experiments for the Dougherty lab. It can be easily transcribed to other electrophysiology experiments (such as EC₅₀ experiments) and allows a new analysis for determining binding parameters not previously accessible from a single temperature study.

4.3.2 Screening for Residues Essential in PAM Potentiation

The second half of this report deals with identification of a PAM binding location on the rat $\alpha 7$ receptor and characterization of the important interactions for potentiation. As noted above, there are two classes of PAMs: Type I, which increase peak currents only, and Type II, which affect several parameters involved in activation, closure, and desensitization. Because Type I PAMs have a single effect on the $\alpha 7$ receptor, interpretation of the results remains simpler and allows easier identification of functional changes. Efforts toward the elucidation of Type I PAM potentiation on $\alpha 7$ are presented and discussed. 5-methoxyindole (5-MI), 5-hydroxyindole (5-HI), and genistein were the main probes in the structure-function studies of this report (**Figure 4.4**).

The T6'S mutation had drastic effects on responses to 5-MI and 5-HI. The signal from co-application with 5-MI was severely attenuated and 5-HI was converted to a negative allosteric modulator (NAM). The T6'S mutation is located on the M2 helix of the receptor pore and has been used previously in $\alpha 7$ nAChR studies because it reduces the rate of desensitization and presents a gain-of-function (30). These properties allow more reliable current measurements at high agonist concentrations and a wider range to observe changes in EC₅₀ values. Another factor to consider is the human Ric3 protein (hRic3), a trafficking protein that is routinely used to increase $\alpha 7$ receptor expression in

oocytes (31). In the present system, the presence of hRic3 had no meaningful effects on PAM potentiation measurements (**Figure 4.4**). Positive signal potentiation for 5-HI was recovered by reverting back to the original $\alpha 7$ wild type receptor, and 5-MI showed a dramatic increase in potency (**Figure 4.4**). Again, potentiation response was unaffected by the presence of hRic3, although receptor expression levels were generally higher while co-expressed with hRic3. These results suggest that further use of hRic3 for PAM studies is acceptable (and was included in further studies), while the T6'S mutation is detrimental. One possible explanation is that the T6'S mutation may act like a pseudo-Type II PAM itself because it affects receptor desensitization. Introduction of this pore mutation severely attenuates or even reverses Type I PAM current potentiation.

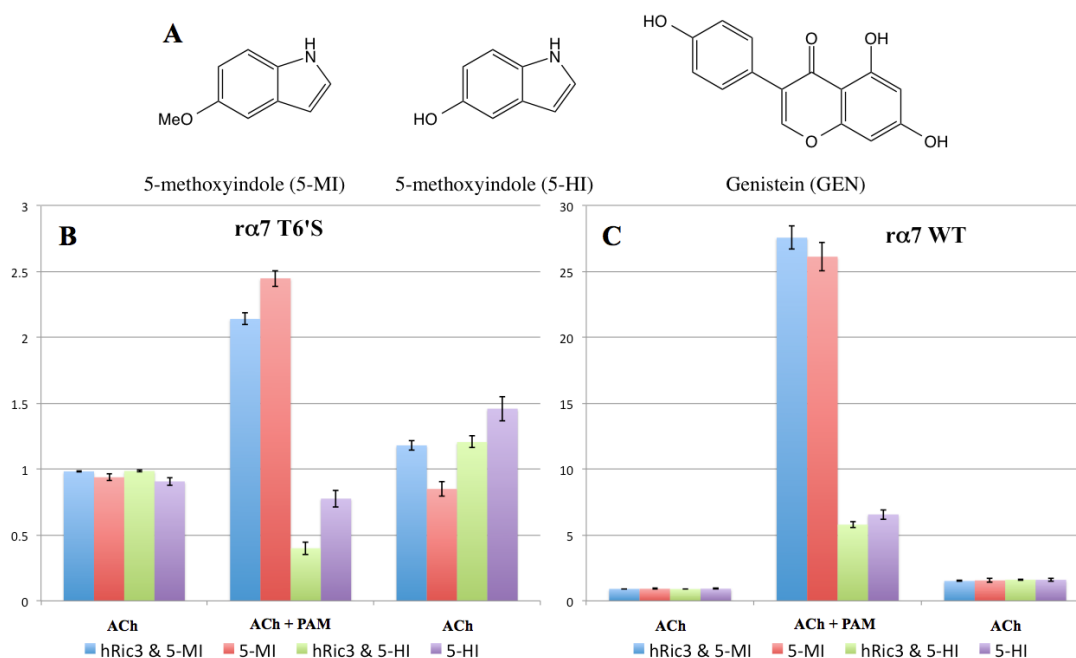


Figure 4.4 PAM function is greatly influenced by the gain-of-function pore mutation T6'S. The hRic3 protein does not affect potentiation. (A) Type I PAMs 5-hydroxyindole (5-HI), 5-methoxyindole (5-MI), and Genistein (GEN). (B) PAM responses for the $\alpha 7$ T6'S nAChR with and without hRic3. The agonist dose was 100 μ M ACh and the PAM concentrations were all 1000 μ M with a 60 s pre-incubation before co-application. (C) PAM responses for the rat $\alpha 7$ WT nAChR with and without hRic3. The agonist dose was 100 μ M ACh and the PAM concentrations were all 1000 μ M. Type I PAM properties are recovered.

Even though 5-MI and 5-HI give large potentiation, they require high doses (1 mM) to elicit potentiation, which is undesirable. Also, the chemical structures are small and provide minimal interactions to probe for structure-function relations. Genistein (a tyrosine kinase inhibitor, see **Figure 4.4**) has a larger structure capable of forming more binding interactions and has been shown to be a Type I PAM of the $\alpha 7$ nAChR (21). Also, it has a potent signal potentiation at a smaller drug concentration (10 μ M). These attributes led to a switch in compounds for further Type I PAM structure-function studies.

At the time of these studies, several different sites were proposed for PAM binding or at least implicated as important for PAM potentiation in the $\alpha 7$ receptor. Several residues in various areas were mutated and put through our adapted methodology. Two different locations in the extracellular region were studied first. Ludwig *et al.* proposed a PAM binding site adjacent to the agonist-binding site (32), and Arias *et al.* proposed a PAM binding site on the opposite side compared to Ludwig's proposal (**See Figure 4.5**) (33). Due to the disparity of these proposed binding sites, several residues from each location were probed through alanine-mutation screening. The mutations and integration analysis results for room temperature and temperature-controlled measurements are outlined in **Table 4.3**. These results suggest that residues K89 and Y153 do not play a role in genistein binding or its potentiation, because the EC_{50} values and the PAM percent increases are essentially the same as for the wild type receptor. Residues' P83, H107, and Y153 effects are less clear due to the varying EC_{50} values and the lack in significant changes in PAM percent increase when compared to the wild type values. An important note, however, is that none of these

mutations dampened or eliminated the PAM response compared to the wild type receptor. The lack of a mutation that decreased or eliminated the PAM response suggests that these residues do not make direct interactions in PAM binding or influence its potentiation.

The $\alpha 7$ receptor transmembrane region was probed next as it has been suggested to be the binding region for a Type II PAM, PNU-120596 (18,20,24). Several key residues were identified to be important in PNU-120596 action because of the significantly reduced peak potentiation: S245, A248, M276, F478, and C482 (numbering adjusted to full length $\alpha 7$ with the signaling sequence). These residues and several others surrounding this region were subjected to an alanine scan or the mutation used in previous studies (**Table 4.4**) (18,20,24). The first observation is that not all of the residues identified for PNU-120596 reduction decreased genistein potentiation. A248D and C482Y did not produce meaningful changes from the wild type response to genistein. Interestingly, C482Y had a large increase in potentiation, which is the opposite of what

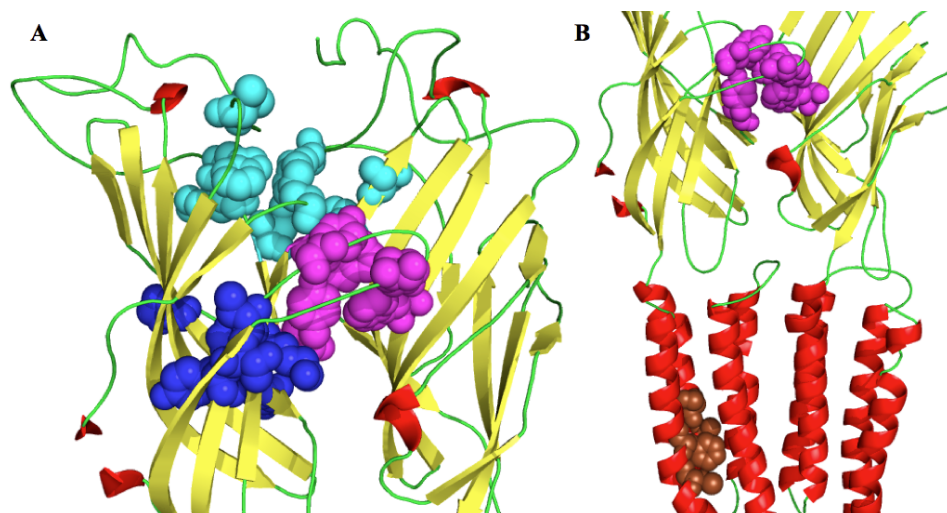


Figure 4.5 A homology model of two adjacent $\alpha 7$ subunits. (A) The binding site proposed by Ludwig *et al.* is colored in blue (32). The binding site proposed by Arias *et al.* is colored in cyan (33). The aromatic box (agonist binding pocket) is in magenta. (B) The binding site proposed by Young *et al.* is colored in brown (24). These residues are situated between the four transmembrane α -helices of one subunit. Several residues from all sites were studied.

Table 4.4 Transmembrane Mutations For Genistein

$\alpha 7$	n	EC ₅₀ (μ M)		%PAM Increase	
		Peak	Area	Peak	Area
Wild Type	11/16	274 \pm 7	78 \pm 5	360 \pm 40	500 \pm 50
G175K*	7/11	17 \pm 2	3.3 \pm 0.2	80 \pm 20	150 \pm 20
Y232A	6/4	<i>No expression</i>		<i>No expression</i>	
N236A	19/10	300 \pm 8	54 \pm 5	7 \pm 8	20 \pm 8
C241A	7/5	224 \pm 10	71 \pm 2	-26 \pm 5	-33 \pm 6
S245A	7/7	—	—	50 \pm 15	220 \pm 20
A248D	3/3	—	—	250 \pm 30	830 \pm 100
T267A	5/5	42 \pm 1	18.3 \pm 0.6	20 \pm 3	80 \pm 6
S271A	5/6	204 \pm 9	51 \pm 3	170 \pm 40	170 \pm 40
F275A	5/5	300 \pm 15	47 \pm 6	66 \pm 12	110 \pm 20
M276L	6/6	93 \pm 6	35 \pm 1	-5 \pm 10	-1 \pm 8
M283A,T6'S	5/7	1800 \pm 100	920 \pm 90	280 \pm 30	240 \pm 14
S287A	10/4	38 \pm 3	20 \pm 1	30 \pm 10	30 \pm 6
D288A,T6'S	4/6	740 \pm 40	410 \pm 20	14 \pm 7	3 \pm 11
S289A	6/6	—	—	310 \pm 40	70 \pm 10
F297A	6/6	—	—	440 \pm 50	490 \pm 40
T300A	3/3	—	—	650 \pm 200	1650 \pm 400
M301A	6/7	19 \pm 1	10.1 \pm 0.3	0.6 \pm 5	-26 \pm 6
F475A	5/5	—	—	570 \pm 80	1500 \pm 200
F478A	13/13	—	—	110 \pm 10	310 \pm 25
C482Y	5/5	—	—	2600 \pm 600	1900 \pm 400

*Extracellular mutations

Cold Buffer (11-16°C), hRic3 used with receptor

was expected. Also, F478A and S245A only had minimal reduction in potentiation strength. Larger effects were found for residues that were above the proposed PNU-120596 binding site and closer to the extracellular domain (**Figure 4.6**). The most distinct mutation involved the N236A, which showed nearly identical waveforms whether genistein was present or not (**Figure 4.7**). These residues comprise a different location that spans the interface of two subunit transmembrane regions and lies closer to the extracellular region. Since Type I PAMs have different pharmacology properties from Type II PAMs, it is not unreasonable to conclude they bind in a similar region close but not identical to each other. Even though loss of potentiation has been used previously to

probe for PAM binding, it is not a definitive measurement since potentiation loss is seen for a gain-of-function mutation found in the extracellular region adjacent to the agonist binding site (Table 4.4). However, it still provides important structure-function observations.

Another notable residue involved M301A, which resides on the M3 α -helix. A large gain-of-function is seen in the EC_{50} as well as a drastic change in receptor closure rates (Table 4.4 and Figure 4.7). This is interesting because mutations affecting desensitization of $\alpha 7$ receptors typically lie on the M2 α -helix. In addition, application of a Type I PAM (genistein) seems to speed up the receptor closure. M301 resides at the bottom of a potential methionine stack that includes M276 (M2 α -helix) and

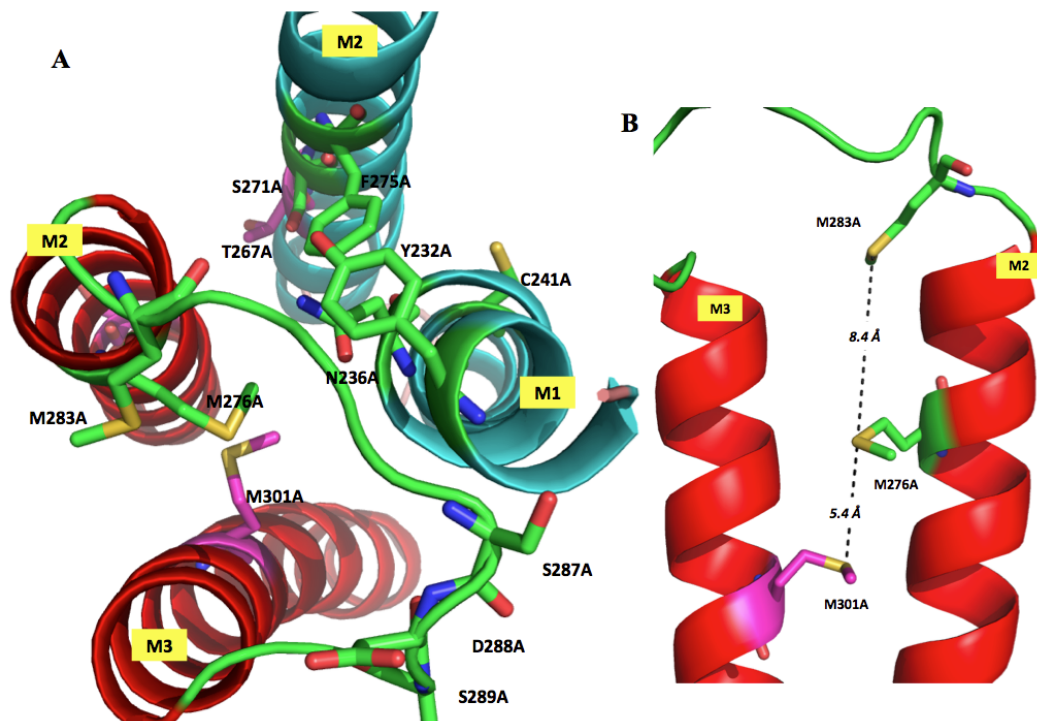


Figure 4.6 Homology model of $\alpha 7$ transmembrane region (A) Residues probed that showed a reduction in genistein potentiation. Residues (green) are labeled as well as the transmembrane helices (two adjacent subunits labeled as red and cyan). Purple residues (T267A and M301A) had large changes in receptor closure rate. (B) Three methionine residues that are vertically stacked in a single subunit.

M283 (M2-M3 loop) (**Figure 4.6**). Methionine residues have been shown to form stabilizing interactions with aromatic groups (34), but they have also been shown to be destabilizing when buried inside the hydrophobic region of a protein (35). Removal of this methionine (301) may release steric interactions that are generated with M2 α -helix movement during receptor activation. This mutation warrants further investigation for use in $\alpha 7$ receptor structure-function studies like the previously used T6'S pore mutation.

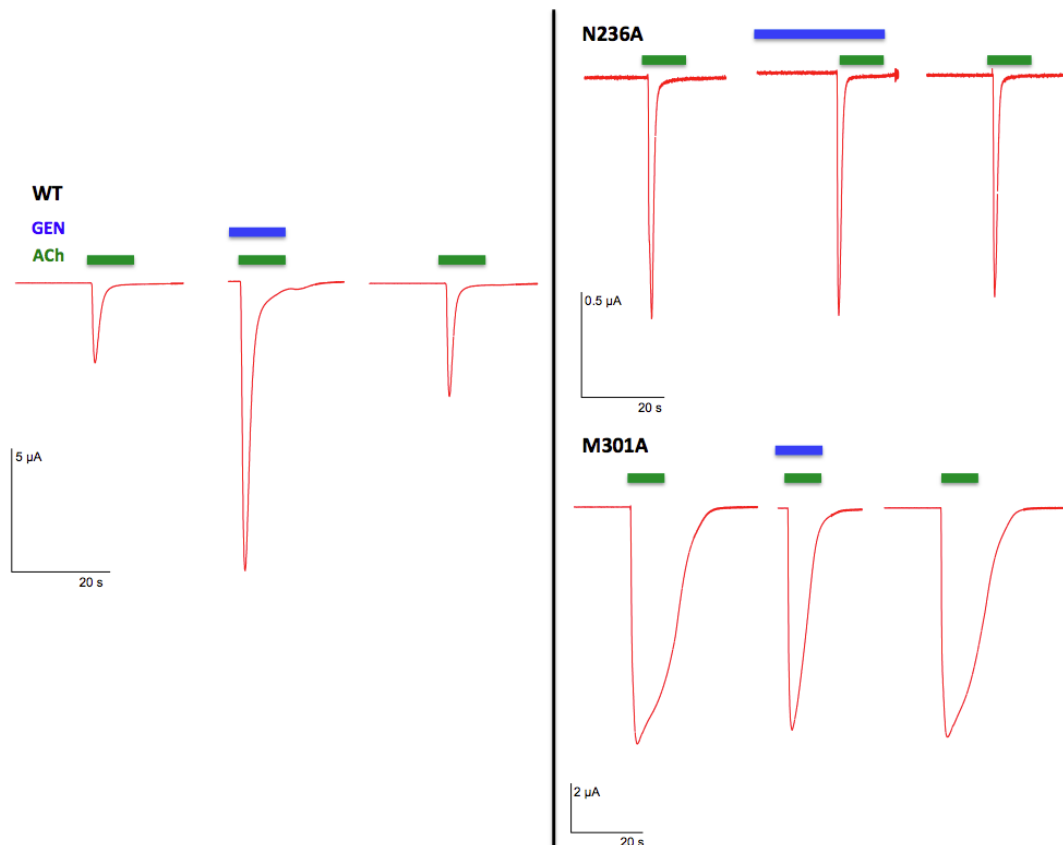


Figure 4.7 Sample traces from PAM potentiation experiments run at colder temperatures. Blue boxes represent genistein (GEN) duration and green represents acetylcholine (ACh). *Left:* wild type (WT) responses show clear potentiation when genistein is present. *Right:* two mutation results. N236A shows the most drastic elimination of genistein potentiation. M301A had a drastic effect on the receptor's closure rate when exposed to acetylcholine only. It also fully eliminated genistein potentiation.

4.4 Conclusions

Research towards understanding and development of allosteric modulators has increased due to several beneficial properties for disease treatment. This study focuses on identifying structure-function relationships of Type I PAMs in $\alpha 7$ nAChRs. An adapted experimental protocol and analysis method was established to increase reproducibility and consistency in potentiation measurements. The electrophysiology rig was modified with a temperature-control device to improve response drifts during experiments. Charge integration was introduced alongside peak height analysis to identify mutations that affect receptor potentiation from allosteric modulators. Then, mutation screening in several proposed PAM binding pockets was performed on the $\alpha 7$ receptor. Type I PAMs (5-HI and 5-MI) were unaffected by several mutations in the extracellular domain, which suggests a transmembrane binding region. Residues linked to PNU-120596 (Type II PAM) binding and those around the site were probed using the Type I PAM genistein. These results reveal that not all residues tied to PNU-120596 binding resulted in a decrease in genistein potentiation. Several new residues closer to the extracellular domain had a larger effect and even eliminated genistein potentiation. These residues are found at the interface of M1 and M2 transmembrane α -helices of one subunit and M2 and M3 α -helices of the adjacent subunit. This resembles interfacial agonist binding in the extracellular region. Even though this is not definitive in identifying a binding site, it strongly suggests these residues are vital in transmission of PAM potentiation during receptor activation. In addition, Type I and Type II PAMs may interact with similar residues, but they are not all the same. Further investigation into these differences would

aid in our understanding of PAM type differentiation and the influences by which they propagate their modulation.

4.5 Methods

4.5.1 Molecular Biology and Homology Models

The $\alpha 7$ and hRic3 plasmids were in the pAMV vector provided by Nyssa Puskar and Walrati Limapichat. Mutations to these receptors were accomplished through site-directed mutagenesis using the QuikChange protocol (Stratagene). The *NotI* restriction enzyme was used for linearizing the $\alpha 7$ and hRic3 plasmids. Post linearization and purification (Qiagen), mRNA was synthesized through run-off transcription by using Ambion's T7 mMessage Machine kits. Purification of the transcribed mRNA was performed using Qiagen's RNeasy RNA kit.

Residue numbering was based on the full-length protein containing the signaling sequence as found on the Ligand Gated Ion Channel Database. The figures were generated using PyMOL and a homology model (generated via MODELLER) of the rat $\alpha 7$ receptor based on the GluCl crystal structure (PDB 3RHW).

4.5.2 Injection of Oocytes and Chemical Preparation

Xenopus laevis stage V and VI oocytes were harvested via standard protocols (36). $\alpha 7$ and hRic3 mRNA were pre-mixed in a 1:1 ratio for a concentration of 0.8 ng of total mRNA per μL . 50 nL were injected per oocyte to deliver 40 ng total of mRNA per cell. For $\alpha 7$ only, 20 ng of mRNA was injected per oocyte. Injected cells

were incubated for 24-72 hours. All cells were incubated at a temperature of 18°C in ND96+ media.

5-hydroxyindole (5-HI) and 5-methoxyindole (5-MI) were purchased from Combi-Blocks Inc. 4',5,7-Trihydroxyisoflavone (genistein) was purchased from Alfa Aesar. Acetylcholine (ACh) was purchased from Sigma-Aldrich. 5-HI, 5-MI, and genistein were dissolved in DMSO for stock solutions. These were then diluted to proper experimental concentrations in buffer with 0.1% v/v DMSO.

4.5.3 Electrophysiology

Electrophysiology recordings were performed using a two electrode voltage clamp technique with the OpusXpress 6000A (Axon Instruments). ND96 w/ Ca^{2+} (96 mM NaCl, 2 mM KCl, 1 mM MgCl_2 , 5 mM HEPES, 1.8 mM CaCl_2 at pH 7.5) was used as the recording buffer. Solution washout rates were 4 mL/min for the first 30 s and then 3 mL/min for the continued duration. Drug applications were 4 mL/min for 15 s. Holding potentials were -60 mV for all cells. Data was collected at 125 Hz and filtered at 50 Hz.

For all $\alpha 7$ experiments, the wash time between drug application doses totaled 5 min. EC_{50} dose response curves were obtained by applying increasing drug concentrations for 15 s (1 mL application total always) with appropriate wash out times. The resulting data was then fit to the Hill equation, $I_{\text{norm}} = 1/[1+(\text{EC}_{50}/A)]^{nH}$, where I_{norm} is the normalized current at a designated agonist concentration, A; EC_{50} is the agonist value that produces half maximal response; nH is the Hill coefficient. Averaging normalized cell response and then fitting to this equation produced the reported EC_{50}

values. For the PAM experiments (**Table 4.1**), the same washing protocols were performed and 100 μ M ACh was used as the agonist. The PAM experiment protocol was as follows: first three doses (dose one is ignored in analysis) were of a constant ACh concentration and washout; two 1 mL doses of PAM only were applied without washout followed immediately with an application of a mix of ACh and PAM followed by washout, which was repeated twice; the final two applications were of a constant ACh concentration and washout. All currents were normalized to the highest response pre-PAM addition. PAM percent increases were calculated by averaging the first two ACh-only responses and the two ACh/PAM co-application responses. The difference between the two values was then taken and multiplied by 100%.

4.6 References

1. Unwin, N. (2005) Refined structure of the nicotinic acetylcholine receptor at 4Å resolution. *J Mol Biol* **346**, 967-989
2. Dougherty, D. A. (2008) Cys-Loop Neuroreceptors: Structure to the Rescue? *Chemical Reviews* **108**, 1642-1653
3. Arias, H. R., Bhumireddy, P., and Bouzat, C. (2006) Molecular mechanisms and binding site locations for noncompetitive antagonists of nicotinic acetylcholine receptors. *Int J Biochem Cell Biol* **38**, 1254-1276
4. Lemoine, D., Jiang, R., Taly, A., Chataigneau, T., Specht, A., and Grutter, T. (2012) Ligand-gated ion channels: new insights into neurological disorders and ligand recognition. *Chem Rev* **112**, 6285-6318
5. Jensen, A. A., Frolund, B., Lijefors, T., and Krogsgaard-Larsen, P. (2005) Neuronal nicotinic acetylcholine receptors: Structural revelations, target identifications, and therapeutic inspirations. *Journal of Medicinal Chemistry* **48**, 4705-4745
6. Taly, A., Corringer, P. J., Guedin, D., Lestage, P., and Changeux, J. P. (2009) Nicotinic receptors: allosteric transitions and therapeutic targets in the nervous system. *Nat Rev Drug Discov* **8**, 733-750
7. Dani, J. A., and Bertrand, D. (2007) Nicotinic acetylcholine receptors and nicotinic cholinergic mechanisms of the central nervous system. *Annual Review of Pharmacology and Toxicology* **47**, 699-729
8. Miwa, J. M., Freedman, R., and Lester, H. A. (2011) Neural systems governed by nicotinic acetylcholine receptors: emerging hypotheses. *Neuron* **70**, 20-33
9. Christopoulos, A. (2002) Allosteric binding sites on cell-surface receptors: novel targets for drug discovery. *Nat Rev Drug Discov* **1**, 198-210
10. Narla, S., Klejbor, I., Birkaya, B., Lee, Y. W., Morys, J., Stachowiak, E. K., Terranova, C., Bencherif, M., and Stachowiak, M. K. (2013) $\alpha 7$ nicotinic receptor agonist reactivates neurogenesis in adult brain. *Biochem Pharmacol* **86**, 1099-1104
11. Parri, H. R., Hernandez, C. M., and Dineley, K. T. (2011) Research update: $\alpha 7$ nicotinic acetylcholine receptor mechanisms in Alzheimer's disease. *Biochem Pharmacol* **82**, 931-942
12. Tong, M., Arora, K., White, M. M., and Nichols, R. A. (2011) Role of key aromatic residues in the ligand-binding domain of $\alpha 7$ nicotinic receptors in the agonist action of β -amyloid. *J Biol Chem* **286**, 34373-34381
13. Williams, D. K., Wang, J., and Papke, R. L. (2011) Positive allosteric modulators as an approach to nicotinic acetylcholine receptor-targeted therapeutics: advantages and limitations. *Biochem Pharmacol* **82**, 915-930
14. Young, J. W., and Geyer, M. A. (2013) Evaluating the role of the $\alpha 7$ nicotinic acetylcholine receptor in the pathophysiology and treatment of schizophrenia. *Biochem Pharmacol* **86**, 1122-1132
15. Horenstein, N. A., Leonik, F. M., and Papke, R. L. (2008) Multiple pharmacophores for the selective activation of nicotinic $\alpha 7$ -type acetylcholine receptors. *Mol Pharmacol* **74**, 1496-1511

16. Pandya, A. A., and Yakel, J. L. (2013) Effects of neuronal nicotinic acetylcholine receptor allosteric modulators in animal behavior studies. *Biochem Pharmacol* **86**, 1054-1062
17. Faghih, R., Gopalakrishnan, M., and Briggs, C. A. (2008) Allosteric Modulators of the $\alpha 7$ Nicotinic Acetylcholine Receptor. *Journal of Medicinal Chemistry* **51**, 701-712
18. Bertrand, D., Bertrand, S., Cassar, S., Gubbins, E., Li, J., and Gopalakrishnan, M. (2008) Positive allosteric modulation of the $\alpha 7$ nicotinic acetylcholine receptor: ligand interactions with distinct binding sites and evidence for a prominent role of the M2-M3 segment. *Mol Pharmacol* **74**, 1407-1416
19. Bertrand, D., and Gopalakrishnan, M. (2007) Allosteric modulation of nicotinic acetylcholine receptors. *Biochem Pharmacol* **74**, 1155-1163
20. Collins, T., Young, G. T., and Millar, N. S. (2011) Competitive binding at a nicotinic receptor transmembrane site of two $\alpha 7$ -selective positive allosteric modulators with differing effects on agonist-evoked desensitization. *Neuropharmacology* **61**, 1306-1313
21. Gronlien, J. H., Hakerud, M., Ween, H., Thorin-Hagene, K., Briggs, C. A., Gopalakrishnan, M., and Malysz, J. (2007) Distinct profiles of $\alpha 7$ nAChR positive allosteric modulation revealed by structurally diverse chemotypes. *Mol Pharmacol* **72**, 715-724
22. Hurst, R. S., Hajos, M., Raggenbass, M., Wall, T. M., Higdon, N. R., Lawson, J. A., Rutherford-Root, K. L., Berkenpas, M. B., Hoffmann, W. E., Piotrowski, D. W., Groppi, V. E., Allaman, G., Ogier, R., Bertrand, S., Bertrand, D., and Arneric, S. P. (2005) A novel positive allosteric modulator of the $\alpha 7$ neuronal nicotinic acetylcholine receptor: in vitro and in vivo characterization. *The Journal of Neuroscience: the Official Journal of the Society for Neuroscience* **25**, 4396-4405
23. Szabo, A. K., Pesti, K., Mike, A., and Vizi, E. S. (2014) Mode of action of the positive modulator PNU-120596 on $\alpha 7$ nicotinic acetylcholine receptors. *Neuropharmacology* **81**, 42-54
24. Young, G. T., Zwart, R., Walker, A. S., Sher, E., and Millar, N. S. (2008) Potentiation of $\alpha 7$ nicotinic acetylcholine receptors via an allosteric transmembrane site. *Proceedings of the National Academy of Sciences of the United States of America* **105**, 14686-14691
25. Hurst, R., Rollema, H., and Bertrand, D. (2013) Nicotinic acetylcholine receptors: from basic science to therapeutics. *Pharmacology & Therapeutics* **137**, 22-54
26. Papke, R. L., Horenstein, N. A., Kulkarni, A. R., Stokes, C., Corrie, L. W., Maeng, C. Y., and Thakur, G. A. (2014) The activity of GAT107, an allosteric activator and positive modulator of $\alpha 7$ nicotinic acetylcholine receptors (nAChR), is regulated by aromatic amino acids that span the subunit interface. *J Biol Chem* **289**, 4515-4531
27. Barron, S. C., McLaughlin, J. T., See, J. A., Richards, V. L., and Rosenberg, R. L. (2009) An allosteric modulator of $\alpha 7$ nicotinic receptors, N-(5-Chloro-2,4-dimethoxyphenyl)-N'-(5-methyl-3-isoxazolyl)-urea (PNU-120596), causes conformational changes in the extracellular ligand binding domain similar to those caused by acetylcholine. *Mol Pharmacol* **76**, 253-263

28. Papke, R. L., and Papke, J. K. P. (2002) Comparative pharmacology of rat and human $\alpha 7$ nAChR conducted with net charge analysis. *British Journal of Industrial Medicine* **137**, 49-61
29. Bataille, N., Helser, T., and Fried, H. M. (1990) Cytoplasmic Transport of Ribosomal Subunits Microinjected into the *Xenopus laevis* Oocyte Nucleus: A Generalized, Facilitated Process. *Journal of Cell Biology* **111**, 1571-1582
30. Placzek, A. N., Grassi, F., Meyer, E. M., and Papke, R. L. (2005) An $\alpha 7$ nicotinic acetylcholine receptor gain-of-function mutant that retains pharmacological fidelity. *Mol Pharmacol* **68**, 1863-1876
31. Halevi, S., McKay, J., Palfreyman, M., Yassin, L., Eshel, M., Jorgensen, E., and Treinin, M. (2002) The *C. elegans* ric-3 gene is required for maturation of nicotinic acetylcholine receptors. *EMBO Journal* **21**, 1012-1020
32. Ludwig, J., Hoffle-Maas, A., Samochocki, M., Luttmann, E., Albuquerque, E. X., Fels, G., and Maelicke, A. (2010) Localization by site-directed mutagenesis of a galantamine binding site on $\alpha 7$ nicotinic acetylcholine receptor extracellular domain. *Journal of Receptors and Signal Transduction* **30**, 469-473
33. Arias, H. R., Gu, R. X., Feuerbach, D., Guo, B. B., Ye, Y., and Wei, D. Q. (2011) Novel positive allosteric modulators of the human $\alpha 7$ nicotinic acetylcholine receptor. *Biochemistry* **50**, 5263-5278
34. Valley, C. C., Cembran, A., Perlmutter, J. D., Lewis, A. K., Labello, N. P., Gao, J., and Sachs, J. N. (2012) The methionine-aromatic motif plays a unique role in stabilizing protein structure. *J Biol Chem* **287**, 34979-34991
35. Lipscomb, L. A., Gassner, N. C., Snow, S. D., Eldridge, A. M., Baase, W. A., Drew, D. L., and Matthews, B. W. (1998) Context-dependent protein stabilization by methionine-to-leucine substitution shown in T4 lysozyme. *Prot. Sci.* **7**, 765-773
36. Nowak, M., Gallivan, J. P., Silverman, S., Labarca, C. G., Dougherty, D. A., and Lester, H. A. (1998) In Vivo Incorporation of Unnatural Amino Acids into Ion Channels in *Xenopus* Oocyte Expression System. *Methods Enzymol* **293**, 504-529

Chapter 5

*An Unaltered Orthosteric Site and a Network of Long-Range Allosteric Interactions for PNU-120596 in $\alpha 7$ Nicotinic Acetylcholine Receptors**

**This chapter is adapted from: Christopher B. Marotta, Henry A. Lester, and Dennis A. Dougherty. An unaltered orthosteric site and a network of long-range allosteric interactions for PNU-120596 in $\alpha 7$ nicotinic acetylcholine receptors. This paper has been submitted to *Chemistry and Biology* for consideration. The work described in this chapter was done in collaboration with Dr. Henry Lester and Dr. Dennis Dougherty.*

5.1 Abstract

Nicotinic acetylcholine receptors (nAChRs) are vital to neuronal signaling, are implicated in important processes such as learning and memory, and are therapeutic targets for neural diseases. The $\alpha 7$ nAChR has been implicated in Alzheimer's disease and schizophrenia, and allosteric modulators have become one focus of drug development efforts. We investigate the mode of action of the $\alpha 7$ -selective positive allosteric modulator, PNU-120596, and show that the higher potency of acetylcholine in the presence of PNU-120596 is not due to an altered agonist binding site. In addition, we propose several residues in the gating interface and transmembrane region that are functionally important to transduction of allosteric properties and link PNU-120596, the acetylcholine binding region, and the receptor's gate. These results suggest global protein stabilization from a communication network through several key residues that alter the gating equilibrium of the receptor while leaving the agonist binding properties unperturbed.

5.2 Introduction

Nicotinic acetylcholine receptors (nAChRs) are pentameric ion channels that are part of the Cys-loop superfamily of ligand-gated ion channels, which includes receptors gated by other neurotransmitters such as glycine, serotonin, and GABA. The $\alpha 7$ nAChR is comprised of five identical subunits that each contain an extracellular domain, transmembrane domain, and a gating interface (**Figure 5.1**) (1-3). This receptor subtype is uncommon among nAChRs in its ability to form homopentamers, and it displays a large and dispersed presence throughout the central nervous system (CNS) (4).

The concepts of allostery, including cooperative transitions between two states of multisubunit proteins (5), have been applied to nAChRs in two ways. First, the nAChR itself has been identified as a protein containing two distinct domains, a binding site for agonists and a conducting pathway (6,7). The existence of one or more additional, desensitized, states was recognized early on (8,9).

Second, and more relevant to the present study, compounds have been identified that do not produce activation on their own, yet modulate activation and desensitization, and bind at sites distinct from both the agonist site (the “orthosteric” site) and channel pore. These are allosteric ligands. At $\alpha 7$ nAChRs, positive allosteric modulators (PAMs) are especially well studied, and two classes can be distinguished. Type I PAMs increase agonist-induced activation. Type II PAMs, such as PNU-120596 (**Figure 5.1**), increase agonist-induced activation and also vastly prolong the waveform of agonist-induced currents; in the usual interpretation, PAMs favor the active states at the expense of the desensitized states (**Figure 5.1**) (10-15).

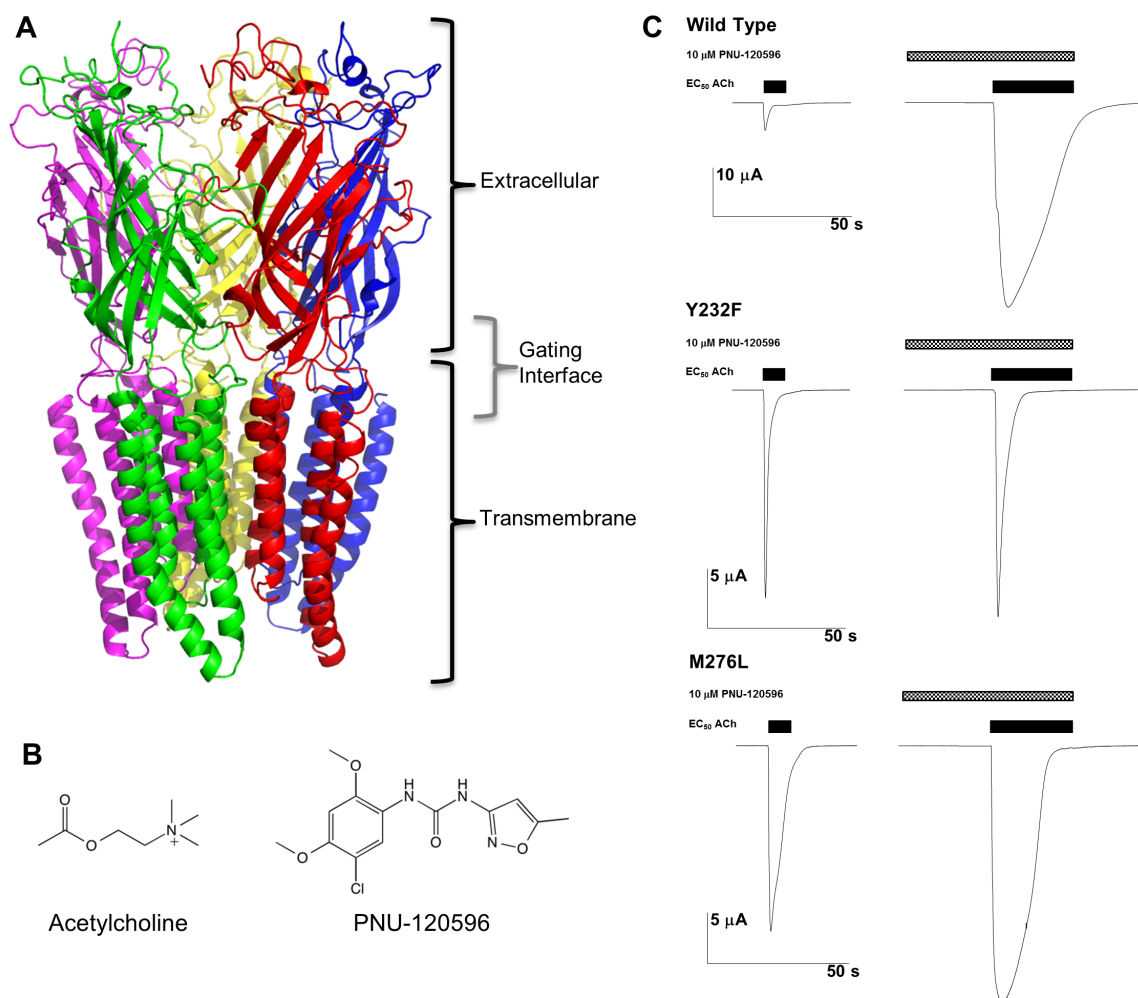


Figure 5.1 Homology model of the rat $\alpha 7$ nAChR. (A) This ligand gated ion channel consists of five subunits arranged in a pentameric fashion, which forms a pore to transmit cations across the membrane. Each subunit consists of a large extracellular domain where the agonist binding site lies between two subunits. In addition, there is a transmembrane region consisting of four α -helices and an intracellular portion used for receptor trafficking (not shown). The region where the extracellular domain and transmembrane physically interact is considered the gating interface and is thought to be important for signal relay from the agonist binding site to the channel gate (33,34). (B) Chemical structures of acetylcholine and PNU-120596. (C) Sample traces of $\alpha 7$ receptor responses for wild type and the cases designated “FAST” and “SLOW” decay currents in **Table 5.4**. Acetylcholine is represented by a black bar and 10 μ M PNU-120596 is represented by a checker-pattern bar. EC₅₀ doses of acetylcholine were used for each respective mutation. For the Y232F mutation in the absence and presence of PNU-120596, both traces show fast decay currents, which closely resembles the wild type response. For the M276L mutation however, the starting acetylcholine application has slowed decay current, which is further amplified when PNU-120596 is introduced.

Inherent to models of allostery is the notion of action at a distance, and it is of interest to ask whether the orthosteric binding site, and/or the channel pore, is affected by the presence of an allosteric modulator. Unfortunately no atomic-scale structural information is available for full $\alpha 7$ nAChRs in any state, let alone all three states in the presence of either an agonist or allosteric modulator. However, the high functional resolution of electrophysiological data allows other approaches to this question. For example, the structurally unrelated allosteric modulator 4PB-TQS has been shown to change the kinetics of gating as well as single-channel conductance of $\alpha 7$ nAChRs (16), indicating that an allosteric modulator can change the structure of the conducting pore.

This study begins by determining to what extent, if any, an allosteric modulator changes the orthosteric site (**Figure 5.2**). Previous data suggested that an allosteric modulator can affect residues within the extracellular domain, but outside the orthosteric site itself (17). Non-canonical amino acid mutagenesis provides high-resolution data that complement those from X-ray crystallography. The key binding interactions at the agonist binding site of nAChRs – a cation- π interaction and two hydrogen bonds – are both sensitive to ligand displacements of <1 Å (18-20). We have therefore applied non-canonical amino acid mutagenesis to ask whether the presence of a PAM in any way modulates these binding interactions at the orthosteric site. The crucial point is that the non-canonical amino acid methodology is sensitive enough to detect even small changes in specific interactions.

Our next goal was to map out the functional coupling pathway from the orthosteric site to the allosteric binding site of PNU-120596 – which is thought to be in the transmembrane region (21,22) – and/or from the allosteric site to the channel gate.

We term our strategy, which again uses functional measurements, “double perturbation cycle analysis” (see **Figure 5.3**). In this analysis, the first perturbation is mutation of the protein (with conventional or non-canonical amino acids); and the second perturbation is not a mutation, but the addition of PNU-120596. Non-additivity of the two perturbations indicates that the protein mutation differentially impacts receptor function depending on whether PNU-120596 is or is not present, suggesting that the residue under study plays an important role in allosteric modulation (23-25).

From these studies, we have identified several residues with significant $\Delta\Delta G$ values, suggesting a potential pathway of communication from the agonist binding site to the PAM binding site and then on to the receptor gate.

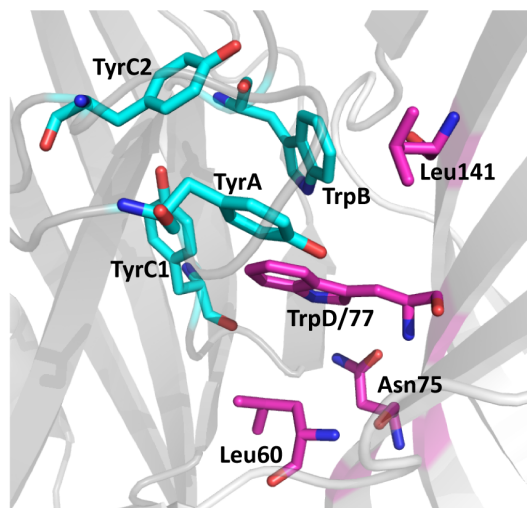


Figure 5.2 Agonist binding site for the $\alpha 7$ nAChR. Several tyrosine and tryptophan residues comprise the aromatic box for the agonist binding site. These residues are labeled thus: TyrA (Y115), TrpB (W171), TyrC1 (Y210), and TyrC2 (Y217) lie on the principal side (cyan) of one subunit while TrpD (W77) lies on the complementary side (magenta) of the adjacent subunit. Backbone hydrogen bonding interactions have been implicated for the carbonyl of TrpB and the backbone amide of Leu141. Residues that have been shown to turn PNU-120596 into a weak agonist – Leu60, Asn75, and TrpD – have been highlighted to show the proximity to and inclusion of (in the case of TrpD) the aromatic box.

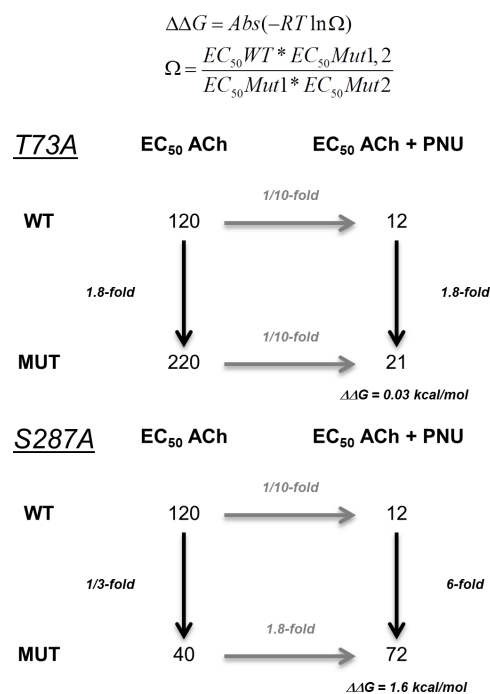


Figure 5.3 Example of the double perturbation cycle analysis. ACh = acetylcholine; PNU = PNU-120596. By keeping one of the “mutations” as the addition of PNU-120596, residues that are important for allosteric propagation through the protein can be assessed by generating a $\Delta\Delta G$ of greater than 0.5 kcal/mol. Here, the equation for generating $\Delta\Delta G$ values is shown along with two mutations – one that is coupled and one that is not – as an example of the non-additivity and basis for this report’s functional coupling comparisons. Room temperature (25°C) was used for the value, T.

5.3 Results

5.3.1 Methodology for Interpretation of Functional Coupling Comparisons

As noted in the Introduction, we sought to identify mutations of the receptor that *differentially* impact function when PNU-120596 is or is not present. Since we wish to evaluate a large number of sites throughout the protein, our metric is EC₅₀, rather than more tedious single-channel methods. We fully appreciate the composite nature of EC₅₀, and have in fact used it to our advantage in evaluating an allosteric modulator.

One can envision two limiting modes of allosteric activation for a ligand-gated ion channel. Binding of the modulator could induce a conformational change in the protein that propagates to the orthosteric site, altering the innate affinity of that site for the natural agonist. Alternatively, the allosteric modulator could impact the gating transition of the receptor, by binding essentially at the metaphorical “gate” or, again, by action through a distance.

We have developed a strategy to distinguish these two possibilities and, in so doing, have removed ambiguities associated with EC_{50} measurements. Beginning in 1995, we have developed methods for probing structure-function relationships at the agonist binding site of nicotinic receptors and related proteins with unprecedented precision. Using non-canonical amino acids, we can reveal key drug-receptor contacts. We can identify cation- π interactions using fluorination, and we can evaluate potential hydrogen bonding interactions using backbone mutagenesis. Importantly, both approaches provide information on the *magnitude* of the non-covalent interaction between drug and receptor. As such, we can detect subtle changes in the agonist binding site that would enhance (or diminish) agonist binding in ways that are just not possible with conventional approaches. As described below, we find no evidence of alteration of the agonist binding site on addition of PNU-120596.

EC_{50} describes a composite of several equilibria, some involving agonist binding, some involving channel gating. Since we can rule out alteration of binding equilibria, we can conclude that changes in EC_{50} induced by PNU-120596 reflect changes in the gating equilibria of the receptor. We have used such analyses before, removing the innate ambiguity in EC_{50} by eliminating one component of the measurement (26,27).

Again, our goal is to identify residues that play a role in the allosteric modulation provided by PNU-120596. To do this, we compare the impact of a mutation on wild type function vs. function when PNU-120596 is present. If the mutation does not affect PNU-120596 in any way, the mutation's impact should be the same whether PNU-120596 is present or not. Stated differently, the impacts on wild type EC_{50} of the mutation and of PNU-120596 should simply have additive energies. Alternatively, if a

mutation alters PNU-120596 function, then the effect of PNU-120596 on receptor function should be different from wild type when the mutation is present. That is, the side chain mutation and the impact of PNU-120596 should be non-additive. By analogy to conventional double mutant cycle analysis, the non-additivity can be expressed as a $\Delta\Delta G$ value (**Figure 5.3**), which, if markedly different from zero, signifies the presence of non-local conformational effects on a large and complex membrane bound protein.

5.3.2 The Orthosteric Site: Binding Interactions are Unaffected by PNU-120596

Previous studies of the $\alpha 7$ nAChR show that acetylcholine makes a single cation- π interaction with TyrA (**Figure 5.2**), which is one of five aromatic residues at the orthosteric binding site (28). One possible way in which the allosteric binding of PNU-120596 could impact receptor function is by influencing the shape of the aromatic box, such that the strength of the cation- π interaction to acetylcholine could change, or the site of the cation- π interaction could move to another aromatic residue instead of or in cooperation with TyrA. Other studies show that mutations outside the agonist binding site can reshape the binding site and significantly alter agonist-receptor contacts (27). One can identify cation- π interactions using progressive fluorination of the aromatic groups that contribute the π electrons. We were able to probe four of the five aromatic box residues for acetylcholine cation- π interactions in the absence and presence of PNU-120596 (**Table 5.1**) (See **Figure 5.4** for structures). TyrC1 could not be probed because of the large loss of function for any substitution made at this residue; TyrC1 has never been implicated in a cation- π interaction in the dozens of studies of Cys-loop receptors we have performed (18).

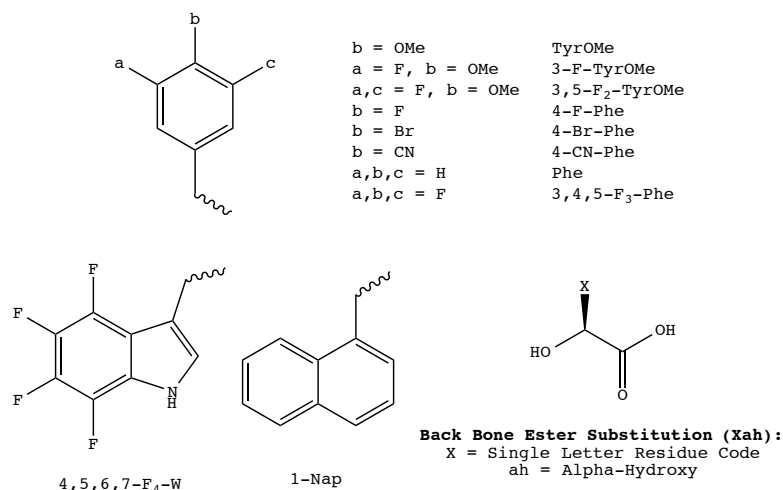


Figure 5.4 Chemical structures of the non-canonical amino acid used to probe the agonist binding site.

The first observation is that acetylcholine continues to make a cation- π interaction with TyrA in the presence of PNU-120596 (**Fig. 5.5**). In addition, the slopes of the two fluorination plots (with and without PNU-120596) are not meaningfully different, which indicates that the strength of the cation- π interaction was also unaltered (18). Since the interaction with TyrA was unchanged, TyrC2 was probed next, because previous data show that a higher sensitivity agonist – epibatidine – makes a cation- π interaction with TyrC2 in addition to TyrA in the $\alpha 7$ nAChR (28). As seen in **Figure 5.5**, a cation- π interaction still does not exist between TyrC2 and acetylcholine in the presence of PNU-120596. However, two observations can be made regarding interactions with the TyrC2 residue. The near wild type receptor response for bulky substituent groups (4-CN-Phe, 4-Br-Phe, and TyrOMe) and severe loss of function for small/no substituents (4-F-Phe and Phe) suggest a large substituent is needed at the 4-position in the aromatic ring to maintain proper receptor function. In addition, the receptor cannot tolerate substitutions at the 3- or 5-position in the ring system, as indicated by the large loss of function for 3-F-TyrOMe and 3,5-F₂-TyrOMe residues. These results suggest a tight

steric environment for TyrC2 at the orthosteric site. Of more relevance here, however, is the fact that the pattern of responses to substitution at TyrC2 is unaltered by the presence of PNU-120596.

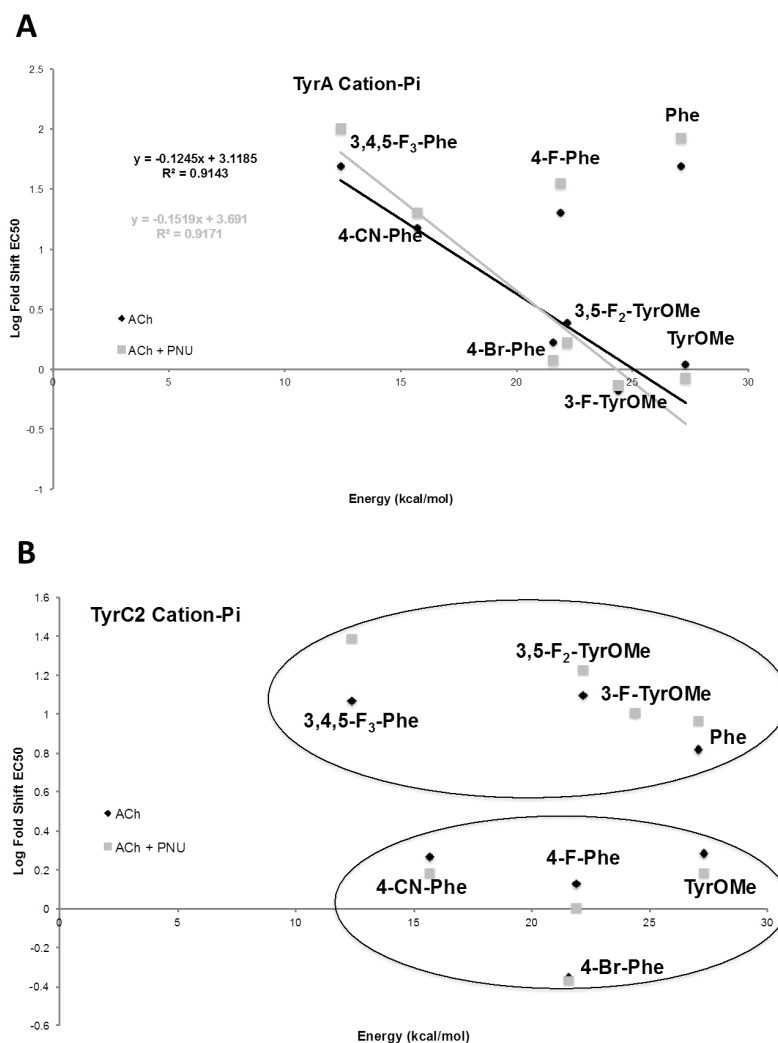


Figure 5.5 Cation- π plots for TyrA and TyrC2 in the rat $\alpha 7$ receptor. ACh = acetylcholine; PNU = PNU-120596. The agonist binding site consists of five aromatic residues, four of which are on the primary subunit and one of which is on the complementary subunit. Previously, TyrA has been shown to make an interaction with acetylcholine and TyrC2 with epibatidine, a more potent partial agonist (28). (A) The cation- π interaction is present at TyrA and does not shift in its relative strength when PNU-120596 is added. (B) TyrC2 shows no cation- π interaction with acetylcholine, even in the presence of PNU-120596. These data suggest that the agonist binding site is not being reshaped from the presence of an allosteric modulator and the effects observed with PNU-120596 reside in altering the protein elsewhere.

Since PNU-120596 did not influence the two critical Tyr residues in the $\alpha 7$ nAChR, the Trp residues were also studied. Note that for most combinations of agonist and nAChR, the cation- π interaction is to TrpB; $\alpha 7$ is unusual in employing TyrA. For both TrpB and TrpD, in the presence and absence of PNU-120596, there was not a meaningful shift in function when we expressed the highly perturbing residue 4,5,6,7-F₄-Trp (**Table 5.1**). This indicates that acetylcholine is not making a cation- π interaction with either of these residues. Previous studies showed that a much more dramatic mutation of TrpD – to Ala – converted PNU-120596 into a partial agonist, while maintaining its function as a positive allosteric modulator (17,29). We find that this mutation shows a $\Delta\Delta G$ of essentially zero (**Table 5.1**).

We also applied a previously described strategy for evaluating the two key H-bonding interactions previously established at the agonist binding site (19,20). Briefly, α -hydroxy analogues of α -amino acids are incorporated in ways that are known to strongly modulate the hydrogen bonding ability of the protein backbone. We found that perturbation of the hydrogen bond acceptor (L141) or the hydrogen bond donor (S172) had little impact on PNU-120596 modulation (**Figure 5.2**) (**Table 5.2**).

Overall, the high-precision methodology of non-canonical amino acid mutagenesis allows us to conclude that the presence PNU-120596 does not measurably alter the key binding interactions to ACh at the orthosteric site.

Table 5.1

α 7 Mutants: Aromatic Box	<i>Acetylcholine</i>					<i>Acetylcholine</i> + <i>PNU-120596</i> (10 μ M)					$\Delta\Delta G$ (kcal/mol)
	EC ₅₀ (μ M)	Hill	Fold Shift From WT	n	I _{max} (μ A)	EC ₅₀ (μ M)	Hill	Fold Shift From WT	n	I _{max} (μ A)	
Wild Type (WT)	120 \pm 8	1.8 \pm 0.2	–	20	1.1 - 23	12 \pm 0.4	3.0 \pm 0.2	–	21	1.7 - 48	0.00
TyrA: TyrOMe	130 \pm 8	2.3 \pm 0.23	1.1	10	2.9 - 48	10 \pm 0.4	2.5 \pm 0.2	0.8	13	4.5 - 51	0.15
TyrA: 3-F-TyrOMe	79 \pm 5	1.7 \pm 0.2	0.7	11	0.22 - 6.7	8.7 \pm 0.5	2.9 \pm 0.5	0.7	15	1.6 - 20	0.05
TyrA: 3,5-F ₂ -TyrOMe	290 \pm 10	1.8 \pm 0.1	2.4	18	1.0 - 11	20 \pm 0.6	2.4 \pm 0.1	1.7	23	1.0 - 41	0.21
TyrA: 4-F-Phe	2400 \pm 100	1.9 \pm 0.1	20	17	0.11 - 1.4	420 \pm 40	2.3 \pm 0.4	35	16	0.43 - 24	0.32
TyrA: 4-Br-Phe	200 \pm 8	1.9 \pm 0.1	1.7	15	0.69 - 15	14 \pm 1	2.8 \pm 0.2	1.2	16	9.3 - 35	0.20
TyrA: 4-CN-Phe	1800 \pm 80	2.2 \pm 0.2	15	17	0.11 - 5.4	240 \pm 10	3.5 \pm 0.8	20	17	9.5 - 44	0.16
TyrA: Phe	5800 \pm 200	1.7 \pm 0.1	48	13	0.041 - 2.1	1000 \pm 80	2.7 \pm 0.5	83	14	0.57 - 53	0.31
TyrA: 3,4,5-F ₃ -Phe	5800 \pm 700	2.2 \pm 0.4	48	9	0.034 - 0.74	1200 \pm 80	4.0 (set)	100	14	0.53 - 25	0.41
TrpB: W	260 \pm 20	1.5 \pm 0.2	2.2	10	2.4 - 26	22 \pm 0.3	3.1 \pm 0.1	1.8	20	0.79 - 47	0.10
TrpB: 4,5,6,7-F ₄ W	670 \pm 20	1.6 \pm 0.1	5.6	14	0.050 - 4.8	60 \pm 3	3.2 \pm 0.4	5	16	0.45 - 68	0.06
TrpB: Wah	13 \pm 1	1.2 \pm 0.1	0.1 (1/10)	14	0.98 - 8.2	0.78 \pm 0.04	2.1 \pm 0.2	0.06 (1/15)	21	0.29 - 21	0.29
TyrC2: TyrOMe	230 \pm 10	1.6 \pm 0.1	2	15	0.76 - 36	18 \pm 1	3.1 \pm 0.2	1.5	15	0.19 - 90	0.14
TyrC2: 3-F-TyrOMe	1200 \pm 120	1.5 \pm 0.2	10	15	0.32 - 6.1	120 \pm 5	4.4 \pm 0.9	10	14	0.88 - 20	0.00
TyrC2: 3,5-F ₂ -TyrOMe	1500 \pm 100	2.0 \pm 0.2	12.5	13	0.091 - 5.1	200 \pm 20	4.7 \pm 1.6	17	13	0.66 - 44	0.16
TyrC2: 4-F-Phe	160 \pm 10	1.4 \pm 0.1	1.3	19	0.84 - 18	12 \pm 0.4	4.5 \pm 0.5	1	16	10 - 33	0.16
TyrC2: 4-Br-Phe	53 \pm 2	1.7 \pm 0.1	0.5 (1/2)	14	3.4 - 21	5.1 \pm 0.1	3.0 \pm 2	0.4 (1/2.5)	16	10 - 39	0.02
TyrC2: 4-CN-Phe	220 \pm 10	1.8 \pm 0.1	1.8	12	4.2 - 34	18 \pm 1	3.1 \pm 0.2	1.5	16	5.7 - 42	0.11
TyrC2: Phe	790 \pm 40	1.9 \pm 0.1	6.6	13	0.34 - 12	110 \pm 7	5.9 \pm 3	9.2	16	0.36 - 21	0.19
TyrC2: 3,4,5-F ₃ -Phe	1400 \pm 60	2.4 \pm 0.2	12	16	0.1 - 2.4	290 \pm 20	4.4 \pm 1.4	24	16	5.0 - 23	0.41
TrpD: W	160 \pm 7	1.9 \pm 0.1	1.3	9	0.59 - 11	18 \pm 0.6	3.2 \pm 0.2	1.5	13	0.31 - 23	0.07
TrpD: 4,5,6,7-F ₄ W	90 \pm 9	1.0 \pm 0.1	0.75 (1/1.3)	20	0.15 - 10	4.1 \pm 0.1	2.2 \pm 0.1	0.3 (1/3)	17	2.8 - 21	0.45
TrpD: 1-Nap	450 \pm 20	1.5 \pm 0.1	3.7	13	0.10 - 4.4	40 \pm 1	3.4 \pm 0.3	3.3	16	3.6 - 17	0.07
TrpD: Wah	360 \pm 20	1.3 \pm 0.1	3	14	0.081 - 4.5	24 \pm 1	4.0 (set)	2	15	0.21 - 24	0.23
W77A	160 \pm 10	2.4 \pm 0.2	1.3	15	8.2 - 28	15 \pm 1	2.1 \pm 0.2	1.2	15	9.6 - 51	0.04

Table 5.2

$\alpha 7$ Mutants: Extracellular	Acetylcholine					Acetylcholine + PNU-120596 (10 μ M)					$\Delta\Delta G$ (kcal/mol)
	EC50 (μ M)	Hill	Fold Shift From WT	n	I _{max} (μ A)	EC50 (μ M)	Hill	Fold Shift From WT	n	I _{max} (μ A)	
Wild Type (WT)	120 \pm 8	1.8 \pm 0.2	-	20	1.1 - 23	12 \pm 0.4	3.0 \pm 0.2	-	21	1.7 - 48	0.00
L60A	27 \pm 2	1.3 \pm 0.1	0.2 (1/4)	15	1.2 - 44	2.0 \pm 0.2	2.3 \pm 0.3	0.2 (1/6)	15	3.9 - 50	0.17
Q61A	44 \pm 4	1.4 \pm 0.2	0.3 (1/3)	16	4.1 - 34	4.0 \pm 0.1	3.2 \pm 0.2	0.3 (1/3)	18	1.3 - 89	0.05
M63A	32 \pm 1	1.9 \pm 0.1	0.27 (1/4)	13	0.42 - 19	2.5 \pm 0.03	3.4 \pm 0.2	0.2 (1/5)	15	2.6 - 39	0.14
E67A	830 \pm 30	1.8 \pm 0.1	7	15	0.13 - 1.1	190 \pm 30	3.6 \pm 1.6	16	24	0.24 - 11	0.47
E67N	720 \pm 100	1.5 \pm 0.3	6	10	0.027 - 0.40	240 \pm 20	2.4 \pm 0.4	20	14	0.085 - 1.6	0.69
K68A	300 \pm 20	1.9 \pm 0.2	2.5	18	0.24 - 39	59 \pm 1	3.7 \pm 0.2	5	16	11 - 44	0.39
N69A	400 \pm 30	1.8 \pm 0.2	3.3	16	1.3 - 39	52 \pm 3	2.7 \pm 0.3	4.3	16	4.4 - 38	0.15
Q70A	450 \pm 30	1.3 \pm 0.1	3.8	20	0.10 - 6.8	29 \pm 1	5.4 \pm 1	2.4	15	0.56 - 18	0.25
T73A	210 \pm 10	1.4 \pm 0.1	1.8	13	0.19 - 8.6	22 \pm 0.8	3.5 \pm 0.4	1.8	16	0.98 - 23	0.03
N75A	8 \pm 1	1.0 \pm 0.1	0.067 (1/15)	15	1.6 - 27	0.29 \pm 0.02	1.7 \pm 0.2	0.025 (1/40)	16	4.6 - 25	0.58
P103G	180 \pm 10	1.9 \pm 0.2	1.5	15	2.3 - 26	21 \pm 1	2.4 \pm 0.3	1.8	16	5.7 - 45	0.09
H127A	48 \pm 3	1.9 \pm 0.2	0.4 (1/2.5)	14	2.4 - 35	5.8 \pm 0.2	3.0 \pm 0.3	0.5 (1/2)	16	3.8 - 42	0.11
Q139F	220 \pm 10	1.8 \pm 0.1	1.8	14	1.3 - 35	25 \pm 1	2.5 \pm 0.3	2.1	16	0.96 - 37	0.07
L141:Leu	120 \pm 7	1.9 \pm 0.2	1	15	0.48 - 17	15 \pm 0.6	2.8 \pm 0.2	1.2	16	1.3 - 41	0.13
L141:Lah**	180 \pm 10	1.9 \pm 0.2	1.5	14	0.23 - 31	27 \pm 1	5.0 \pm 1.3	1.8	15	1.5 - 26	0.10
Y151A	120 \pm 20	1.2 \pm 0.1	1	15	3.2 - 43	8.3 \pm 0.3	2.3 \pm 0.2	0.7	12	11 - 37	0.21
D153A	170 \pm 10	1.8 \pm 0.2	1.4	15	0.27 - 9.6	25 \pm 1	4.0 (set)	2.1	14	1.6 - 17	0.22
W156A	240 \pm 30	1.9 \pm 0.4	2	12	0.16 - 8.8	65 \pm 3	1.9 \pm 0.2	5.4	15	0.18 - 23	0.57
S172:Ser	480 \pm 20	1.3 \pm 0.1	4	15	0.21 - 4.8	23 \pm 0.5	3.2 \pm 0.2	1.9	16	0.30 - 7.8	0.42
S172:Sah*	130 \pm 10	1.2 \pm 0.1	0.3 (1/3)*	15	0.088 - 3.1	8.4 \pm 0.6	3.5 \pm 0.8	0.36 (1/3)*	15	0.54 - 18	0.17
S172:Thr	120 \pm 10	1.2 \pm 0.1	1	15	0.28 - 35	8.0 \pm 0.5	2.8 \pm 0.5	0.67 (1/1.5)	16	5.3 - 31	0.23
S172:Tah*	48 \pm 10	0.93 \pm 0.2	0.4 (1/2.5)*	13	0.18 - 7.9	1.6 \pm 0.05	3.5 \pm 0.2	0.2 (1/5)*	16	0.33 - 26	0.39
G175K	7.5 \pm 0.7	1.6 \pm 0.2	0.06 (1/17)	17	0.42 - 30	1.0 \pm 0.2	2.5 \pm 0.9	0.08 (1/12)	19	2.1 - 42	0.16
S189A	210 \pm 20	1.4 \pm 0.1	1.8	15	0.20 - 48	16 \pm 0.7	2.9 \pm 0.2	1.3	16	4.6 - 49	0.15
N193A	210 \pm 5	1.7 \pm 0.1	1.8	14	0.22 - 12	18 \pm 1	2.4 \pm 0.2	1.5	21	0.18 - 18	0.09
E195A	620 \pm 60	1.7 \pm 0.3	5.2	13	0.050 - 0.17	170 \pm 8	3.6 \pm 0.4	14	15	0.54 - 13	0.57
E195N	530 \pm 20	1.4 \pm 0.1	4.4	22	0.17 - 14	40 \pm 2	2.7 \pm 0.2	3.3	15	0.56 - 25	0.16
D197A	130 \pm 10	1.6 \pm 0.2	1.1	14	0.54 - 19	16 \pm 0.4	3.0 \pm 0.1	1.3	16	2.6 - 40	0.12
D219A	860 \pm 20	2.1 \pm 0.1	7.2	13	0.37 - 31	130 \pm 5	5.1 \pm 0.7	11	16	3.6 - 23	0.24

*Fold shift from canonical amino acid incorporation (Ser and Thr) using the non-canonical amino acid method

Table 5.3

$\alpha 7$ Mutants: Transmembrane	Acetylcholine					Acetylcholine + PNU-120596 (10 μ M)					
	EC ₅₀ (μ M)	Hill	Fold Shift (WT)	n	I _{max} (μ A)	EC ₅₀ (μ M)	Hill	Fold Shift (WT)	n	I _{max} (μ A)	$\Delta\Delta G$ (kcal/mol)
Wild Type	120 \pm 8	1.8 \pm 0.2	-	20	1.1 - 23	12 \pm 0.4	3.0 \pm 0.2	-	21	1.7 - 48	0.00
T6'S	64 \pm 1	2.4 \pm 0.1	0.5 (1/2)	15	4.8 - 67	21 \pm 2	3.2 \pm 0.7	1.8	16	0.48 - 23	0.68
R229A	78 \pm 8	1.3 \pm 0.1	0.6	12	0.42 - 42	8.1 \pm 0.3	2.6 \pm 0.2	0.7	14	0.12 - 8.1	0.02
Y232F	52 \pm 2	1.9 \pm 0.2	0.4 (1/2.5)	15	2.4 - 20	73 \pm 2	2.1 \pm 0.1	6	17	0.85 - 20	1.50
N236A	480 \pm 40	1.2 \pm 0.1	4	17	0.32 - 6.8	430 \pm 40	1.1 \pm 0.1	36	16	0.087 - 0.77	1.25
C241A	180 \pm 10	3.1 \pm 0.4	1.5	16	0.19 - 31	73 \pm 3	4.1 \pm 0.5	6	15	0.61 - 15	0.80
S245A	160 \pm 10	1.3 \pm 0.1	1.3	15	1.2 - 15	3.2 \pm 0.2	2.5 \pm 0.4	0.27 (1/4)	15	13 - 57	0.92
A248D	92 \pm 5	1.3 \pm 0.1	0.8	12	0.16 - 7.7	10 \pm 0.4	2.8 \pm 0.3	0.8	16	0.089 - 10	0.05
S271A	110 \pm 7	2.2 \pm 0.2	0.9	14	9.1 - 32	14 \pm 0.3	2.6 \pm 0.1	1.2	15	1.2 - 58	0.14
F275A	280 \pm 20	1.8 \pm 0.2	2.3	15	0.35 - 23	510 \pm 30	1.4 \pm 0.1	43	18	0.16 - 18	1.65
M276L	46 \pm 1	3.0 \pm 0.1	0.4 (1/2.5)	15	9.9 - 39	32 \pm 2	2.0 \pm 0.2	2.7	16	7.3 - 43	1.10
M283A T6'S**	2100 \pm 70	2.3 \pm 0.1	33**	14	0.52 - 18	440 \pm 30	4.4 \pm 1.2	21**	16	3.6 - 37	0.26
S287A	40 \pm 2	2.0 \pm 0.2	0.3 (1/3)	16	8.7 - 36	72 \pm 7	1.3 \pm 0.1	6	15	3.1 - 31	1.65
D288A T6'S**	750 \pm 30	2.3 \pm 0.2	12**	13	4.8 - 46	230 \pm 10	5.7 \pm 3	11**	16	1.6 - 84	0.04
S289A	52 \pm 2	1.7 \pm 0.1	0.4 (1/2.5)	16	3.3 - 51	6.6 \pm 0.5	2.1 \pm 0.3	0.5 (1/2)	15	6.4 - 42	0.14
F297A	150 \pm 10	1.8 \pm 0.2	1.3	15	0.93 - 52	16 \pm 1	2.6 \pm 0.2	1.3	16	6.9 - 45	0.04
M301A	19 \pm 1	2.1 \pm 0.1	0.2 (1/5)	10	11 - 53	23 \pm 1	1.7 \pm 0.1	1.9	15	8.2 - 60	1.42
F475A	78 \pm 3	1.8 \pm 0.1	0.6	16	1.3 - 22	5.8 \pm 0.7	2.0 \pm 0.4	0.5 (1/2)	16	13 - 30	0.17
F478A	74 \pm 1	2.3 \pm 0.1	0.6	16	1.3 - 30	12 \pm 0.7	3.4 \pm 0.6	1.0	15	8.1 - 48	0.28
C482Y	210 \pm 20	2.0 \pm 0.3	1.8	19	0.84 - 27	44 \pm 1	3.0 \pm 0.2	3.7	16	2.4 - 37	0.42

**** Fold shift from the T6'S value since it is a background mutation for the point in question.**

5.3.3 *A Double Perturbation Cycle Analysis to Identify Residues Critical to PNU-120596 Function*

We assessed numerous residues throughout the $\alpha 7$ subunit to determine whether they played a role in the allosteric modulation by PNU-120596. Previous studies have emphasized how mutations impact the potentiation produced by PNU-120596, an approach that has produced useful insights such as identification of the PNU-120596 binding site in the transmembrane region. We extended previous data by adopting the double perturbation cycle analysis, which is appropriate for identifying long-range communication between two sites of interest (described in **Figure 5.3**). Results are tabulated for all residues studied in **Tables 5.1, 5.2, and 5.3**. If the absolute value of the calculated $\Delta\Delta G$ is ≥ 0.5 kcal/mol, we consider the protein residue to be functionally important to the allosteric modulatory activity of PNU-120596. This approach may minimize possible complications arising from changes to the receptor that do not influence the allosteric communication pathway. (23).

Previous experiments probing agonist-binding interactions in $\alpha 7$ nAChRs were aided by the inclusion of a pore mutation (T6'S) that produces a modest gain of function and slows $\alpha 7$ desensitization, allowing more precise waveform analysis (19,28). However, this mutation is coupled to PNU-120596, with a $\Delta\Delta G$ of 0.68 kcal/mol. As such, this mutation was disregarded for the majority of this study except in two cases where the introduced mutations generated a non-functional receptor that was recoverable through the introduction of a gain-of-function pore mutation (30).

5.3.4 *Measuring the Coupling at the Proposed PNU-120596 Binding Site*

Several studies of the impact of mutations on PNU-120596 potentiation of acetylcholine response suggested that PNU-120596 binds in the transmembrane region, across α -helices M1 (S245 & A248), M2 (M276), and M4 (F478 & C482) of a single subunit (**Figure 5.6**) (22,31). Since the goal of the present work was to map out the functional coupling pathway between the binding site for PNU-120596 and the agonist binding site, we mutated a large number of residues throughout the receptor (**Tables 5.1, 5.2, 5.3**). For purposes of discussion, we will begin at the “bottom” and work our way up to the agonist binding site.

Of the five residues thought to contribute to the PNU-120596 binding site, only two show a meaningful functional coupling. However, several nearby residues did show meaningful coupling (**Table 5.3**). Interestingly, these residues generally lie “above” the three residues that were previously implicated in binding but show no coupling (A248, F478, C482). Further exploration of the area around this region yielded several other residues – C241 (M1), F275 (M2), and M301 (M3) – that resulted in a large coupling, as reflected in the $\Delta\Delta G$ values. As seen in **Figure 5.6**, these residues lie outside the previously proposed PNU-120596 binding pocket (32).

Some of these residues produced interesting response waveforms. F275A showed responses that – regardless of the addition of PNU-120596 – resembled wild type $\alpha 7$ acetylcholine waveforms. Conversely, M276L and M301A provided the opposite observation for the decay phase: they showed a slowed response whether PNU-120596 was added or not.

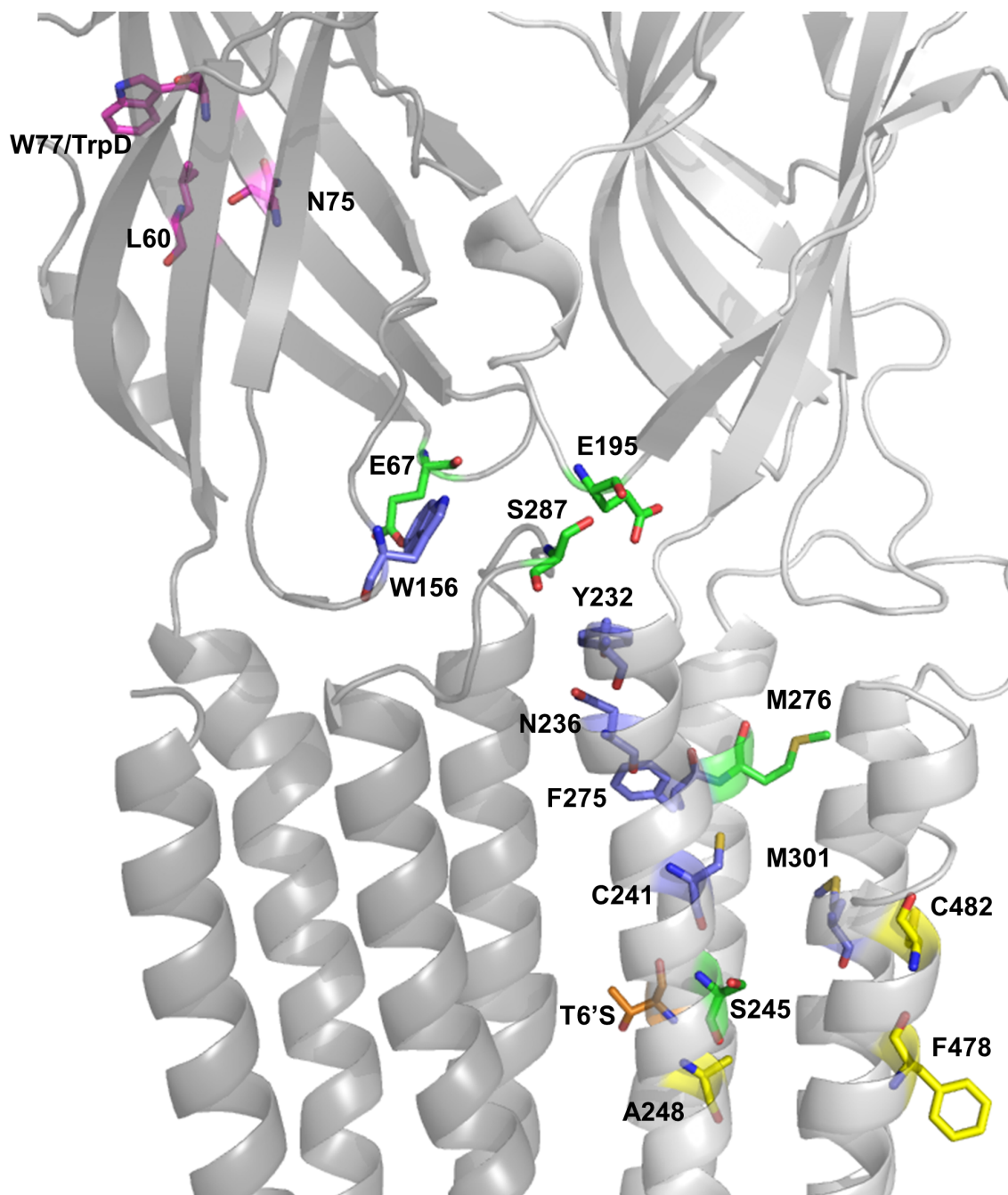


Figure 5.6 Summary of residues that generated a $\Delta\Delta G$ greater than 0.5 kcal/mol for the functional coupling comparison or caused PNU-120596 to become a weak agonist. Only two subunits are shown for clarity. The color scheme is as follows: magenta, PNU-120596 becomes a partial agonist; orange, T6'S on the M2 helix; blue, new residues discovered to have a $\Delta\Delta G \geq 0.5$ kcal/mol; green, residues previously studied that also show a $\Delta\Delta G \geq 0.5$ kcal/mol; yellow, residues previously implicated in the PNU-120596 binding site that do not show a $\Delta\Delta G \geq 0.5$ kcal/mol.

5.3.5 Important Residues in the Gating Interface and the Extracellular Domain

Previous cysteine labeling experiments by Barron et al. showed several extracellular residues positioned at the interface of two adjacent subunits that underwent conformational changes in the $\alpha 7$ nAChR when exposed to either PNU-120596 or acetylcholine (17). These residues (L60, M63, E67, N75, N193, and E195) were evaluated along with several others in the surrounding region (**Table 5.2**). **Figure 5.6** shows the residues in the gating interface with $\Delta\Delta G \geq 0.5$ kcal/mol (33,34). Tillman et al. showed, through chimera analysis, that specific loops and linkers were necessary for PNU-120596 potentiation of $\alpha 7$ receptors (34). Here, we were able to isolate specific residues on some of these identified regions: in Loop 2, E67; in Loop 9, E195; and in the M2-M3 Linker, S287. Again, we observed distinct response waveforms. Results for E67A/N, E195A, Y232F, N236A, and S287A all resembled $\alpha 7$ wild type acetylcholine waveforms, even in the presence of PNU-120596 (**Figure 5.1 and Table 5.4**).

All the mutations that had markedly affected $\Delta\Delta G$, or that rendered PNU-120596 an agonist, define a network of residues necessary for propagation of the PNU-120596 effects throughout the full receptor (**Figure 5.6**). In addition, this can suggest a conformational wave of movement upon activation and gives insight into the molecular motions that potentially take place between the closed and open forms of the receptor.

Table 5.4 Summary of Residues that Show Coupling of PNU-120596 and Acetylcholine

The left panel lists in descending absolute value the mutations found to have a $\Delta\Delta G \geq 0.5$ kcal/mol and thus are considered here to be important for allosteric modulation. They also contain the abbreviation for the relative location on the protein (Figure 5.6). The right panel contains the residues (listed in residue numerical order) previously probed and implicated in PNU-120596 function but did not show a $\Delta\Delta G \geq 0.5$ kcal/mol. Both panels also contain references associated with each mutation and the effect on the electrophysiology observations that were seen when comparing traces from the EC_{50} s measured (See Figure 5.1 for examples). Mutations without a reference are newly discovered locations that showed importance to allosteric function.

Coupled Mutations (Location)	$\Delta\Delta G$ (kcal/mol)	Previously Probed: Reference	Electrophysiology Response Observations	Uncoupled Mutations (Location)	$\Delta\Delta G$ (kcal/mol)	Previously Probed: Reference	Electrophysiology Response Observations
F275A (TM)	1.65	–	FAST	L60A (EC)	0.17	c	PNU Weak Partial Agonist
S287A (GI)	1.65	d	FAST	M63A (EC)	0.14	c	
Y232F (GI)	1.50	–	FAST	W77A (EC)	0.04	e	PNU Weak Partial Agonist
M301A (TM)	1.42	–	SLOW	N193A (GI)	0.09	c	
N236A (GI)	1.25	–	FAST	A248D (TM)	0.05	a,b	
M276L (TM)	1.10	a,b	SLOW	F478A (TM)	0.28	a,b	
S245A (TM)	0.92	a,b		C482Y (TM)	0.42	a,b	
C241A (TM)	0.80	–					
E67N (GI)	0.69	c,d	FAST				
T6'S (TM)	0.68	–					
N75A (EC)	0.58	c	PNU Weak Partial Agonist				
E195A (GI)	0.57	c,d	FAST				
W156A (GI)	0.57	–					
E67A (GI)	0.47	c,d	FAST				

*Needed the T6'S mutation to generate receptor response

TM = transmembrane, EC = extracellular, GI = gating interface

FAST = Normal $\alpha 7$ trace for both EC_{50} measurements (Acetylcholine & Acetylcholine + PNU-120596)

SLOW = Slower decay current for both EC_{50} measurements (Acetylcholine & Acetylcholine + PNU-120596)

a = Collins et al. (31); b = Young et al. (22); c = Barron et al. (17); d = Tillman et al. (34); e = Papke et al. (29)

5.4 Discussion

The present work aims to evaluate the influences of the positive allosteric modulator PNU-120596 on $\alpha 7$ nAChRs. Through the use of non-canonical amino acids, the binding region of acetylcholine was probed for potential changes in interactions with acetylcholine when PNU-120596 was introduced. These studies produced three key results: 1) the cation- π interaction with the TyrA residue is not perturbed by the introduction of PNU-120596, 2) no other cation- π interactions are gained when PNU-120596 is present, and 3) the overall shape of the agonist binding site seems unperturbed. The aromatic fluorination series and introduction of α -hydroxy acid residues give compelling evidence that no significant rearrangements propagate to the orthosteric binding site from the allosteric binding site of PNU-120596.

Since no distinct change to the agonist binding motif was observed, we suggest that PNU-120596 does not alter the binding step of the agonist to the receptor and instead exerts its effects only on the gating equilibrium. As explained above, this result effectively removes the ambiguity in comparing EC_{50} values for various mutations. Since the agonist binding site is unperturbed, it is reasonable to assume that PNU-120596 primarily, if not solely, influences receptor function by perturbing gating equilibria. The binding of PNU-120596 apparently impacts important residues required for signal transduction from the agonist binding site to the channel gate. In evaluating long-range interactions between residues, functional coupling comparisons based on a double perturbation cycle analysis provide an appropriate and rigorous method (23-25). The functional coupling comparisons were used to probe for mutations that coupled acetylcholine and PNU-120596 together, thus allowing for identification of residues

necessary for proper PAM function and influence. **Table 5.4** summarizes the major observations and results of this study. **Figure 5.7** shows the fold shift data from **Tables 5.1, 5.2, and 5.3** in a graphical form, which supports the analysis of the double perturbation cycle. The non-additive mutations do not adhere to the linear relationship seen with the those that do not influence PNU-120596 effects. From these data, several observations and conclusions can be drawn to elicit new information on allosteric modulation of $\alpha 7$ nAChRs by PNU-120596.

An interesting observation concerned the mutations M276L and M301A, which changed the decay current rate of acetylcholine-only waveforms (**Table 5.4**). This effect is quite similar to that seen with the T6'S mutation. Again, coupling was seen here, because all of these mutations seemed to aid in changing the gating equilibrium and thus

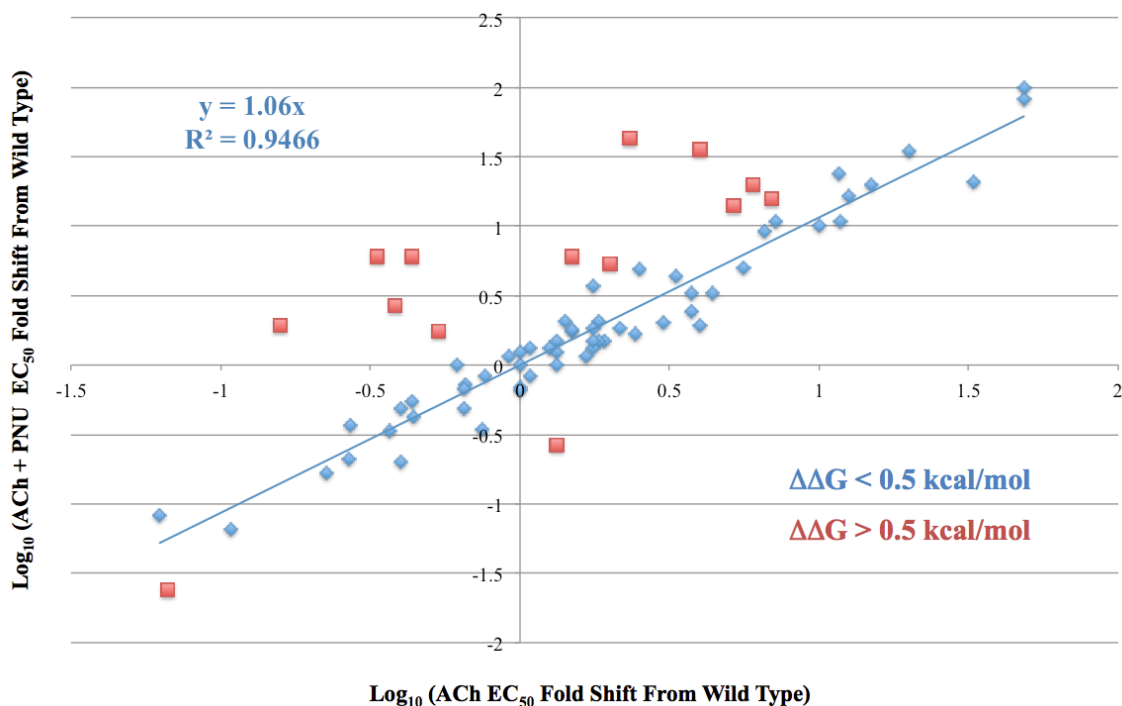


Figure 5.7 Plot of log EC_{50} fold shifts with and without PNU-120596. Mutations that show no coupling ($\Delta\Delta G < 0.5$ kcal/mol) form a linear line while those with values of $\Delta\Delta G > 0.5$ kcal/mol lie off the relationship. Based on the double perturbation cycle analysis, this type of result is expected. This way graphically represents the fold shift data in this report and visually shows the non-additivity from the introduced mutations.

diminish the total effect PNU-120596 can exert on the system. M301A (adjacent to the putative PNU-120596 binding site) and M276L (on the M2 pore-lining helix) most likely contribute to structural rearrangements in the transmembrane region. In addition, the mutation L60 shows a large gain of function for acetylcholine alone, which suggests a possible re-structuring coupled to the agonist binding site. Thus, the allosteric propagation between acetylcholine and PNU-120596 is highly disrupted and could cause the PNU-120596 to become a weak agonist.

Another surprising result seen here is that several residues previously implicated in PNU-120596 binding do not show functional coupling with respect to transmitting the effects of PNU-120596. Previously, the binding pocket had been proposed to lie in the transmembrane region and to interact with residues on the M1, M2, and M4 α -helices (22,31). Even though these residues were implicated in comprising the PNU-120596 binding, they may not contribute to allosteric propagation in the protein – which is analogous to the residues critical for acetylcholine binding shown above. Residues adjacent to the pockets were implicated in the communication pathway: N75 lies on the β 2 strand connected to loop 2; C241 & S245 lie on the M1 helix and F275 on the M2 helix. Remarkably, both of these edges of the binding sites seem to be oriented for interaction with residues at the gating interface. The residues E195 (Loop 9), Y232 (M1), and N236 (M1) of one subunit are located in the vicinity of E67 (Loop 2), W156 (Loop 7), and S287 (M2-3 Linker) of the adjacent subunit. This suggests the presence of a collection of residues in the gating interface region that communicates the allosteric potentiation between the extracellular and transmembrane regions (**Figure 5.6**). This interpretation is reinforced by the fact that five of these six residues (excluding W156)

show nearly $\alpha 7$ wild type response waveforms even when PNU-120596 is present (**Table 5.4**). The increase in decay current rates back to wild type waveforms even when PNU-120596 is present suggests that these residues are vital to propagation of the PNU-120596 allosteric properties. Even though the residue N193 is not included in this complex despite its proximity, a possible explanation for the effects previously seen by Barron et al. is that its physical location can be reorienting because the above-mentioned complex movements change the solvent exposure (17).

PNU-120596 thus exerts positive allosteric modulation by binding in the transmembrane region, which stabilizes the gating interface and changes the gating equilibrium of the receptor, allowing for a lower concentration of the agonist to open the channel. Also, stabilizing this interaction prolongs channel activation, presumably by decelerating desensitization of the $\alpha 7$ receptor, which is the most rapidly desensitizing nAChR known (30). Naturally this suggests a global interaction involving a complex change in the stability of the wild type receptor after agonist binding. Here we have provided a quantitative analysis for identification of residues necessary for proper propagation of allosteric effects.

5.5 Conclusions

Nicotinic acetylcholine receptors (nAChRs) are critical contributors to neuronal communication, which also implicates them in vital normal brain processes as well as neural diseases. The $\alpha 7$ nAChR in particular has been implicated in Alzheimer's disease; thus the molecular understanding of how compounds affect this receptor has attracted much interest (35-39). Attempts to design small molecules that are specific to $\alpha 7$ have

yielded numerous agonists with some therapeutic success (40). As an alternative to selective agonist design, research towards the development and understanding of allosteric modulators – which have the potential to be more target specific and thus produce fewer side effects – has generated progress (32,41). In this study, the use of non-canonical amino acids allowed individual chemical interactions of the agonist binding to the protein to be probed in the presence of the $\alpha 7$ -specific positive allosteric modulator PNU-120596. The conclusion from this analysis is that PNU-120596 does not alter the agonist binding pocket. To further probe the molecular basis of the properties of PNU-120596, conventional mutagenesis throughout the receptor was performed. Several gating interface residues as well as transmembrane residues were identified as vital for propagating PNU-120596 properties throughout the receptor. This network of residues links the agonist binding site to the PNU-120596 binding site and to the channel gate in the pore of the receptor, influencing the global stabilization of the gating equilibrium.

5.6 Methods

5.6.1 Residue Numbering and Protein Modeling

Residue numbering was based on the full-length protein containing the signaling sequence as found on the Ligand Gated Ion Channel Database (<http://lenoverelab.org/LGICdb/LGICdb.php>). The figures were generated using PyMOL and a homology model (generated via MODELLER) of the rat $\alpha 7$ receptor based on the GluCl crystal structure (PDB 3RHW) (42).

5.6.2 Molecular Biology

The QuikChange protocol (Stratagene) was used for site-directed mutagenesis of the rat nAChR $\alpha 7$ subunit (pAMV vector). *NotI* was used to linearize the circular plasmid. The DNA was purified (Qiagen) and *in vitro* transcription of mRNA from the linearized DNA templates was performed using the T7 mMessage Machine kit (Ambion). The resulting mRNA was purified and isolated using Qiagen's RNeasy RNA purification kit. The same linearization and mRNA synthesis protocols were used for the human Ric3 (pAMV) accessory protein.

For non-canonical amino acid incorporation, the amber (UAG) stop codon was used for all $\alpha 7$ subunit incorporation. The 74-nucleotide THG73 tRNA and 76-nucleotide THG73 tRNA were *in vitro* transcribed using the MEGAscript T7 (Ambion) kit and isolated using Chroma Spin DEPC-H₂O columns (Clontech). Synthesized non-canonical amino acids coupled to the dinucleotide dCA were enzymatically ligated to the 74-nucleotide tRNA as previously described (27,43).

ND96 media was used for all experimental running/wash buffer (96 mM NaCl, 1.8mM CaCl₂, 2 mM KCl, 1 mM MgCl₂, 5 mM HEPES at pH 7.5). ND96+ media was used for oocyte storage media (2.5mM sodium pyruvate and 6.7mM theophylline). No gentamicin was added to the ND96+ storage media in order to avoid distorting ACh-induced responses (44).

5.6.3 Oocyte Preparation and Injection

Xenopus laevis stage V and VI oocytes were harvested via standard protocols (43). For conventional mutagenesis, mRNA mixtures of $\alpha 7$ and Ric3 (45-49) were mixed

at a ratio of 1:1 by weight to a final concentration of 0.8 ng/nL. Each oocyte received a 50 nL injection for a 40 ng total mRNA mass delivery. Oocytes were incubated at 18° C for 24-48 h. For non-canonical amino acid incorporation, mRNA mixtures of $\alpha 7$ and Ric3 were made in a 1:1 ratio to a final concentration of 1.6 ng/nL. These mRNA mixtures were then mixed in a 1:1 volume ratio with de-protected (photolysis) tRNA, and 50 nL were injected into each oocyte. Oocytes were incubated at 18° C for 24 h. For non-canonical amino acids that showed no response after 24 h, the oocyte was subjected to a second injection and incubation following the aforementioned procedure. Read-through/reaminoacylation tests (76-nucleotide THG73 tRNA) were performed to confirm non-canonical amino acid incorporation (19).

5.6.4 Chemical Preparation

Acetylcholine Chloride (Sigma-Aldrich) was dissolved to 1 M stock solutions in ND96 buffer. PNU-120596 (Selleckchem) was dissolved in DMSO to 150 mM stock solutions. Further dilution was performed to make a 10 μ M and 0.1% v/v DMSO solution for experimentation.

5.6.5 Electrophysiology

The two-electrode voltage clamp mode of an OpusXpress 6000A (Axon Instruments) was used. A holding potential of -60 mV and ND96 media for running buffer were used.

For acetylcholine EC₅₀ measurements, 2-fold and 2.5-fold acetylcholine concentration steps were applied over several orders of magnitude for dose-response

measurements. Drug applications consisted of applying 1 mL of solution over 8 s. Then the oocytes were washed with buffer for 3 min at a rate of 3 mL min⁻¹ before the next application of drug. For the acetylcholine and PNU-120596 EC₅₀ measurements, a similar protocol was used. PNU-120596 at a 10 μM concentration was pumped in at a rate of 3 mL min⁻¹ for 30 s (1.5 mL total volume per oocyte) prior to the co-application of acetylcholine and 10 μM PNU-120596. The co-application dose was 1 mL of solution over 15 s followed by an additional 15 s pause to allow each response to reach its maximum value. Then the oocytes were washed with buffer for 5 min at a rate of 3 mL min⁻¹ before the next co-application of drug. Again, 2-fold and 2.5-fold acetylcholine concentration steps were used over several orders of magnitude.

Data were sampled at 50 Hz and then low-passed filtered at 5 Hz. Data were normalized on a per cell basis, response was averaged on a per concentration basis, and then fit to a single Hill term to generate EC₅₀ and Hill coefficient (nH) values. Error bars represent standard error of the mean (SEM) values.

5.7 Acknowledgments

We thank Matt Rienzo and Noah Duffy for their work in making the dCA-coupled fluorinated-OMe-Tyrosines and tRNA, and Emily Blythe for developing the α7 homology model. Support for this work came from the NIH (NS 34407).

5.8 References

1. Lemoine, D., Jiang, R., Taly, A., Chataigneau, T., Specht, A., and Grutter, T. (2012) Ligand-gated ion channels: new insights into neurological disorders and ligand recognition. *Chemical Reviews* **112**, 6285-6318
2. Unwin, N. (2005) Refined structure of the nicotinic acetylcholine receptor at 4Å resolution. *Journal of Molecular Biology* **346**, 967-989
3. Dougherty, D. A. (2008) Cys-Loop Neuroreceptors: Structure to the Rescue? *Chemical Reviews* **108**, 1642-1653
4. Millar, N. S., and Gotti, C. (2009) Diversity of vertebrate nicotinic acetylcholine receptors. *Neuropharmacology* **56**, 237-246
5. Monod, J., Wyman, J., and Changeux, J. P. (1965) On the nature of allosteric transitions: A plausible model. *J. Mol. Biol.* **12**, 88-118
6. Edelstein, S. J., and Changeux, J. P. (1998) Allosteric transitions of the acetylcholine receptor. *Adv Protein Chem* **51**, 121-184
7. Karlin, A. (1967) On the application of "a plausible model" of allosteric proteins to the receptor for acetylcholine. *Journal of Theoretical Biology* **16**, 306-320
8. Heidmann, T., and Changeux, J. P. (1986) Characterization of the transient agonist-triggered state of the acetylcholine receptor rapidly labeled by the noncompetitive blocker [3H]chlorpromazine: additional evidence for the open channel conformation. *Biochemistry* **25**, 6109-6113
9. Katz, B., and Thesleff, S. (1957) A study of 'desensitization' produced by acetylcholine at the motor end-plate. *J Physiol (Lond.)* **138**, 63-80
10. Gronlien, J. H., Hakerud, M., Ween, H., Thorin-Hagene, K., Briggs, C. A., Gopalakrishnan, M., and Malysz, J. (2007) Distinct profiles of $\alpha 7$ nAChR positive allosteric modulation revealed by structurally diverse chemotypes. *Molecular Pharmacology* **72**, 715-724
11. Faghih, R., Gopalakrishnan, M., and Briggs, C. A. (2008) Allosteric Modulators of the $\alpha 7$ Nicotinic Acetylcholine Receptor. *Journal of Medicinal Chemistry* **51**, 701-712
12. Bertrand, D., and Gopalakrishnan, M. (2007) Allosteric modulation of nicotinic acetylcholine receptors. *Biochemical Pharmacology* **74**, 1155-1163
13. Hurst, R. S., Hajos, M., Raggenbass, M., Wall, T. M., Higdon, N. R., Lawson, J. A., Rutherford-Root, K. L., Berkenpas, M. B., Hoffmann, W. E., Piotrowski, D. W., Groppi, V. E., Allaman, G., Ogier, R., Bertrand, S., Bertrand, D., and Arneric, S. P. (2005) A novel positive allosteric modulator of the $\alpha 7$ neuronal nicotinic acetylcholine receptor: in vitro and in vivo characterization. *The Journal of Neuroscience: the Official Journal of the Society for Neuroscience* **25**, 4396-4405
14. Szabo, A. K., Pesti, K., Mike, A., and Vizi, E. S. (2014) Mode of action of the positive modulator PNU-120596 on $\alpha 7$ nicotinic acetylcholine receptors. *Neuropharmacology* **81**, 42-54
15. Williams, D. K., Wang, J., and Papke, R. L. (2011) Investigation of the molecular mechanism of the $\alpha 7$ nicotinic acetylcholine receptor positive allosteric modulator PNU-120596 provides evidence for two distinct desensitized states. *Molecular Pharmacology* **80**, 1013-1032

16. Pałczyńska, M. M., Jindrichova, M., Gibb, A. J., and Millar, N. S. (2012) Activation of $\alpha 7$ Nicotinic Receptors by Orthosteric and Allosteric Agonists: Influence on Single-Channel Kinetics and Conductance. *Molecular Pharmacology* **82**, 910-917
17. Barron, S. C., McLaughlin, J. T., See, J. A., Richards, V. L., and Rosenberg, R. L. (2009) An allosteric modulator of $\alpha 7$ nicotinic receptors, N-(5-Chloro-2,4-dimethoxyphenyl)-N'-(5-methyl-3-isoxazolyl)-urea (PNU-120596), causes conformational changes in the extracellular ligand binding domain similar to those caused by acetylcholine. *Molecular Pharmacology* **76**, 253-263
18. Dougherty, D. A., and Van Arnem, E. B. (2014) In vivo incorporation of non-canonical amino acids by using the chemical aminoacylation strategy: a broadly applicable mechanistic tool. *Chembiochem : a European Journal of Chemical Biology* **15**, 1710-1720
19. Van Arnem, E. B., Blythe, E. E., Lester, H. A., and Dougherty, D. A. (2013) An unusual pattern of ligand-receptor interactions for the $\alpha 7$ nicotinic acetylcholine receptor, with implications for the binding of varenicline. *Molecular Pharmacology* **84**, 201-207
20. Tavares Xda, S., Blum, A. P., Nakamura, D. T., Puskar, N. L., Shanata, J. A., Lester, H. A., and Dougherty, D. A. (2012) Variations in binding among several agonists at two stoichiometries of the neuronal, $\alpha 4\beta 2$ nicotinic receptor. *Journal of the American Chemical Society* **134**, 11474-11480
21. Bertrand, D., Bertrand, S., Cassar, S., Gubbins, E., Li, J., and Gopalakrishnan, M. (2008) Positive allosteric modulation of the $\alpha 7$ nicotinic acetylcholine receptor: ligand interactions with distinct binding sites and evidence for a prominent role of the M2-M3 segment. *Molecular Pharmacology* **74**, 1407-1416
22. Young, G. T., Zwart, R., Walker, A. S., Sher, E., and Millar, N. S. (2008) Potentiation of $\alpha 7$ nicotinic acetylcholine receptors via an allosteric transmembrane site. *Proceedings of the National Academy of Sciences of the United States of America* **105**, 14686-14691
23. Gleitsman, K. R., Shanata, J. A., Frazier, S. J., Lester, H. A., and Dougherty, D. A. (2009) Long-range coupling in an allosteric receptor revealed by mutant cycle analysis. *Biophysical Journal* **96**, 3168-3178
24. Daeffler, K. N., Lester, H. A., and Dougherty, D. A. (2012) Functionally important aromatic-aromatic and sulfur- π interactions in the D2 dopamine receptor. *Journal of the American Chemical Society* **134**, 14890-14896
25. Miles, T. F., Bower, K. S., Lester, H. A., and Dougherty, D. A. (2012) A coupled array of noncovalent interactions impacts the function of the 5-HT3A serotonin receptor in an agonist-specific way. *ACS Chemical Neuroscience* **3**, 753-760
26. Lummis, S. C., Beene, D. L., Lee, L. W., Lester, H. A., Broadhurst, R. W., and Dougherty, D. A. (2005) Cis-trans isomerization at a proline opens the pore of a neurotransmitter-gated ion channel. *Nature* **438**, 248-252
27. Xiu, X., Puskar, N. L., Shanata, J. A., Lester, H. A., and Dougherty, D. A. (2009) Nicotine binding to brain receptors requires a strong cation- π interaction. *Nature* **458**, 534-537

28. Puskar, N. L., Xiu, X., Lester, H. A., and Dougherty, D. A. (2011) Two neuronal nicotinic acetylcholine receptors, $\alpha 4\beta 4$ and $\alpha 7$, show differential agonist binding modes. *The Journal of Biological Chemistry* **286**, 14618-14627
29. Papke, R. L., Horenstein, N. A., Kulkarni, A. R., Stokes, C., Corrie, L. W., Maeng, C. Y., and Thakur, G. A. (2014) The activity of GAT107, an allosteric activator and positive modulator of $\alpha 7$ nicotinic acetylcholine receptors (nAChR), is regulated by aromatic amino acids that span the subunit interface. *The Journal of Biological Chemistry* **289**, 4515-4531
30. Zhang, J., Xue, F., Whiteaker, P., Li, C., Wu, W., Shen, B., Huang, Y., Lukas, R. J., and Chang, Y. (2011) Desensitization of $\alpha 7$ nicotinic receptor is governed by coupling strength relative to gate tightness. *The Journal of Biological Chemistry* **286**, 25331-25340
31. Collins, T., Young, G. T., and Millar, N. S. (2011) Competitive binding at a nicotinic receptor transmembrane site of two $\alpha 7$ -selective positive allosteric modulators with differing effects on agonist-evoked desensitization. *Neuropharmacology* **61**, 1306-1313
32. Williams, D. K., Wang, J., and Papke, R. L. (2011) Positive allosteric modulators as an approach to nicotinic acetylcholine receptor-targeted therapeutics: advantages and limitations. *Biochemical Pharmacology* **82**, 915-930
33. Hanek, A. P., Lester, H. A., and Dougherty, D. A. (2008) A Stereochemical Test of a Proposed Structural Feature of the Nicotinic Acetylcholine Receptor. *Journal of the American Chemical Society* **130**, 13216-13218
34. Tillman, T. S., Seyoum, E., Mowrey, D. D., Xu, Y., and Tang, P. (2014) ELIC- $\alpha 7$ Nicotinic acetylcholine receptor ($\alpha 7$ nAChR) chimeras reveal a prominent role of the extracellular-transmembrane domain interface in allosteric modulation. *The Journal of Biological Chemistry* **289**, 13851-13857
35. Young, J. W., and Geyer, M. A. (2013) Evaluating the role of the $\alpha 7$ nicotinic acetylcholine receptor in the pathophysiology and treatment of schizophrenia. *Biochemical Pharmacology* **86**, 1122-1132
36. Pandya, A. A., and Yakel, J. L. (2013) Effects of neuronal nicotinic acetylcholine receptor allosteric modulators in animal behavior studies. *Biochemical Pharmacology* **86**, 1054-1062
37. Narla, S., Klejbor, I., Birkaya, B., Lee, Y. W., Morys, J., Stachowiak, E. K., Terranova, C., Bencherif, M., and Stachowiak, M. K. (2013) $\alpha 7$ nicotinic receptor agonist reactivates neurogenesis in adult brain. *Biochemical Pharmacology* **86**, 1099-1104
38. Tong, M., Arora, K., White, M. M., and Nichols, R. A. (2011) Role of key aromatic residues in the ligand-binding domain of $\alpha 7$ nicotinic receptors in the agonist action of β -amyloid. *The Journal of Biological Chemistry* **286**, 34373-34381
39. Parri, H. R., Hernandez, C. M., and Dineley, K. T. (2011) Research update: $\alpha 7$ nicotinic acetylcholine receptor mechanisms in Alzheimer's disease. *Biochemical Pharmacology* **82**, 931-942
40. Horenstein, N. A., Leonik, F. M., and Papke, R. L. (2008) Multiple pharmacophores for the selective activation of nicotinic $\alpha 7$ -type acetylcholine receptors. *Molecular Pharmacology* **74**, 1496-1511

41. Christopoulos, A. (2002) Allosteric binding sites on cell-surface receptors: novel targets for drug discovery. *Nature Reviews. Drug Discovery* **1**, 198-210
42. Hibbs, R. E., and Gouaux, E. (2011) Principles of activation and permeation in an anion-selective Cys-loop receptor. *Nature* **474**, 54-60
43. Nowak, M., Gallivan, J. P., Silverman, S., Labarca, C. G., Dougherty, D. A., and Lester, H. A. (1998) In Vivo Incorporation of Unnatural Amino Acids into Ion Channels in *Xenopus* Oocyte Expression System. *Methods Enzymol* **293**, 504-529
44. Amici, M., Eusebi, F., and Miledi, R. (2005) Effects of the antibiotic gentamicin on nicotinic acetylcholine receptors. *Neuropharmacology* **49**, 627-637
45. Ben-Ami, H. C., Yassin, L., Farah, H., Michaeli, A., Eshel, M., and Treinin, M. (2005) RIC-3 affects properties and quantity of nicotinic acetylcholine receptors via a mechanism that does not require the coiled-coil domains. *The Journal of Biological Chemistry* **280**, 28053-28060
46. Castillo, M., Mulet, J., Gutierrez, L. M., Ortiz, J. A., Castelan, F., Gerber, S., Sala, S., Sala, F., and Criado, M. (2005) Dual role of the RIC-3 protein in trafficking of serotonin and nicotinic acetylcholine receptors. *The Journal of Biological Chemistry* **280**, 27062-27068
47. Cheng, A., McDonald, N. A., and Connolly, C. N. (2005) Cell surface expression of 5-hydroxytryptamine type 3 receptors is promoted by RIC-3. *The Journal of Biological Chemistry* **280**, 22502-22507
48. Halevi, S., McKay, J., Palfreyman, M., Yassin, L., Eshel, M., Jorgensen, E., and Treinin, M. (2002) The *C. elegans* ric-3 gene is required for maturation of nicotinic acetylcholine receptors. *EMBO J* **21**, 1012-1020
49. Williams, M. E., Burton, B., Urrutia, A., Shcherbatko, A., Chavez-Noriega, L. E., Cohen, C. J., and Aiyar, J. (2005) Ric-3 promotes functional expression of the nicotinic acetylcholine receptor $\alpha 7$ subunit in mammalian cells. *The Journal of Biological Chemistry* **280**, 1257-1263

Appendix 1

*Autosomal Dominant Nocturnal Frontal Lobe Epilepsy Mutation Suppresses Low-Sensitivity ($\alpha 4$)₃($\beta 2$)₂ Nicotinic Acetylcholine Receptor Expression**

**The work described in this section was done in collaboration with Dr. Weston Nichols, Dr. Brandon Henderson, Caroline Yu, Dr. Chris Richards, and Dr. Bruce Cohen.*

A1.1 Abstract

Autosomal dominant nocturnal frontal lobe epilepsy (ADNFLE) is linked to mutations in $\alpha 2$, $\alpha 4$, and $\beta 2$ nicotinic acetylcholine receptor (nAChR) subunits (1), as well as in a sodium-gated potassium channel (2). ADNFLE results in brief nocturnal seizures that occur mainly during slow-wave sleep. A number of ADNFLE nAChR mutations increase the sensitivity of $\alpha 4\beta 2$ nAChRs to the endogenous agonist ACh and reduce allosteric Ca^{2+} potentiation (1,3). One ADNFLE mutation, V287L, is located in the pore-lining region of the nAChR $\beta 2$ subunit (4,5). Previous studies have shown that agonist sensitivity, desensitization, single-channel conductance, and allosteric Ca^{2+} potentiation of $\alpha 4\beta 2$ nAChRs change when this mutation is introduced to the receptor (4,5). The $\alpha 4\beta 2$ receptor can assemble into several functional receptors with different stoichiometries, two of which are the high sensitivity ($\alpha 4$)₂($\beta 2$)₃ and low sensitivity ($\alpha 4$)₃($\beta 2$)₂ receptors (6,7). These two stoichiometries have been shown to be expressed and functional in native neuronal environments (8). In addition, the accessory subunit $\alpha 5$ can co-assemble with $\alpha 4\beta 2$ subunits to form $\alpha 5\alpha 4\beta 2$ nAChRs (9).

The effects of ADNFLE mutations on $\alpha 4\beta 2$ subunit stoichiometry are vague (10). The goal of this collaboration was to use a combination of electrophysiological and fluorescent imaging techniques to resolve these ambiguities. The functional effects of $\beta 2$ V287L were measured via dose-response relationships of $\alpha 4\beta 2$ and $\alpha 5\alpha 4\beta 2$ nAChRs expressed in oocytes using two-electrode voltage clamp electrophysiology. Total internal reflection fluorescence (TIRF) microscopy using superecliptic pHluorin (SEP)-labeled $\alpha 5$, $\alpha 4$, $\beta 2$, and $\beta 2$ V287L nAChR subunits in HEK293 cells were used to measure surface expression of the different receptors. The results from these studies show that $\beta 2$ V287L provides a gain-of-function to the $(\alpha 4)_2(\beta 2)_3$ and $(\alpha 4)_3(\beta 2)_2$ receptors, and suppresses $(\alpha 4)_3(\beta 2)_2$ expression. In addition, $\beta 2$ V287L increases $\alpha 5\alpha 4\beta 2$ surface expression but does not affect functional responses to acetylcholine (ACh).

Appendix 1 focuses on the interpretation of the oocyte experimental results I obtained for this collaboration.

A1.2 Results and Discussion

To determine whether $(\alpha 4)_3(\beta 2)_2$ receptor suppression was inherent to the $\beta 2$ V287L mutation, oocytes were injected with either $\alpha 4\beta 2$ or $\alpha 4\beta 2$ V287L mRNAs in a 1:1 or 10:1 $\alpha 4:\beta 2$ ratio, and ACh EC_{50} measurements were obtained. *Xenopus laevis* oocytes can be biased in receptor expression by varying ratios of injected mRNAs. Equal amounts of $\alpha 4$ and $\beta 2$ mRNA yields a mixture of $(\alpha 4)_2(\beta 2)_3$ and $(\alpha 4)_3(\beta 2)_2$ receptors, while an excess of $\alpha 4$ mRNA favors $(\alpha 4)_3(\beta 2)_2$ receptor formation and an excess of $\beta 2$ favors $(\alpha 4)_2(\beta 2)_3$ formation (6,7).

Injecting $\alpha 4:\beta 2$ wild type (WT) mRNAs in a 1:1 ratio produced a biphasic ACh EC_{50} curve (**Figure A1.1**). Data fitting yielded EC_{50} values for the two components differing by more than tenfold, with $(\alpha 4)_2(\beta 2)_3$ receptors accounting for $65 \pm 2\%$ of the maximum WT response (**Table A1.1**). In contrast, injecting $\alpha 4:\beta 2$ V287L mRNAs in a 1:1 ratio produced a monophasic ACh EC_{50} curve of high sensitivity (**Figure A1.1**), which suggests $(\alpha 4)_3(\beta 2)_2$ receptor suppression from inclusion of the $\beta 2$ V287L mutation. The EC_{50} of the $(\alpha 4)_2(\beta 2$ V287L) $_3$ mutant receptor shows a six-fold gain-of-function compared to $(\alpha 4)_2(\beta 2)_3$ receptors (**Table A1.1**). Thus, the $\beta 2$ V287L mutation increased the sensitivity of $(\alpha 4)_2(\beta 2)_3$ receptors while appearing to suppress the expression of $(\alpha 4)_3(\beta 2)_2$ receptors.

Injecting $\alpha 4:\beta 2$ mRNAs in a 10:1 ratio shifted the WT ACh EC_{50} curve rightward, indicating a more enriched $(\alpha 4)_3(\beta 2)_2$ population (**Figure A1.1**). To estimate the percentage of the high sensitivity component, a biphasic ACh EC_{50} curve was fit after constraining the $(\alpha 4)_2(\beta 2)_3$ contribution of the two components to the values obtained from fitting the $\alpha 4:\beta 2$ 1:1 data above (**Table A1.1**). The percent of $(\alpha 4)_2(\beta 2)_3$ receptors in the population was $7 \pm 4\%$ and that of $(\alpha 4)_3(\beta 2)_2$ receptors was $93 \pm 4\%$ (**Table A1.1**). Thus, the WT 10:1 ACh EC_{50} curve relation was nearly monophasic, suggesting an almost complete suppression of $(\alpha 4)_2(\beta 2)_3$ expression.

Again a similar suppression and gain-of-function observation is seen when introducing the $\beta 2$ V287L mutation. The 10:1 ratio of $\alpha 4:\beta 2$ V287L mRNAs produced a notably biphasic ACh EC_{50} curve (**Figure A1.1**). Fitting the biphasic curve in a similar manner to the WT case by constraining the value for the $(\alpha 4)_2(\beta 2$ V287L) $_3$ contribution,

the $(\alpha 4)_2(\beta 2 \text{ V287L})_3$ receptors accounted for $23 \pm 3\%$ of the maximum response, and the $(\alpha 4)_3(\beta 2 \text{ V287L})_2$ receptors for $77 \pm 3\%$ (Table 1). The percentage of $(\alpha 4)_2(\beta 2 \text{ V287L})_3$ receptors for the 10:1 injection ratio was significantly larger than the corresponding value for the WT (**Table A1.1**). The $\beta 2 \text{ V287L}$ mutation also reduced the EC_{50} of the $(\alpha 4)_3(\beta 2 \text{ V287L})_2$ receptors by a factor of five (**Table A1.1**). In summary, the $\beta 2 \text{ V287L}$ mutation favors formation of the $(\alpha 4)_2(\beta 2)_3$ stoichiometry, and it produces gain-of-function for ACh responses for both the $(\alpha 4)_2(\beta 2 \text{ V287L})_3$ and $(\alpha 4)_3(\beta 2 \text{ V287L})_2$ receptors by similar factors.

Since the $\beta 2 \text{ V287L}$ mutation had significant effects in sensitivity and stoichiometry of the $\alpha 4\beta 2$ receptors, $\alpha 5\alpha 4\beta 2$ receptors were also investigated for functional and assembly changes. Again, ratio biasing is used to generate enriched populations of the $\alpha 5\alpha 4\beta 2$ receptors. Oocytes were injected with $\alpha 5:\alpha 4:\beta 2$ or $\alpha 5:\alpha 4:\beta 2 \text{ V287L}$ mRNAs, using a large excess of $\alpha 5$ ($\alpha 5:\alpha 4:\beta 2$ ratio of 10:1:1) to favor $\alpha 5:\alpha 4:\beta 2$ assembly (**Figure A1.2**). The WT and $\beta 2 \text{ V287L}$ ACh EC_{50} curves were monophasic and essentially identical to one another (**Figure A1.2, Table A1.1**). Surprisingly, the $\beta 2 \text{ V287L}$ mutation did not alter the EC_{50} of $\alpha 5\alpha 4\beta 2$ nAChRs. These results suggest that $\beta 2 \text{ V287L}$ does not affect the ACh sensitivity of $\alpha 5^*$ nAChRs despite the large effects seen in $\alpha 4\beta 2$ nAChRs.

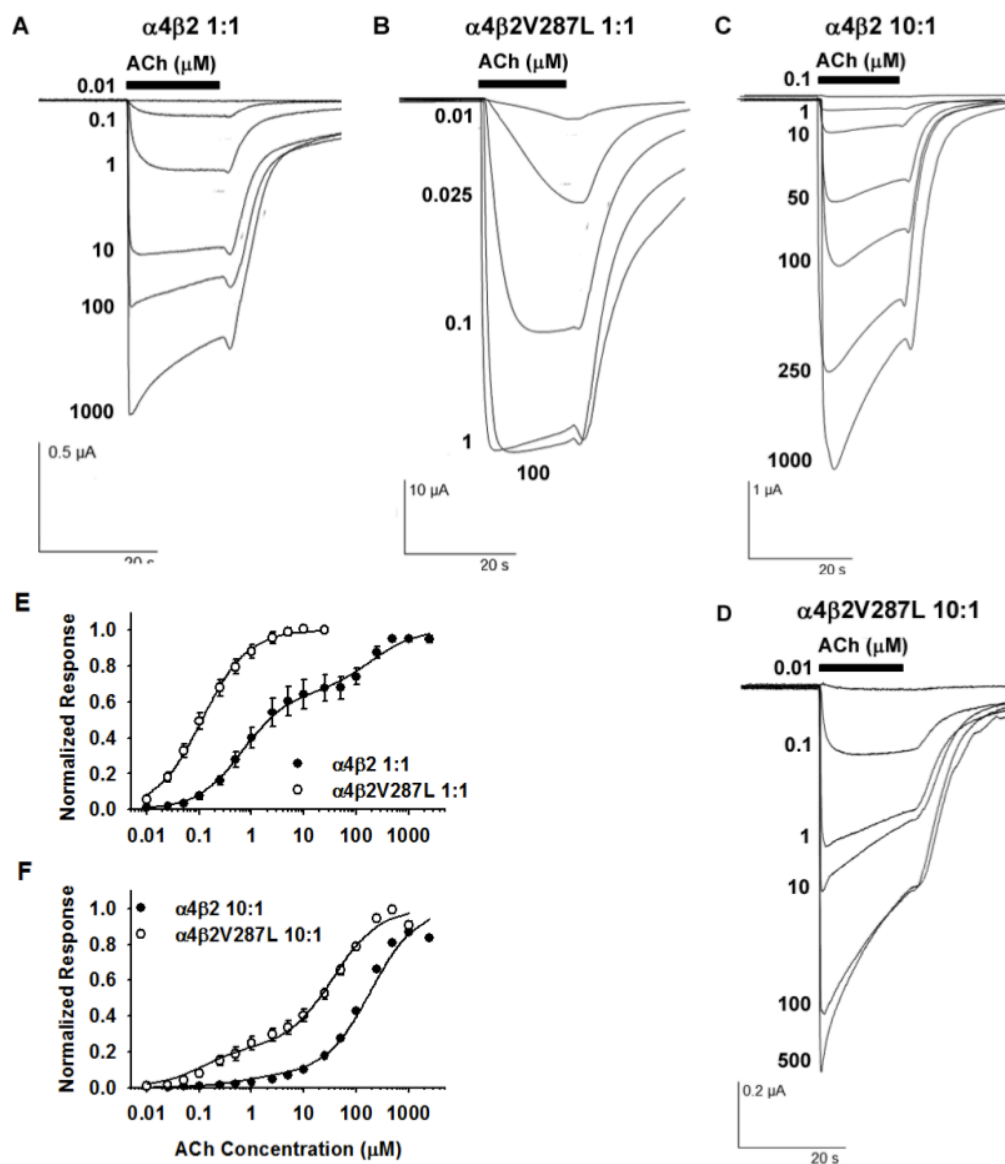


Figure A1.1 ACh EC₅₀ curves for $\alpha 4\beta 2$ and $\alpha 4\beta 2$ V287L nAChRs expressed in *Xenopus* oocytes using 1:1 (A-B, E) and 10:1 $\alpha 4:\beta 2$ mRNA injection ratios (C-D, F). The traces are voltage-clamped ACh responses of oocytes injected with (A) $\alpha 4\beta 2$ or (B) $\alpha 4\beta 2$ V287L in a 1:1 $\alpha 4:\beta 2$ stoichiometric ratio (*w/w*). The ACh concentrations (in μM) are listed to the left of, or below, the traces. The bars above the traces show the timing and duration of the ACh application. For clarity, only a subset of the 18 responses recorded from each oocyte is shown. Voltage-clamped traces of (C) $\alpha 4\beta 2$ and (D) $\alpha 4\beta 2$ V287L responses using a 10:1 $\alpha 4:\beta 2$ injection ratio. (E-F) Normalized ACh EC₅₀ curves for the $\alpha 4\beta 2$ (filled circles) and $\alpha 4\beta 2$ V287L nAChRs (open circles) using (E) 1:1 and (F) 10:1 $\alpha 4:\beta 2$ injection ratios. Lines are fit to one or two Hill terms to generate EC₅₀ and Hill coefficient (nH) values.

TABLE A1.1

Receptor	α : β mRNA Injection Ratio	Component	% of Total	EC ₅₀ (μ M)
$\alpha 4\beta 2$	1:1	HS	65 \pm 2 (8)	0.67 \pm 0.08 (8)
		LS	35 \pm 2 (8)	190 \pm 60 (8)
$\alpha 4\beta 2$ V287L	1:1	HS	100	0.11 \pm 0.01 (8)***
$\alpha 4\beta 2$	10:1	HS	7 \pm 4 (17)	0.67 (fixed)
		LS	93 \pm 4 (17)	190 (fixed)
$\alpha 4\beta 2$ V287L	10:1	HS	23 \pm 3 (7)**	0.11 (fixed)
		LS	77 \pm 3 (7)	36 \pm 7 (7)*
$\alpha 5\alpha 4\beta 2$	10:1:1	HS	100	0.26 \pm 0.04 (4)
$\alpha 5\alpha 4\beta 2$ V287L	10:1:1	HS	100	0.32 \pm 0.01 (8)

Fitted parameters for the ACh concentration-response relations of $\alpha 4\beta 2$, $\alpha 4\beta 2$ V287L, $\alpha 5\alpha 4\beta 2$, and $\alpha 5\alpha 4\beta 2$ V287L nAChRs expressed in oocytes. Values are mean \pm S.E. (number of oocytes). HS and LS denote $(\alpha 4)_2(\beta 2)_3$ and $(\alpha 4)_2(\beta 2)_3$ components of the concentration-response relations, respectively. For single-component concentration-response relations the percent of total (% of total) was fixed at 100%. Parameters constrained to a particular value are denoted as (fixed). Mutant values that differ significantly from WT ($\alpha 4\beta 2$) at the 0.05, 0.01, and 0.001 levels are marked (*), (**), and (***), respectively.

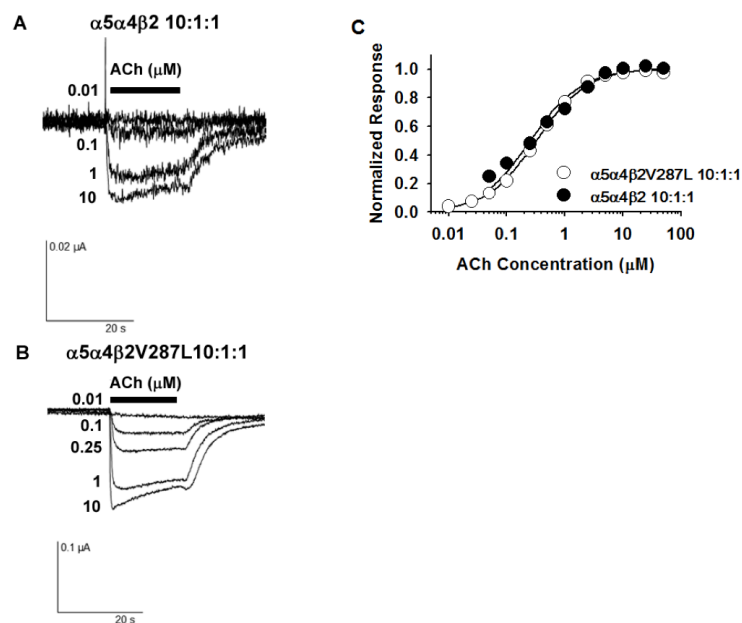


Figure A2.2 ACh EC₅₀ curves for $\alpha 5\alpha 4\beta 2$ and $\alpha 5\alpha 4\beta 2$ V287L nAChRs expressed in *Xenopus* oocytes using a large excess of $\alpha 5$ mRNA ensure that $\alpha 5$ -containing ($\alpha 5^*$) nAChRs were the predominant subtype ($\alpha 5$: $\alpha 4$: $\beta 2$ mRNA injection ratio of 10:1:1 w/w/w). Voltage-clamped ACh responses of oocytes injected with (A) $\alpha 5\alpha 4\beta 2$ or (B) $\alpha 5\alpha 4\beta 2$ V287L. (C) Normalized ACh EC₅₀ curves for the WT $\alpha 5\alpha 4\beta 2$ (filled circles), and $\alpha 5\alpha 4\beta 2$ V287L (open circles).

A1.3 Methods

A1.3.1 Molecular Biology

Mouse nAChR $\alpha 5$, $\alpha 4$, and $\beta 2$ subunits were subcloned into pGEMhe, and the QuikChange protocol (Stratagene) was used for site-directed mutagenesis. The resulting plasmids of $\alpha 4$ and $\beta 2$ DNA were linearized using the *SbfI* restriction enzyme. Plasmids of $\alpha 5$ DNA were linearized using the *SphI* restriction enzyme. The linearized DNA template was purified (Qiagen) and used for mRNA synthesis via the T7 mMessage Machine kit (Ambion) run-off transcription. Qiagen's RNeasy RNA purification kit was used to purify the resulting mRNA.

A1.3.2 Oocyte Injection

Standard protocols were performed to harvest *Xenopus laevis* stage V and VI oocytes (11). The $\alpha 5$, $\alpha 4$, and $\beta 2$ mRNA were mixed with a 10:1:1 ratio by mass to produce a 0.8 ng/nL concentration. 50 nL were injected into the oocytes delivering 40 ng of total mRNA. The $\alpha 4$ and $\beta 2$ mRNA were mixed with a mass ratio of 1:1 to produce a 0.13 ng/nL concentration and a mass ratio of 10:1 to produce a 0.42 ng/nL concentration. 50 nL were injected to deliver 6.7 ng and 21 ng of total mRNA, respectively. Oocytes were stored in ND96+ medium and incubated at 18°C for 24-96 h post injection.

A1.3.3 Electrophysiology

Acetylcholine chloride was purchased from Sigma-Aldrich and dissolved to a 1 M stock solution in ND96 Ca^{2+} free buffer (96 mM NaCl, 2 mM KCl, 1 mM MgCl_2 , 5 mM HEPES at pH 7.5).

The OpusXpress 6000A (Axon Instruments) two electrode voltage clamp mode was used for electrophysiological recordings. For all recordings, the holding potential was -60 mV and the ND96 Ca^{2+} free solution was used as the running buffer. All measurements involved 1 mL of drug solution applied over 15 s followed by a 2 min buffer wash. Dose-response curves involved a three concentration series (approximately three-fold between each) spanning several orders of magnitude, which totaled eight to eighteen doses. Data were low-pass filtered at 5 Hz before determining the current response for each dose application.

Each cell was individually normalized to its own max response. These results were then averaged and fit to one or two Hill terms to generate EC_{50} and Hill coefficient (nH) values. Error is represented by standard error of the mean (SEM).

A1.4 References

1. Ferini-Strambi, L., Sansoni, V., and Combi, R. (2012) Nocturnal frontal lobe epilepsy and the acetylcholine receptor. *The Neurologist* **18**, 343-349
2. Heron, S. E., Smith, K. R., Bahlo, M., Nobili, L., Kahana, E., Licchetta, L., Oliver, K. L., Mazarib, A., Afawi, Z., Korczyn, A., Plazzi, G., Petrou, S., Berkovic, S. F., Scheffer, I. E., and Dibbens, L. M. (2012) Missense mutations in the sodium-gated potassium channel gene KCNT1 cause severe autosomal dominant nocturnal frontal lobe epilepsy. *Nature Genetics* **44**, 1188-1190
3. Raggenbass, M., and Bertrand, D. (2002) Nicotinic receptors in circuit excitability and epilepsy. *Journal of Neurobiology* **53**, 580-589
4. De Fusco, M., Becchetti, A., Patrignani, A., Annesi, G., Gambardella, A., Quattrone, A., Ballabio, A., Wanke, E., and Casari, G. (2000) The nicotinic receptor $\beta 2$ subunit is mutant in nocturnal frontal lobe epilepsy. *Nature Genetics* **26**, 275-276
5. Gambardella, A., Annesi, G., De Fusco, M., Patrignani, A., Aguglia, U., Annesi, F., Pasqua, A. A., Spadafora, P., Oliveri, R. L., Valentino, P., Zappia, M., Ballabio, A., Casari, G., and Quattrone, A. (2000) A new locus for autosomal dominant nocturnal frontal lobe epilepsy maps to chromosome 1. *Neurology* **55**, 1467-1471
6. Zwart, R., and Vijverberg, H. P. (1998) Four pharmacologically distinct subtypes of $\alpha 4\beta 2$ nicotinic acetylcholine receptor expressed in *Xenopus laevis* oocytes. *Mol Pharmacol* **54**, 1124-1131.
7. Moroni, M., Zwart, R., Sher, E., Cassels, B. K., and Bermudez, I. (2006) $\alpha 4\beta 2$ nicotinic receptors with high and low acetylcholine sensitivity: pharmacology, stoichiometry, and sensitivity to long-term exposure to nicotine. *Mol Pharmacol* **70**, 755-768
8. Gotti, C., Moretti, M., Meinerz, N., Clementi, F., Gaimarri, A., Collins, A. C., and Marks, M. J. (2008) Partial deletion of the nicotinic cholinergic receptor $\alpha 4$ and $\beta 2$ subunit genes changes the acetylcholine sensitivity of receptor mediated $^{86}\text{Rb}^+$ efflux in cortex and thalamus and alters relative expression of $\alpha 4$ and $\beta 2$ subunits. *Mol Pharmacol*
9. Brown, R. W., Collins, A. C., Lindstrom, J. M., and Whiteaker, P. (2007) Nicotinic $\alpha 5$ subunit deletion locally reduces high-affinity agonist activation without altering nicotinic receptor numbers. *J Neurochem* **103**, 204-215
10. O'Neill, H. C., Lavery, D. C., Patzlaff, N. E., Cohen, B. N., Fonck, C., McKinney, S., McIntosh, J. M., Lindstrom, J. M., Lester, H. A., Grady, S. R., and Marks, M. J. (2013) Mice expressing the ADNFLE valine 287 leucine mutation of the $\beta 2$ nicotinic acetylcholine receptor subunit display increased sensitivity to acute nicotine administration and altered presynaptic nicotinic receptor function. *Pharmacol Biochem Behav* **103**, 603-621
11. Nowak, M., Gallivan, J. P., Silverman, S., Labarca, C. G., Dougherty, D. A., and Lester, H. A. (1998) In Vivo Incorporation of Unnatural Amino Acids into Ion Channels in *Xenopus* Oocyte Expression System. *Methods Enzymol* **293**, 504-530

Appendix 2

*Ligand-Gated Ion Channel Screen of Physostigmine Derivatives for Allosteric Modulation and Receptor Agonism**

**The work described in this section was done in collaboration with Dr. Kristina Daeffler, Dr. Lindsey Repka, and Alex Maolanon.*

A2.1 Abstract

The goal of this collaboration was to screen synthetic, drug-like compounds for activation, potentiation, or inhibition of several ligand-gated ion channels (LGICs). Dr. Lindsey Repka and Alex Maolanon of the Reisman group developed and utilized a novel synthetic scheme for organic compounds that are structurally similar to physostigmine, which is a clinically used acetylcholinesterase inhibitor and positive allosteric modulator (PAM) of nicotinic acetylcholine receptors (nAChRs) (1,2). The Reisman group provided five compounds that were screened with the help of Dr. Kristina Daeffler against seven LGICs: the $\alpha 7$ (T6'S), $(\alpha 4 L 9' A)_3(\beta 2)_2$, and muscle-type nAChRs and the 5-HT_{3A}, GABA_A($\alpha\beta\gamma$), glycine, and GluR2 receptors. Most compounds were either channel blockers with varying levels of potencies for nicotinic acetylcholine receptors or non-interacting for other channels probed. However, compound AMAO-1-86 showed weak partial agonism and demonstrated PAM properties at the GABA_A($\alpha\beta\gamma$) receptor. Agonism was eliminated and PAM properties diminished when tested against the GABA_A($\alpha\beta$) receptor, which suggests potential binding at the α - γ interface, like

benzodiazepines. Further studies are needed to confirm the results from the GABA_A($\alpha\beta$) study and to identify the actual binding site of AMAO-1-86.

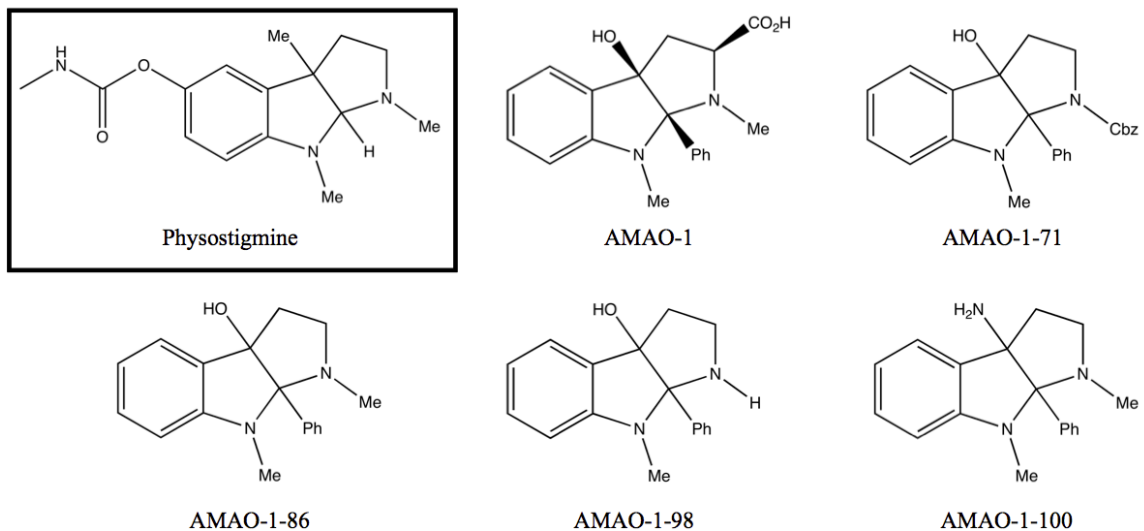


Figure A2.1 Chemical structures of physostigmine and the synthetic derivatives provided by Dr. Lindsey Repka and Alex Maolanon.

A2.2 Results and Discussion

A2.2.1 Screening Compounds for Functional Properties at Various LGICs

Five derivatives (**Figure A2.1**) based on the core ring structure of physostigmine were tested across the seven LGICs. The PAM protocol from **Chapter 4** was used to study these molecules. This included three native agonist EC₅₀ doses, one 60 s incubation of the compound with an immediate co-application of an EC₅₀ dose, and two native agonist EC₅₀ doses (**Figure A2.2**). Since the goal was to screen for “hit” compounds, the concentration of molecule being tested was 20-40 μ M. This protocol allows for identification of activation, inhibition, and/or positive allosteric modulation of the receptor. All percent increases or decreases are relative to the EC₅₀ response of the receptor. These values may change based on higher or lower doses of agonist or ligand

tested; however these concentrations provide an adequate range in order to observe increasing (PAM) or decreasing (inhibition) receptor response.

Nearly all the compounds studied showed either no effect or inhibition of receptor response (**Table A2.1**). The one exception was AMAO-1-86, which was a weak partial agonist (~10% channel activation at 40 μM) and a PAM (~50% increase of the EC_{50} response) for the $\text{GABA}_A(\alpha\beta\gamma)$ receptor (**Table A2.1 and Figure A2.2**). Increasing the concentration of AMAO-1-86 showed an increase in receptor response, indicating that it acts in a dose-dependent manner. However, available quantity and solubility issues hampered efforts to obtain a full EC_{50} curve due to lack of potency (possibly high μM EC_{50}). Removal of the γ subunit generates the $\text{GABA}_A(\alpha\beta)$ receptor, which showed elimination of agonist activity and marked reduction of positive allosteric modulation (~15% increase of the EC_{50} response). This suggests interactions with the α - γ interface for AMAO-1-86 or at least a strong role for the γ subunit in AMAO-1-86 receptor modulation. Further studies are needed for replication of the $\text{GABA}_A(\alpha\beta)$ experiment and

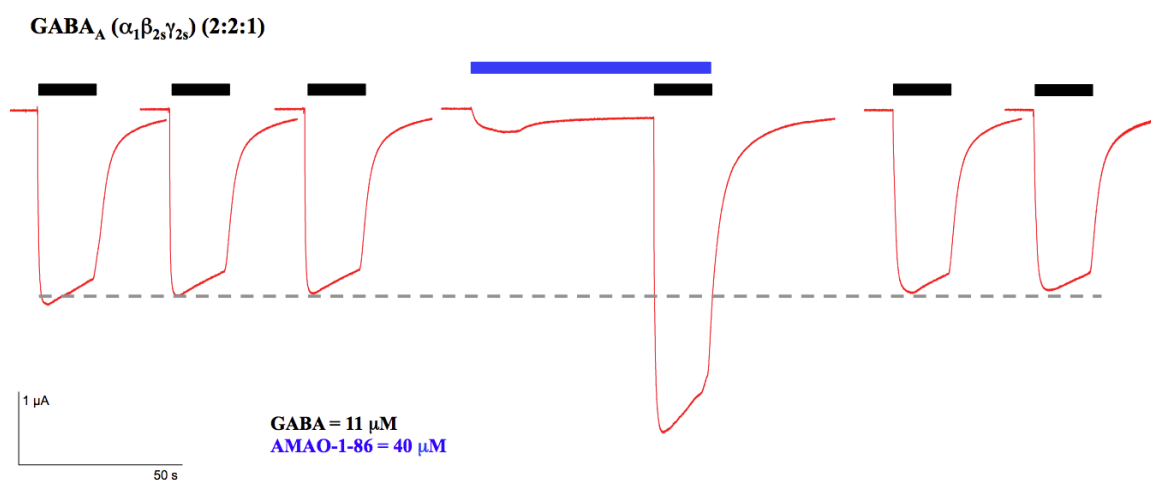


Figure A2.2 Example of protocol used for screening the compounds against LGICs. The black bars represent native agonist EC_{50} doses. The blue bar represents the compound being tested. The novel result of AMAO-1-86 being a weak partial agonist and PAM of $\text{GABA}_A(\alpha\beta\gamma)$ is shown in these traces.

Table A2.1

Percent change in EC₅₀ response when co-applied with indicated ligand. Negative values represent signal decreases while positive values represent signal increases.

Receptor	Percent (%) change in current with co-application of EC ₅₀ dose and 20-40 μ M of Compound				
	AMAO-1	AMAO-1-71	AMAO-1-86	AMAO-1-98	AMAO-1-100
Muscle (9')	-21 \pm 1	-29 \pm 3	-53 \pm 3	-7 \pm 3	-81 \pm 6
(α 4L9'A) ₃ (β 2) ₂	-28 \pm 2	-47 \pm 4	-29 \pm 6	-11 \pm 2	-44 \pm 2
α 7 (T6'S)	-62 \pm 4	-68 \pm 7	-92 \pm 4	-57 \pm 10	-96 \pm 3
5-HT _{3A}	-3 \pm 2	-23 \pm 4	-3 \pm 5	3 \pm 12	-11 \pm 8
GABA _A ($\alpha\beta\gamma$)	-27 \pm 4	-27 \pm 11	52 \pm 10	-27 \pm 21	10 \pm 5
GABA _A ($\alpha\beta$)			16 \pm 2		
GluR2	-6 \pm 1	0 \pm 2	-9 \pm 6	-11 \pm 5	-12 \pm 5
Glycine	-6	-9 \pm 9	3 \pm 7	18 \pm 10	-16 \pm 6

further mutational screening will be needed to identify the binding site of AMAO-1-86.

The first place to try would involve the α 1 H129R mutation which has been shown to eliminate benzodiazepine modulation of the GABA_A($\alpha\beta\gamma$) (3). Other studies have shown differential residue movements on activation when benzodiazepines are co-applied with receptor agonists (4,5).

For the rest of the receptors and compounds, co-application resulted in either no effect or inhibition. GluR and glycine receptors were relatively inert to the ligands applied here. 5-HT_{3A} exhibited a similar trend except ~25% drop in signal for the AMAO-1-71 compound. The largest inhibition results were seen for the nAChRs: muscle-type, (α 4L9'A)₃(β 2)₂, and α 7 (T6'S) (**Table A2.1**). The α 7 (T6'S) receptor consistently had the highest inhibition values. The muscle-type and (α 4L9'A)₃(β 2)₂ receptors had modest inhibition across all the compounds except for AMAO-1-98, which only inhibited the α 7 (T6'S) receptor. This is not surprising due to the promiscuity in compound activation, inhibition, and modulation for α 7 nAChRs (6,7). No other positive modulation was observed for the remaining receptors screened. All derivatives had different levels of inhibition, indicating some receptor specificity. To better understand

the mode of inhibition, further studies were performed on AMAO-1 because it was the most water-soluble and most abundant analog synthesized.

A2.2.1 Physostigmine Analog Inhibition Characterization

Receptor inhibition can occur in several different modes: channel block, antagonism, and negative allosteric modulation (NAM). IC₅₀ curves and voltage-jump experiments were performed to delineate how AMAO-1 was inhibiting the nAChRs. **Figure A2.3** shows the IC₅₀ curves for $\alpha 7$ (T6'S) and ($\alpha 4L9'A$)₃($\beta 2$)₂ receptors. Lower doses of AMAO-1 showed a large variability in inhibition, suggesting a slow on-rate of the compound. The $\alpha 7$ (T6'S) and ($\alpha 4L9'A$)₃($\beta 2$)₂ receptor IC₅₀ values were 5 μ M and 8 μ M and Hill coefficients were -0.8 and -1.2, respectively. The Hill coefficient of near 1 suggests that only one molecule is needed to inhibit the channel. This seems to rule out AMAO-1 as an antagonist since there are five binding sites for the $\alpha 7$ (T6'S) nAChR and

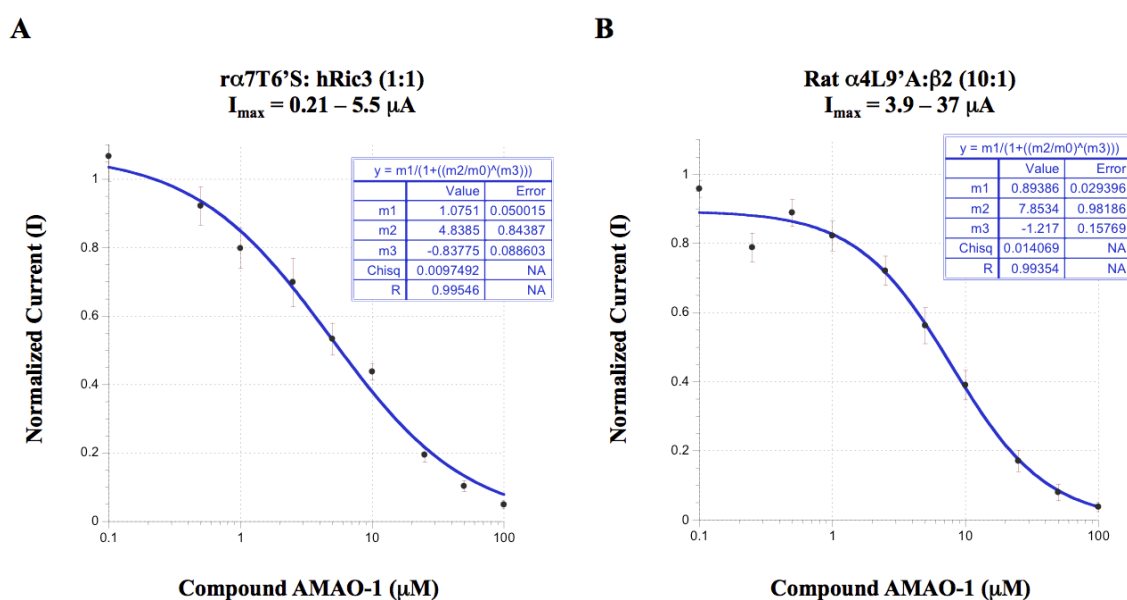


Figure A2.3 IC₅₀ curves of AMAO-1 at (A) $\alpha 7$ (T6'S) and (B) ($\alpha 4L9'A$)₃($\beta 2$)₂. m2 and m3 represent the IC₅₀ and Hill coefficient, respectively.

three sites for the $(\alpha 4L9'A)_3(\beta 2)_2$ receptor. This still leaves the channel blocker and NAM profile. However, the NAM profile is unlikely since there tends to be multiple binding locations for allosteric modulators, which is similar to agonist binding sites.

Voltage-jump experiments were performed on $(\alpha 4L9'A)_3(\beta 2)_2$ receptors to test if AMAO-1 is acting through a channel blocker mechanism. Comparison of positive-to-negative and negative-to-positive voltage-jumps can indicate if a compound is acting as a channel blocker and this has been previously done for characterization of hexamethonium at $\alpha 4\beta 2$ nAChRs (8). AMAO-1 did not exhibit similar voltage-dependence as hexamethonium (**Figure A2.4**). This is probably due to AMAO-1 having a net neutral charge and hexamethonium being positively charged, which is influenced more by relative cell holding potentials. It is more likely that AMAO-1 is a channel blocker and further studies on the other charged derivatives would most likely resemble the voltage-jump results of hexamethonium.

Rat $(\alpha 4L9'A)_3(\beta 2)_2$

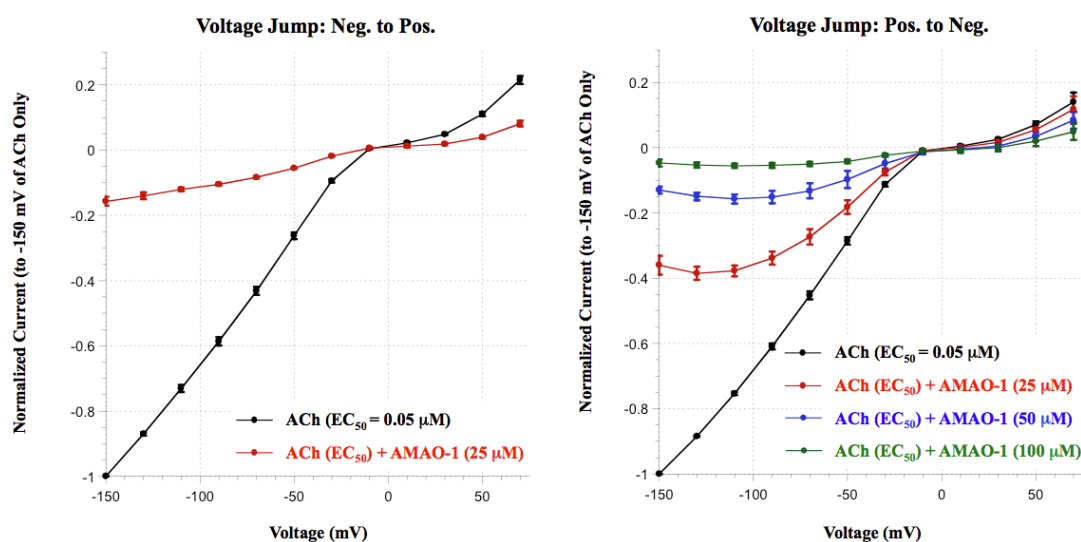


Figure A2.4 Example of voltage jump results of a single cell expressing $(\alpha 4L9'A)_3(\beta 2)_2$. Minor changes are seen when varying the voltage from negative-to-positive (left) and positive-to-negative (right) when AMAO-1 is present.

A2.3 Conclusions

The physostigmine analogs exhibited here show a variety of activities among a series of LGICs. For the most part, these compounds behave as inhibitors of nAChRs and generally are inactive at other Cys-loop receptors, with minor exceptions (GABA_A and one instance at 5-HT_{3A}). Due to the low Hill coefficients and low sensitivity (mid- μ M range) for inhibition of nAChRs, they most likely are acting via a channel blocker mechanism. Although the voltage-jump experiments performed here do not corroborate this observation, the compound tested was net neutral and differs from the original comparison (positively charged channel blocker). Testing a charged analog would probably resemble a voltage-jump experiment for hexamethonium channel blocking.

The more exciting result involved the partial activation and positive allosteric modulation of GABA_A($\alpha\beta\gamma$) with AMAO-1-86. The effects were eliminated with introduction of small chemical changes: alcohol to amine (AMAO-1-100), tertiary to secondary amine (AMAO-1-98), and addition of a carboxyl group (AMAO-1). In addition, preliminary results show elimination of the agonist activity and reduction of the allosteric modulation when the γ subunit is removed to form GABA_A($\alpha\beta$). These data suggests a distinct binding environment for the compound and point to a binding region possibly involving the α - γ subunit interface. Further investigation involving receptor mutation screening as well as synthesis of other derivatives of AMAO-1-86 would prove useful in identifying the binding region of a structurally novel PAM for GABA_A($\alpha\beta\gamma$) receptors

A2.4 Methods

An adapted PAM protocol outlined in **Chapter 4** was used for the LGIC screen experiments. First, three EC₅₀ doses (of which the first was ignored) of the native agonist were applied with a 2-5 min washout in between applications. All cell responses were normalized to the largest response pre-ligand exposure. The next application in the series involved a 60 s pre-incubation of 20-40 μ M of the ligand followed immediately by a co-application of the ligand and native agonist EC₅₀ dose. This tested for direct receptor activation (agonist with the pre-incubation dose) and allosteric modulation/inhibition (co-application dose). Finally, two EC₅₀ doses similar to the first three were performed to show the ligand's ability to be washed out and have receptor response returned to the baseline agonist-only applications. Averaging current responses from doses two and three (EC₅₀ agonist response only) and subtracting from the co-application dose (ligand and EC₅₀ agonist) gave the calculated change in response. Multiplying this value by 100% gave the percent inhibition/activation of the ligand. Agonist EC₅₀ values for each receptor studied were: 100 μ M ACh ($\alpha 7$ T6'S), 1.2 μ M (muscle-type L9'A), 0.05 μ M (($\alpha 4$ L9'A)₃($\beta 2$)₂), 3 μ M 5-HT (5-HT_{3A} receptor), 110 μ M glycine (glycine receptor), 14 μ M glutamate (GluR2), 11 μ M GABA (GABA_A($\alpha\beta\gamma$)), and 3 μ M GABA (GABA_A($\alpha\beta$)). ND96 Ca²⁺ free buffer was used for the muscle type, ($\alpha 4$ L9'A)₃($\beta 2$)₂, glycine, 5-HT3A, and GluR2 receptors. ND96 buffer was used for the GABA_A and $\alpha 7$ (T6'S) nAChRs.

A2.5 References

1. Militante, J., Ma, B. W., Akk, G., and Steinbach, J. H. (2008) Activation and block of the adult muscle-type nicotinic receptor by physostigmine: single-channel studies. *Molecular Pharmacology* **74**, 764-776
2. Hamouda, A. K., Kimm, T., and Cohen, J. B. (2013) Physostigmine and galanthamine bind in the presence of agonist at the canonical and noncanonical subunit interfaces of a nicotinic acetylcholine receptor. *The Journal of Neuroscience: the Official Journal of the Society for Neuroscience* **33**, 485-494
3. Wieland, H. A., Luddens, H., and Seeburg, P. H. (1992) A Single Histidine in GABA_A Receptors Is Essential for Benzodiazepine Agonist Binding. *J Biol Chem* **267**, 1426-1429
4. Bergmann, R., Kongsbak, K., Sorensen, P. L., Sander, T., and Balle, T. (2013) A unified model of the GABA_A receptor comprising agonist and benzodiazepine binding sites. *PloS One* **8**, e52323
5. May, A. C., Fleischer, W., Kletke, O., Haas, H. L., and Sergeeva, O. A. (2013) Benzodiazepine-site pharmacology on GABA_A receptors in histaminergic neurons. *British Journal of Pharmacology* **170**, 222-232
6. Faghi, R., Gopalakrishnan, M., and Briggs, C. A. (2008) Allosteric Modulators of the $\alpha 7$ Nicotinic Acetylcholine Receptor. *J Med Chem* **51**, 701-712
7. Horenstein, N. A., Leonik, F. M., and Papke, R. L. (2008) Multiple pharmacophores for the selective activation of nicotinic $\alpha 7$ -type acetylcholine receptors. *Molecular Pharmacology* **74**, 1496-1511
8. Buisson, B., and Bertrand, D. (1998) Open-Channel Blockers at the Human $\alpha 4\beta 2$ Neuronal Nicotinic Acetylcholine Receptor. *Molecular Pharmacology* **53**, 555-563

